

POLITECNICO DI TORINO

Dipartimento di Ingegneria Meccanica ed Aerospaziale



Tesi di Laurea Magistrale

Trajectories Analysis towards Asteroids
using Indirect Methods

Laurea Magistrale in Ingegneria Aerospaziale

Relatore

Prof. Lorenzo Casalino

Candidato

Fabiano Sgarbi

Sessione di Laurea Marzo 2018

Contents

LIST OF FIGURES	III
LIST OF TABLES	IV
ABSTRACT.....	1
ACKNOWLEDGEMENTS.....	2
1. INTRODUCTION.....	3
1.1 NASA ARM PROGRAM	3
1.2 ASTEROID 2008 EV ₅	5
1.3 INTERPLANETARY TRAJECTORIES OPTIMIZATION	9
2. OPTIMIZATION OF SPACE TRAJECTORIES WITH THE INDIRECT METHOD.....	11
2.1 INTRODUCTION.....	11
2.1.1 <i>Advantages and disadvantages of the indirect methods</i>	11
2.2 THEORY OF THE OPTIMAL CONTROL	12
2.3 DIFFERENTIAL PROBLEM TO LIMITS	18
2.3.1 <i>Boundary values problem (BVP) resolution method</i>	18
2.4 OPTIMIZATION OF SPACE TRAJECTORIES	24
2.5 ELECTRIC PROPULSION.....	27
3. FORTRAN CODE TO FIND AND ANALYSE THE TRAJECTORIES	29
3.1 INTRODUCTION.....	29
3.2 ARM1v0.....	29
3.3 ARM2VF.....	32
3.4 EXPECTED RESULTS	34
4. RESULTS: FROM INDIVIDUAL TRIPS TO THE COMPLETE MISSION.....	35
4.1 INITIAL CONDITIONS	35
4.2 GOING TRIP	35
4.3 RETURN TRIP.....	39
4.4 COMPLETE TRIP	45
4.4.1 <i>Results summary</i>	54
5. CONCLUSION.....	56
BIBLIOGRAPHY	57
APPENDIXES	58
APPENDIX I: RESULTS FOR THE GOING TRIP	58

<i>Case: Default</i>	58
<i>Case: +6 months</i>	59
<i>Case: -6 months</i>	60
<i>Case: +12 months</i>	61
<i>Case: -12 months</i>	62
<i>Case: +18 months</i>	63
<i>Case: -24 months</i>	64
APPENDIX II: RESULTS FOR THE RETURN TRIP	66
<i>Case: Default</i>	66
<i>Case: Default (+1FB)</i>	67
<i>Case: Default (+1FB & trip)</i>	68
<i>Case: Default (+2FB)</i>	69
<i>Case: -12 months</i>	70
<i>Case: -12 months (+1FB)</i>	71
<i>Case: -12 months (+1FB & trip)</i>	72
<i>Case: -12 months (+2FB)</i>	73
<i>Case: +12 months</i>	74
<i>Case: +12 months (+1FB)</i>	75
<i>Case: +12 months (+1FB & trip)</i>	76
<i>Case: +12 months (+2FB)</i>	77
<i>Case: +24 months</i>	78
<i>Case: +24 months (+1FB)</i>	79
<i>Case: +24 months (+2FB)</i>	80
APPENDIX III: OPTIMAL RESULTS FOR THE RETURN TRIP	82

List of Figures

FIGURE 1: POSSIBLE SCENARIOS OF ARM PROGRAM [2]	4
FIGURE 2: ASTEROID 2008 EV₅'S ORBIT (WHITE) COMPARED WITH THE NEAREST PLANETS, IN THE HELIOCENTRIC REFERENCE SYSTEM	7
FIGURE 3: 3D VISUAL OF THE ASTEROID AND EARTH ORBIT IN THE HELIOCENTRIC REFERENCE SYSTEM	8
FIGURE 4: A 2008 EV₅ REPRESENTATION	8
FIGURE 5: DEFAULT INPUT VALUES FOR THE ARM1V0 CODE	30
FIGURE 6: DEFAULT INPUT VALUES FOR THE ARM2VF CODE	32
FIGURE 7: GRAPH FOR THE DEFAULT CASE, WHERE THE DIMENSIONLESS MASS IS COMPARED WITH THE DURATION	37
FIGURE 8: GRAPH FOR THE OVERALL DEPARTURES	38
FIGURE 9: ARM2VF RESULTS FOR THE DEFAULT CASE	40
FIGURE 10: GRAPH OF THE RETURN TRIP (DEFAULT CASE)	42
FIGURE 11: NODES POSITION FOR THE ASTEROID'S ORBIT	8
FIGURE 12: GRAPH OF OVERALL ARRIVALS	44
FIGURE 13: 3D TRAJECTORY TRAVELLED BY THE SATELLITE (REFERRED TO THE BEST SOLUTION FOR THE GOING TRIP)	45
FIGURE 14: 2D TRAJECTORY TRAVELLED BY THE SATELLITE (REFERRED TO THE BEST SOLUTION FOR THE GOING TRIP)	46
FIGURE 15: SATELLITE VERTICAL MOTION FOR THE OPTIMAL SOLUTION DURING THE GOING TRIP	37
FIGURE 16: SWITCHING FUNCTION FOR THE OPTIMAL SOLUTION DURING THE GOING TRIP	47
FIGURE 17: APOGEE AND PERIGEE RADIUS VALUES FOR THE OPTIMAL GOING TRIP	48
FIGURE 18: 3D TRAJECTORY TRAVELLED BY THE SATELLITE (REFERRED TO THE BEST SOLUTION FOR THE RETURN TRIP)	50
FIGURE 19: 2D TRAJECTORY TRAVELLED BY THE SATELLITE (REFERRED TO THE BEST SOLUTION FOR THE RETURN TRIP)	50
FIGURE 20: SATELLITE VERTICAL MOTION FOR THE OPTIMAL SOLUTION DURING THE RETURN TRIP	51
FIGURE 21: APOGEE AND PERIGEE RADIUS VALUES FOR THE OPTIMAL RETURN TRIP	52
FIGURE 22: SWITCHING FUNCTION FOR THE OPTIMAL SOLUTION DURING THE RETURN TRIP	32
FIGURE 23: FLYBY RESULTS FOR THE OPTIMAL CASE	53
FIGURE 24: FLYBY SCHEME	53

List of Tables

TABLE 1: 2008 EV₅'S ORBITAL PARAMETERS REFERRED AT THE HELIOCENTRIC REFERENCE SYSTEM AND REFERRED AT 23 MARCH 2018..... 6

TABLE 2: EARTH'S ORBITAL PARAMETER IN THE HELIOCENTRIC REFERENCE SYSTEM..... 6

TABLE 3: DEFAULT CASE RESULTS FOR THE GOING TRIP..... 36

TABLE 4: OPTIMAL RESULTS FOR THE GOING TRIP 39

TABLE 5: DEFAULT RESULTS FOR THE RETURN TRIP..... 41

TABLE 6: OPTIMAL RESULT FOR THE GOING TRIP..... 45

TABLE 7: OPTIMAL RESULTS FOR THE RETURN TRIP..... 49

TABLE 8: COMPLETE TRIP INFORMATION..... 55

Abstract

The following study deals the trajectories analysis towards asteroids.

In particular, the asteroid 2008 EV₅, which it is part of the NASA ARM program, has been considered following the importance of its composition and for its orbit.

In fact, for its composition will be possible to see as it is a C-type asteroid, which means that it may have 40% of extractable volatile material and about 18% metals, while its orbit is similar at the Earth's orbit.

The ARM (Asteroid Redirect Mission) program consists of two mission segments:

1. the ARRM (Asteroid Redirect Robotic Mission), the first robotic mission to visit a large (greater than ~100 m diameter) near-Earth asteroid (NEA), in order to collect a multi-ton boulder from its surface and return it to a stable orbit around the Moon or the Earth;
2. the Asteroid Redirect Crewed Mission (ARCM), in which astronauts will explore the boulder and return to Earth with samples.

In this study, the first mission segment will be considered and studied.

In order to do this, the indirect methods will be used: these methods are based on the theory of optimal control and solve the optimization problem by defining and solving a boundary value problem.

All this will allow to found, considering different duration and different launch windows, the different solutions for the going and return trip (and their trajectories) and then, analysing these data and evaluating the best solutions, the optimal solutions for the complete trip will be found and analysed, in order to obtain the best mission which will be able to satisfy the imposed constraints.

In this case, the imposed constrains will allow to obtain a mission with the lowest propellant consumption and the higher boulder mass available.

Acknowledgements

I would first like to thank my thesis advisor Professor Lorenzo Casalino of the Mechanics and Aerospace department (DIMEAS) at Politecnico of Turin.

I owe him a special thanks to Professor Casalino, because he was always available for every problem or doubt about this thesis and his help it was essential for the success of the work.

In addition, I must express my very profound gratitude to my family for providing me with unfailing support and continuous encouragement throughout my years of study and through the process of researching and writing this thesis.

This accomplishment would not have been possible without them.

Thank you so much.

Chapter 1

1. Introduction

1.1 NASA ARM program

The ARM program is part of NASA's plan to advance the new technologies and spaceflight capabilities needed for a human mission to the Martian system in the 2030s, as well as other future human and robotic missions.

This program includes the Asteroid Redirect Robotic Mission (ARRM) and the Asteroid Redirect Crewed Mission (ARCM), along with leveraging the global asteroid-observation community's efforts to detect, track and characterize candidate asteroids.

At the beginning, NASA intention was to capture an entire small asteroid (around 4–10 m in size) using a robotic mission, in order to test the developed technology and to obtain additional data on the human exploration and planetary defence but, subsequently, a new approach in order to collect a boulder from a large asteroid was evaluated.

From this, after that the different about these two approaches were evaluated (where their feasibility, the identification about the most important differences between them and the evaluation of the key risks and figures of merit for each concept was considered/evaluated), the ARRM program was born.

Then, as consequence of this, the ARRM program will be the first robotic mission to visit a large (greater than ~100 m diameter) near-Earth asteroid and collect a multi-ton boulder from its surface, along with regolith samples.

This mission will allow to capture an asteroid boulder and then to return it in a stable orbit around the Earth (or around the Moon), in order that the astronauts will be able to explore, study and use it. In order to perform this, a multi-ton boulder will be mounted on the spacecraft.

In this way, the human and robotic missions could be performed to capture these asteroids so to use their material, so to benefit scientific and partnership interests (domestic and international) and expanding the knowledge of small celestial bodies, besides being able to mining asteroid resources for commercial and exploration needs.

The second ARM program is the ARCM, which will provide a compelling science focus for the early flights of the Orion program (this will take place before the infrastructure for more ambitious flights will be available). In addition, this program will provide the opportunity for astronauts to work in space with unaltered asteroid material, testing the activities that would be performed and tools that would be needed for later exploration of primitive body surfaces in deep space.

1. Introduction

Then, in order to perform all these aims, it is clear that an adequate propulsion system must be designed. In fact, another main objective of the ARM concerns with the development of a high-power Solar Electric Propulsion (SEP) vehicle, which could be able to operate for many years in interplanetary space, which is critical for deep-space exploration missions.

In addition, all that will be useful for the following human spaceflight missions, in order to provide the systems and operational experience that will be required for the future human exploration of Mars (including the Martian moons). [1]

Then, summarizing, it is so possible to understand as the Asteroid Redirect Mission includes the following three segments:

- IDENTITY: Ground and space-based assets detect and characterize potential target asteroids;
- REDIRECT: Solar electric propulsion (SEP) based system redirects asteroid to cislunar space;
- EXPLORE: Crew launches aboard SLS rocket, travels to redirected asteroid, study and returns samples to Earth.

In this way, the mission will be useful even for its contribution at the Deep Space Human Exploration and all that will be useful in order to:

- Demonstrate advanced autonomous proximity operations in deep-space and with a natural body;
- Using high-power solar electric propulsion to transport multi-ton masses in space;
- Demonstrate integrated crewed/robotic vehicle operations in deep-space;
- Use astronaut EVA (Extra Vehicular Activity) in deep space for sample selection, handling, and containment on just the second extra-terrestrial body in history. [2] [3]



Figure 1: Possible scenarios of ARM program [2]

1. Introduction

1.2 Asteroid 2008 EV₅

As known, the solar system includes a high number of asteroids with different dimension, shape and composition, then to choose one in order to perform the ARM program may be complicated. However, NASA has identified, among different candidate targets (as Ryugu, Bennu, and Itokawa) the asteroid 2008 EV₅ as the reference target for the ARRM.

The asteroid 2008 EV₅ (discovered on 4 March 2008), scientifically called 341843, is a sub-kilometer asteroid, classified as near-Earth object and potentially hazardous asteroid of the Aten group (a group of asteroids, whose orbit brings them into proximity with Earth, with a semi-major axis of less than 1 AU and with an high eccentricity).

During the years, this asteroid has been well characterized by ground-based radar and by the infrared wavelengths, so as to allow the discovery the satellite composition. In fact, 2008 EV₅ is a carbonaceous chondrite asteroid (C-type), which is believed to be water/volatile-rich (up to 40%) and may contain significant amounts of organic materials (about 18% metals).

For example, 1000 metric ton C-type asteroid may contain 400 ton of volatile elements (water, carbon dioxide, nitrogen, ammonia, etc), 180 ton of metal (roughly 170 ton of iron, 13 ton of nickel and 2 ton of cobalt) and 400 ton of other elements. [4]

In this way is explained because these satellites are studied and analysed, being them an excellent source of raw materials useful in every industrial field.

However, this particular composition may have been caused by its creation process: in fact, the asteroid 2008 EV₅ was initially a part of a much larger body in the asteroid belt (with a likely diameter greater than 100 kilometres), but was product as a reassembly of ejected fragments after that its parent body experienced a large cratering event or, more likely, a catastrophic disruption event that resulted in a highly fractured, shattered, or reaccumulated object. [5]

In addition to its composition, another important reason that allow to explain why this asteroid has been choose is in its orbital and physical characteristics, because these proprieties are similar at the Earth's orbit and even compatible with the planned ARM timeline and operations.

In this way, a significant mass return (even greater than 20 t) will be possible with the start of ARRM program in the 2020 and of ARCM in late 2025.

Another reason, about the choice of this asteroid, it is that his orbital parameters are known in accurate way, besides being an asteroid big enough and therefore such as to allow a landing on its surface. In fact, for the orbital parameter, it is possible to see as the asteroid 2008 EV₅ orbital parameter [6] [7] in the heliocentric reference system frame are the following

1. Introduction

Asteroid 2008 EV₅'s orbital parameters	
Semimajor axis	0.958242 AU
Eccentricity	0.083401
Inclination	7.437°
Ascending node	93.384°
Argument of Perihelion	234.848°
Mean anomaly	63.658°
Perihelion	0.8783 AU
Aphelion	1.0382 AU
Orbit period	342.619 days

Table 1: 2008 EV₅'s orbital parameters referred at the heliocentric reference system and referred at 23 March 2018

and, for an easier comparison, the Earth's orbital parameters [8] are the following

Earth's orbital parameters	
Semimajor axis	1.0000001 AU
Eccentricity	0.01671022
Inclination	0.00005°
Ascending node	174.9°
Argument of Perihelion	288.1°
Perihelion	0.98329 AU
Aphelion	1.0167 AU
Orbit period	365.256 days

Table 2: Earth's orbital parameter in the heliocentric reference system

Now, using these parameters, could be useful to compared the 2008 EV₅'s orbit with the Earth one.

1. Introduction

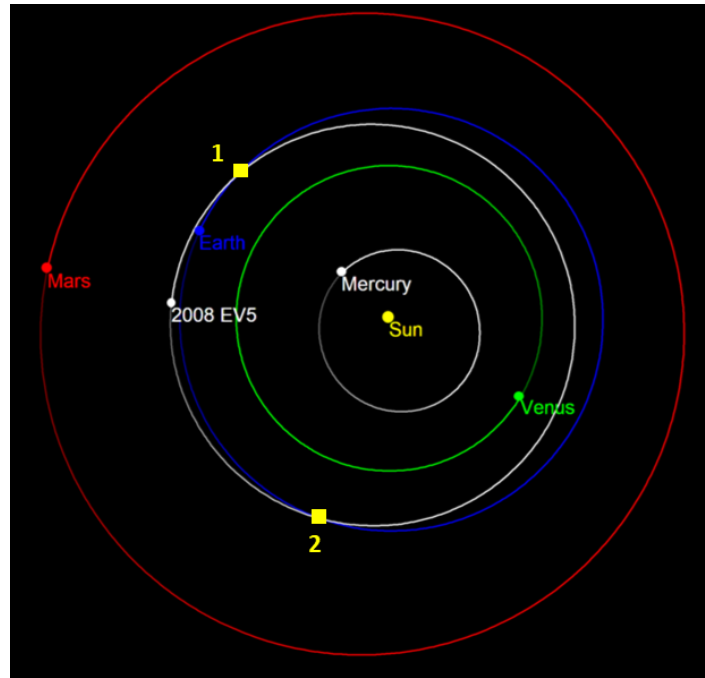


Figure 2: Asteroid 2008 EV₅'s orbit (white) compared with the nearest planets, in the heliocentric reference system

From this figure, and just like previously said about the Athena's asteroids characteristics, it is possible to see how the asteroid's orbit intersects the Earth one in two different points: this represent an important aspect to consider during the trajectories analysis, because this has a high repercussion on the propellant consumption. In fact, a lower propellant consumption will be required if a manoeuvre in the asteroid descending node (point 1) will be achieve, while a higher propellant consumption will be required in the ascending node (point 2).

In addition, a 3D view can be useful in order to see the relative position of each orbit in the heliocentric reference system.

1. Introduction

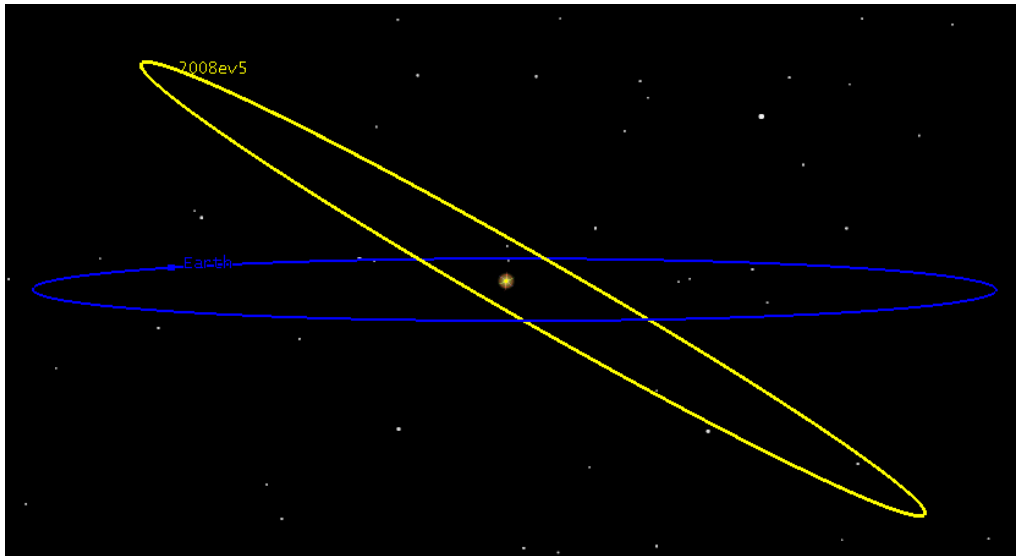


Figure 3: 3D visual of the asteroid and Earth orbit in the heliocentric reference system

At this point, it could be even interesting to report the asteroid dimensions: it is possible to notice how 2008 EV₅ is an oblate spheroid of 400 m in diameter, with a very slow rotation in a retrograde direction; furthermore, it presents a 150 m diameter concave feature, that maybe could be an impact crater or a relic feature from a previous episode of rapid rotation that caused the asteroid's shape to reconfigure. [9]



Figure 4: A 2008 EV₅ representation

1. Introduction

1.3 Interplanetary Trajectories Optimization

In order to perform any interplanetary mission, it is important to adopt a control on one parameter (for example the thrust vector) in order to have an optimal problem that allows to find the optimal control law to maximize or minimize a specified performance index. In fact, for the great propellant consumption influence on the orbital transfers and manoeuvres, it is essential to minimize the required propellant consumption or to maximize the final satellite/vehicle mass, having the initial mass fixed.

In this way, the optimal problem allows to persecute a strategy where the interplanetary mission is achieved with a maximum final mass.

Then, it is possible to affirm that this peculiar procedure allows for an almost mechanical derivation of the boundary conditions, which must be satisfied by an optimal trajectory, depending on the specific constraints of the problem under analysis.

To use this method, there is a problem concerning its utilization: in fact, this method not allow to obtain an analytics solution, because too much simplifications are required; so, the only way to use it, in order to found the optimal solution, it is to solve the problem using approximate solutions or numerical methods. For these numerical methods, three cases could be used: the direct methods, the indirect methods and the evolutionary algorithmic.

The first one transforms the problem into a parameter optimization (nonlinear programming, where the trajectory is discretised) and solve it by means of gradient-based procedures, over to be an approach that requires a tentative solution; the indirect methods use the optimal control theory to transform the optimization problem into a boundary value problem (BVP) solved by means of shooting procedures, while the evolutionary algorithms exploit large populations of solutions which evolve according to specific rules towards the global optimum.

Now, focusing on the indirect methods, it is possible to see as their offer many advantages:

first, they allow for an exact, even though numerical, optimization (in the limits of the adopted dynamical model and integration accuracy); in addition, as far as low-thrust missions are concerned, the computational cost of indirect methods is typically lower compared to direct methods, which require a much larger number of variables for an accurate trajectory description and, in the end, the indirect approach provides useful theoretical information on the problem which is dealt with.

However, alongside the advantages, there are also disadvantages:

for example, some difficult could be available in order to reach the convergence, and this could be possible if a flyby is present, because the trajectory will assumes constrains in the intermediate points (should be even the problem related to thermal or dynamic loads, but in this case, not being in the

1. Introduction

atmosphere, this is not considered); furthermore, it is even possible to have problems caused by the state variables discontinuity, in particular for the terms related at the impulsive manoeuvres, flyby and the disposal of exhausted stages. Another problem could interest the difficult to integrated the values because of the controls discontinuity, in particular for the thrust control (here, the switching function plays an important role).

At the end, it is important to notice that, as the direct methods, the indirect methods require a tentative solution and convergence to the optimum is typically obtained if the tentative solution is sufficiently close to the optimal one.

Nevertheless, the indirect methods allow to assume in advance the structure of the trajectory. In fact, the trajectory is divided into phases called "arcs", where there are homogeneous control laws in each arc, with constraints and discontinuities in correspondence of the arcs extremes. Besides that, it is always possible to check and modify the structure of the trajectory. [10] [11] [12]

The aim of the thesis is to find return trajectories for the asteroid objective of different duration and for different launch windows, in order to explore all the possible opportunities and find among them the most convenient ones. In order to perform this, the indirect methods have been used in order to analysed the trajectories in order to reach the asteroid 2008 EV₅ and to return in a stable orbit around Earth (with a boulder takes from 2008 EV₅).

Chapter 2

2. Optimization of space trajectories with the indirect method

2.1 Introduction

The spacecraft trajectory has a big impact on the feasibility and cost of a space mission, where the minimization of required propellant may be fundamental to deliver a sufficient payload mass and guarantee the mission feasibility, or to allow for a less expensive launcher, and thus reducing costs. Furthermore, even the final mass or payload maximization and propellant mass or flight time minimization are aspects that must be typically dealt during a mission planning. Then, to allow to achieve these aspects, an efficient optimization method is required and, to do this, three different methods could be used.

The first one is the direct method, which it transforms the problem into a parameter optimization (nonlinear programming) and solve it by means of gradient-based procedures; the second one is the indirect method, which uses the optimal control theory to transform the optimization problem into a boundary value problem (BVP) solved by means of shooting procedures; the last includes the evolutionary algorithms, exploit large populations of solutions which evolve according to specific rules towards the global optimum.

2.1.1 Advantages and disadvantages of the indirect methods

Considering the different methods useful to perform a space trajectory optimization, in this thesis only the indirect method will be used, and to better understand this choice, the advantages and disadvantages of this method will be highlighted.

Starting from the advantages, it is possible to see as this method:

- allows to have an exact, even though numerical, optimization (in the limits of the adopted dynamical model and integration accuracy);
- the computational cost of this method is typically lower compared to direct methods, which require a much larger number of variables for an accurate trajectory;
- the indirect approach provides useful theoretical information on the problem which is dealt with.

Unfortunately, just like previously said, this method includes even the following three drawbacks:

2. Optimization of space trajectories with the indirect method

- the necessity of deriving analytic expressions for the necessary conditions, that could become discouraging when dealing with complex problems;
- the convergence region for a shooting algorithm may be quite small, as it is necessary to guess values for adjoint variables that may not have an obvious physical meaning;
- for problems with path inequalities, it is necessary to guess the sequence of constrained and unconstrained sub-arcs.

Nevertheless, exist a way that allows to mitigates the drawbacks of the indirect methods by simply making the position of the problem and the derivation of the optimal conditions more general and easy.

It is even important to notice like the capability of achieving the numerical solution is dependent on the tentative solution which is assumed to start the procedure. However, the simplicity of the theoretical approach permits a fast formulation of a series of optimization problems with increasing difficulty: in fact, the solution of the most complex problem is obtained via the solution of similar but easier problems (just like direct methods).

In the end, a last important aspect to notice is about the two-body problem model, which will be considered in order to find the optimal trajectory.

2.2 Optimal control theory

The indirect approach to optimization uses the optimal control theory (OCT), which is based on calculus of variations and it is adapted at the optimization of space trajectories and to exploit the capabilities of the numerical procedure that has been selected to solve the BVP (boundary values problem) resulting from the OCT application.

Here, it is possible to notice as the system is described by a set of state variables \mathbf{x} , and the differential equations that rule the evolution from the initial to the final state (the external boundaries) are functions of \mathbf{x} , of the control variables \mathbf{u} and the independent variable t (usually, the time). So, it is possible to have the following formulation

$$\frac{d\mathbf{x}}{dt} = \mathbf{f}(\mathbf{x}, \mathbf{u}, t) \quad (1)$$

2. Optimization of space trajectories with the indirect method

Moreover, the trajectory between the initial and final point (the external boundaries) is usefully split into n arcs at the points (internal boundaries), where the state or control variables are discontinuous or constraints are imposed.

The j -th arc starts at $t_{(j-1)+}$ and ends at t_{j-} , where the state variables are $x_{(j-1)+}$ and x_{j-} respectively (j_- and j_+ denote values just before and after point j): in this way, it is possible to take into account the possible discontinuities of the variables (for example, the velocity and the mass are discontinuous after an impulsive manoeuvre) and, in the limits, also of time (for example in the case of flyby around a planet, if the time of stay inside the sphere of influence is not overlooked) that apply to the junction points between the various arches (internal contours). Furthermore, mixed-type boundary conditions may be imposed where these conditions involve the values of the variables of state and of the independent variable time both at the external contours than internal ones.

In general, nonlinear constraints are imposed at both internal and external boundaries, and where these boundary conditions are grouped into a χ vector

$$\chi (x_{(j-1)+}, x_{j-}, t_{(j-1)+}, t_{j-}) = 0 \quad J = 1, \dots, n \quad (2)$$

Additional path constraints may hold along an entire arc; constraints may also concern the control variables \mathbf{u} .

The optimal problem is to look for extremal values (that is maximum or minimum values relative) of a functional which, in its general form, has the following formulation

$$J = \varphi (x_{(j-1)+}, x_{j-}, t_{(j-1)+}, t_{j-}) + \sum_j \int_{t_{(j-1)+}}^{t_{j-}} \phi (\mathbf{x}(t), \mathbf{u}(t), t) dt \quad j = 1, \dots, n \quad (3)$$

Here, it is possible to see like the functional J is the sum of two terms:

the function φ , which depends on the values assumed from variables and time at the boundaries (internal and external) and the integral extended to the entire trajectory of function ϕ , which depends on time and on the values assumed at each point by variables and controls.

In addition, it is possible to notice how with the use of suitable auxiliary variables it is possible to refer to the case $\varphi = 0$ (Lagrange formulation) or $\phi = 0$ (formulation of Mayer, which is preferred).

At this point may be useful to rewrite the functional by introducing the Lagrange multipliers, the μ constants associated with boundary conditions and the λ variables (also called ‘‘added variables’’) associated to the equations of state. Then, doing this, the following formulation has been obtained

2. Optimization of space trajectories with the indirect method

$$J^* = \varphi + \mu^T \chi + \sum_j \int_{t_{(j-1)+}}^{t_{j-}} (\phi + \lambda^T (f - \dot{x})) dt \quad j = 1, \dots, n \quad (4)$$

where the temporal derivative is indicated by the dot “.”.

At this point, it is possible to see that the two functionals J and J^* depend on time t , on state variables \mathbf{x} and their $\dot{\mathbf{x}}$ derivatives (in particular from the values that time and variables assume at the extremes of each arc, t_j and \mathbf{x}_j) and from the \mathbf{u} controls. Obviously, if boundary conditions and state equations are satisfied, the two functional and their extremal values coincide.

Now, by integrating by parts in order to eliminate the dependence on the derivatives of the $\dot{\mathbf{x}}$ variables, it is possible to obtain

$$\begin{aligned} J^* = \varphi + \mu^T \chi + \sum_j (\lambda^T_{(j-1)+} x_{(j-1)+} - \lambda^T_{j-} x_{j-}) + \\ + \sum_j \int_{t_{(j-1)+}}^{t_{j-}} (\phi + \lambda^T f - \dot{\lambda}^T x) dt \quad j = 1, \dots, n \end{aligned} \quad (5)$$

and differentiating it is possible to get the variation before the δJ^* functional itself (in this case, the matrix is indicated by the square brackets)

$$\begin{aligned} \delta J^* = \left(-H_{(j-1)+} + \frac{\partial \varphi}{\partial t_{(j-1)+}} + \mu^T \frac{\partial \chi}{\partial t_{(j-1)+}} \right) \delta t_{(j-1)+} + \\ + \left(H_{j-} + \frac{\partial \varphi}{\partial t_{j-}} + \mu^T \frac{\partial \chi}{\partial t_{j-}} \right) \delta t_{j-} + \left(\lambda^T_{(j-1)+} + \frac{\partial \varphi}{\partial x_{(j-1)+}} + \mu^T \left[\frac{\partial \chi}{\partial x_{(j-1)+}} \right] \right) \delta x_{(j-1)+} + \\ + \left(-\lambda^T_{j-} + \frac{\partial \varphi}{\partial x_{j-}} + \mu^T \left[\frac{\partial \chi}{\partial x_{j-}} \right] \right) \delta x_{j-} + \sum_j \int_{t_{(j-1)+}}^{t_{j-}} \left(\left(\frac{\partial H}{\partial x} + \dot{\lambda}^T \right) \delta x + \frac{\partial H}{\partial x} \delta u \right) dt \quad j = 1, \dots, n \end{aligned} \quad (6)$$

and so, the system Hamiltonian has been defined as

$$H = \phi + \lambda^T f \quad (7)$$

The (necessary) condition of optimum prescribes the stationarity of the functional and therefore the cancellation of its first variation for any choice of δx , δu , $\delta x_{(j-1)+}$, δx_{j-} , $\delta t_{(j-1)+}$, δt_{j-} variations, compatible with differential equations and boundary conditions.

2. Optimization of space trajectories with the indirect method

The introduction of additive variables and constant allows, with an appropriate choice, to cancel the coefficient of each variations in the expression at the same time (6), so to ensuring the stationarity of the functional expressed by the condition $\delta J^* = 0$.

Now, in order to obtain the Euler-Lagrange differential equations for the added variables, the δx and δu coefficients inside the integral should be cancelling for each point of the trajectory. Then

$$\frac{d\lambda}{dt} = - \left(\frac{\partial H}{\partial x} \right)^T \quad (8)$$

and the algebraic equations for the controls appear as

$$\left(\frac{\partial H}{\partial u} \right)^T = 0 \quad (9)$$

By this, it is interesting to note how the control laws are formally independent from the search of maximum or minimum values of J .

In addition, particular attention must be paid if one of the checks is subject to a constraint, because this must belong to a given admissibility domain (for example, the thrust value must be between the minimum value 0 and the maximum value T_{max}); furthermore, the cases where the constraint depends on the time or the state variables are not considered, while those are where it is explicit and constant.

In the presence of a such constraint, the optimal value of the control at each point of the trajectory is that which, belonging to the eligibility domain, it makes maximum, if the maximum values of J are investigating, or minimum, if the minima are investigating, the Hamiltonian (7) at that point (here all is on Pontryagin's Maximus Principle based, which is used to find the best possible control for taking a dynamical system from one state to another, especially in the presence of constraints for the state or input controls, so that the control Hamiltonian take an extreme value over controls in the set of all permissible controls).

In this way, basically two possibilities are available:

- the optimal value of the control is given by equation (9), if it falls within the eligibility domain and therefore the constraint does not intervene at that point (locally "not bound" control);
- the optimal value is at the ends of the domain, that is the control assumes the maximum value or minimum, if the one provided by equation (9) does not fall within the eligibility domain ("bound" control).

2. Optimization of space trajectories with the indirect method

A particular case is available if the Hamiltonian H is linear with respect to one of the controls subject to constraints, as in equation (9), where the control does not appear explicitly and can therefore not be determined. In this case, there are still two possibilities (refers to the case where J should be maximized):

- if in the equation (7) the coefficient of the control in question is not null, then H is maximized for the maximum control value if the coefficient is positive and minimum if it is negative (bang-bang control), in accordance with the Pontryagin's Maximus Principle;
- if in the equation (7) the coefficient of the control in question is identically zero during a finite interval of time (singular arc), then it is necessary to impose the cancellation of all subsequent derivatives of the coefficient with respect to time, up when in one of them there is no explicit control: the optimal control it is then determined by setting the latter derivative equal to zero.

Here, for the missing boundary conditions, it is convenient to refer to the j -th boundary, writing for this the conditions that derive from considering it as extreme final of $(j - 1)$ -th sub-interval or as initial extreme of the j -th sub-interval; in this way, cancelling in order the coefficients of $\delta x_{j-}, \delta x_{j+}, \delta t_{j-}, \delta t_{j+}$ (these values must be cancelling in this order) in the expression (6), it is possible to obtain:

$$-\lambda^T_{j-} + \frac{\partial \varphi}{\partial x_{j-}} + \mu^T \left[\frac{\partial \chi}{\partial x_{j-}} \right] = 0 \quad j = 1, \dots, n \quad (10)$$

$$\lambda^T_{j+} + \frac{\partial \varphi}{\partial x_{j+}} + \mu^T \left[\frac{\partial \chi}{\partial x_{j+}} \right] = 0 \quad j = 1, \dots, n - 1 \quad (11)$$

$$H_{j-} + \frac{\partial \varphi}{\partial t_{j-}} + \mu^T \frac{\partial \chi}{\partial t_{j-}} = 0 \quad j = 1, \dots, n \quad (12)$$

$$-H_{j+} + \frac{\partial \varphi}{\partial t_{j+}} + \mu^T \frac{\partial \chi}{\partial t_{j+}} = 0 \quad j = 1, \dots, n - 1 \quad (13)$$

where the subscripts j_- and j_+ indicate the values assumed respectively immediately before and after the point j (it is necessary to distinguish as they may occur, as said, discontinuity in junction points between sub-intervals). The equations (10) and (12) have no meaning at the beginning of the trajectory ($j = 0$), while equations (11) and (13) do not have them term ($j = n$).

2. Optimization of space trajectories with the indirect method

By that, eliminating the additional constants μ from equations (10) ÷ (13), the optimal boundary conditions have been obtained

$$\sigma (x_{(j-1)+}, x_{j-}, \lambda_{(j-1)+}, \lambda_{j-}, t_{(j-1)+}, t_{j-}) = 0 \quad (14)$$

which, with the assigned conditions (2), they complete the differential system given by the equations (1) and (8).

Now, considering a generic state variable \mathbf{x} , if it is subjected to particular conditions at the boundary, equations (10) and (11) provide particular conditions of optimum for the corresponding additional λ_x variable:

- if the \mathbf{x} status variable is explicitly assigned to the initial instant (the vector of the χ conditions imposed contains the equation $x_0 - a = 0$ with an assigned value), on the corresponding added variable there are no conditions ("free" λ_{x_0}); the similar situation occurs at the end time if the variable is there assigned;
- if the initial value of the x_0 state variable does not appear in the φ function and even not in the boundary conditions, the corresponding added variable is nothing at initial time ($\lambda_{x_0} = 0$); even in this case where these considerations are extended to a similar situation at the final time;
- if a status variable is continuous and not assigned to the i internal point (where the equation $x_{j+} = x_{j-}$ is contained by χ), the corresponding added variable is also continuous ($\lambda_{x_{j+}} = \lambda_{x_{j-}}$);
- if a status variable is continued and explicitly assigned to an internal contour (χ contains the equations $x_{j+} = x_{j-} = a$), the corresponding variable added has a "free" discontinuity, that is the value of $\lambda_{x_{j+}}$ and it is independent by $\lambda_{x_{j-}}$ and must be determined by the optimization procedure.

Similarly, if H does not explicitly depend on time, equations (12) and (13) also they provide, in some cases, particular boundary conditions:

- if the initial t_0 time does not explicitly appear in the boundary conditions and even not in the φ function, the Hamiltonian is null at the initial instant ($H_0 = 0$); similarly, the Hamiltonian is annulled at the final time if this does not explicitly intervene in χ and φ .

2. Optimization of space trajectories with the indirect method

- if the intermediate t_j time does not appear explicitly in the φ function (the only one condition in χ which involves the continuity of time $t_{j+} = t_{j-}$) the Hamiltonian is in j continuous ($H_{j+} = H_{j-}$);
- if the t_j time is explicitly assigned, (in χ the equations appear $t_{j+} = t_{j-} = a$) the Hamiltonian has at that point a "free" discontinuity.

2.3 Differential problem to limits

The indirect method adopted for the optimization of orbital transfers provides the application of the theory of optimal control to the system of equations (1), which has boundary conditions depending on the type of orbits between which the transfer takes place. The optimal control theory formulates a new system of differential equations (BVP) in which some of the initial values of the variables are unknown. The solution to this problem consists in finding which initial values allow, by numerically integrating the differential system, to satisfy all the boundary conditions, both imposed and optimal.

2.3.1 Boundary values problem (BVP) resolution method

In this paragraph, the BVP resolution method and how the optimal problem comes formulated to adapt to its characteristics will be described.

As seen in the previous chapter, the optimal control theory formulates the optimal problem as a mathematical problem subject to differential and algebraic constraints. Since some initial values of the state variables and additions are unknown, the optimal problem results in a differential problem at the limits (BVP), with the differential equations (1) and (8), in which the controls are determined by the algebraic equations (9), supported from the imposed boundary conditions (2) and excellent conditions (14). It is important to notice as the problem presents some features:

- the integration interval is subdivided into sub-intervals, where the differential equations could have different expression;
- the duration of each sub-interval is generally unknown;

2. Optimization of space trajectories with the indirect method

- the boundary conditions may be non-linear and involve the values of the variables both external and internal contours;
- the variables could be discontinuous to the internal contours and their value after the discontinuity could be unknown.

The main difficulty of the indirect optimization techniques is the solution of the problem to the limits that emerge from their application: the method, for its solution, is an indispensable tool and the correspondence between its characteristics and those of the problem under consideration. The BVP solution is obtained by reducing it to a succession of problems at the initial values, which is brought to convergence according to the Newton method.

In order to resolve the indefiniteness of each sub-interval duration, the independent variable t has been substituted with a new ε variable defined in the j -th sub-interval, so to allow integration.

By this, the following relation has been obtained:

$$\varepsilon = j - 1 + \frac{t - t_{j-1}}{t_j - t_{j-1}} = j - 1 + \frac{t - t_{j-1}}{\tau_j} \quad (15)$$

where τ_j is the duration (usually unknown) of the sub-interval.

In this way, the internal and external contours are fixed, thanks to the introduction of the τ_j unknown parameters and correspond to consecutive whole values of the new independent variable ε .

To describe the method, the generic equations system given by (1) and (8) has been considered, in which the expressions (9) have been substituted for the controls. There is therefore a differential problem in the state and additions variables $\mathbf{y} = (\mathbf{x}, \boldsymbol{\lambda})$:

$$\frac{d\mathbf{y}}{dt} = f^*(\mathbf{y}, t) \quad (16)$$

It is necessary to keep in mind that also constant parameters appear in the problem under examination, such as the durations of the τ_j sub-intervals or the variables values after one discontinuity: it is therefore useful to refer to a new vector $\mathbf{z} = (\mathbf{y}, \mathbf{c})$, which contains the status and additions variables and the new \mathbf{c} vector of the constant parameters.

At this point, applying the change of independent variable, the differential equations system takes the following formulation

$$\frac{d\mathbf{z}}{d\varepsilon} = f(\mathbf{z}, \varepsilon) \quad (17)$$

2. Optimization of space trajectories with the indirect method

By explicating the second member of the equations (17), for the state and additions variables, it is possible to have:

$$\frac{dy}{d\varepsilon} = \tau_j \frac{dy}{dt} \quad (18)$$

while for the constant parameters

$$\frac{dc}{d\varepsilon} = 0 \quad (19)$$

The boundary conditions are generically expressed, without distinguishing between imposed and optimal conditions, such as

$$\psi (s) = 0 \quad (20)$$

where s is a vector that contains the values that the variables assume at each contour (internal or external) $\varepsilon = 0, 1, \dots, n$, and the unknown parameters.

$$s = (y_0, y_1, \dots, y_n, c) \quad (21)$$

The initial values of some variables are usually unknown, and the search must allow to determining, through an iterative process, which values must be assumed in order to satisfy the equations (20).

The procedure will be described assuming that none of the initial values is known.

The r -th iteration begins with the integration of equations (17) with the initial p^r values found at the end of the previous iteration, so to fix

$$z (0) = p^r \quad (22)$$

Made this, the next step is to proceed to the integrate the equations along the entire trajectory, taking into account any discontinuities to the internal contours (to start the procedure, at the first iteration it is necessary to choose attempt values p^1). In each contour the state variables value is determined and at the end of the integration the error is calculated on the boundary conditions ψ^r to the r -th iteration.

A Δp variation leads to varying the error on the boundary conditions of a quantity that, taking into account only the terms of the first order, is equal to

$$\Delta\psi = \left[\frac{\partial\psi}{\partial p} \right] \Delta p \quad (23)$$

2. Optimization of space trajectories with the indirect method

Having to cancel the error on the boundary conditions, so to get $\psi = -\psi^r$, at each iteration the initial values are corrected by a quantity

$$\Delta p = p^{r+1} - p^r = - \left[\frac{\partial \psi}{\partial p} \right]^{-1} \psi^r \quad (24)$$

until the boundary conditions (20) are verified with the desired precision.

The matrix that appears in equation (24) is calculated as a product of two matrices:

$$\left[\frac{\partial \psi}{\partial p} \right] = \left[\frac{\partial \psi}{\partial s} \right] \left[\frac{\partial s}{\partial p} \right] \quad (25)$$

where the former can be immediately obtained by deriving the boundary conditions with respect to the quantities that appear. The second matrix contains the derivatives values of the variables to the contours with respect to the initial values, that are the values that are assumed to the contours ε ($= 0, 1, \dots, n$) from the matrix

$$\left[\frac{\partial z}{\partial p} \right] = [g(\varepsilon)] \quad (26)$$

and it is obtained by integrating the differential equation system obtained by deriving the main system (17) with respect to each of the initial values:

$$[\dot{g}] = \frac{d}{d\varepsilon} \left[\frac{\partial z}{\partial p} \right] = \left[\frac{\partial}{\partial p} \left(\frac{dz}{d\varepsilon} \right) \right] = \left[\frac{\partial f}{\partial p} \right] \quad (27)$$

where the dot “.” indicates the derivative with respect to the new independent ε variable.

Now, explicating the Jacobian of the principal system (17), equation (27) takes the following form

$$[\dot{g}] = \left[\frac{\partial f}{\partial z} \right] \left[\frac{\partial z}{\partial p} \right] = \left[\frac{\partial f}{\partial z} \right] [g] \quad (28)$$

A particularity about the application of this method to indirect optimization problems are the symmetry properties of some Jacobian terms.

The initial values for homogeneous system (28) are derived from the relation (22); thus, the identical matrix is obtained

$$[g(0)] = \left[\frac{\partial z(0)}{\partial p} \right] = [I] \quad (29)$$

2. Optimization of space trajectories with the indirect method

It should be noted that this method also allows discontinuities in the variables to be treated.

In fact, for a discontinuity in the i point, it is sufficient to update both the vector of z variables that the g matrix through the relation h , that binds the variables values before and after the discontinuity

$$z_{i+} = h(z_{i-}) \quad (30)$$

$$[g_{i+}] = \left[\frac{\partial h}{\partial z} \right] [g_{i-}] \quad (31)$$

(for this reason, defining the s vector it is not distinct between the vectors y_{i+} and y_{i-} , in as the one known function, through h , of the other and of the c vector).

Obviously, if some of the initial values variables are known, the problem results simplified since the vector p is reduced to the unknown components of $z(0)$ estimation and the ψ vector only to not explicit conditions at the initial time.

In addition, the matrix that appears in equation (24) can also be evaluated numerically:

its i -th row is obtained by varying the i -th p component of a small Δp quantity (keeping the others fixed) and then integrating the equations (17).

Done this, it is possible to calculate the variation of the boundary conditions $\Delta\psi$ (Δp) and, by linearizing, get the corresponding line as $\Delta\psi^T / \Delta p$.

This procedure allows, in some cases, to obtain a simpler and rapid solution of BVP (values suitable for Δp , found empirically, are of the order of $10^{-6} - 10^{-7}$) but it is not always able to guarantee the convergence: the determination of the matrix in equation (24) is, in fact, less accurate than its calculation through the solution of the system (28) and, given the great sensitivity of the problem, the numerical approximations introduced could compromise the convergence.

A similar numerical procedure can also be used for the calculation of the Jacobian and the matrix $\left[\frac{\partial\psi}{\partial s} \right]$: it is therefore preferred to maintain the analytical evaluation and use, in the code setting, the values obtained numerically for verify, through comparison with those provided by the analytical expressions of the Jacobian and the matrix $\left[\frac{\partial\psi}{\partial s} \right]$, the accuracy of these expressions.

The integration of all differential equations, both for the main system (17) and for the homogeneous one (28), it is performed with a variable pitch and order method based on the Adams' formulas (a linear multistep method used for the numerical solution of ordinary differential equations).

2. Optimization of space trajectories with the indirect method

For example, if the required accuracy is equal to 10^{-7} , it is required that the maximum error $E_{max} = \max_i (\psi_i)$ on the boundary conditions is lower than this value.

The introduced linearization for the calculation of the Δp correction given by the equation (24), to be made to the initial values of the attempt, introduces errors that can compromise the convergence by increasing rather than decreasing the error on the boundary conditions and to improve the procedure, some tricks have been used:

- to avoid getting too far from the solution, the correction made is actually a fraction of the determined one, that is

$$p^{r+1} = p^r + K_1 \Delta p \quad (32)$$

with $K_1 = 0.1 \div 1$, values determined empirically during the first tests of the codes, depending on whether the starting solution is relatively distant or close to the one searched.

- at each iteration, after that the new vector of the initial attempt values p^{r+1} has been determined through the (32) and the motion equations have been integrated, the maximum error on the E_{max}^{r+1} boundary conditions is compared with the one obtained to the previous E_{max}^r iteration: if the maximum error is less than a multiple of the previous one, that is, if $E_{max}^{r+1} < K_2 E_{max}^r$, proceed with the new iteration. In order to converge to the solution, the error on the boundary conditions could, in the first iterations, increase, the K_2 value must be higher than the unit: so, a $K_2 = 2 \div 3$ value guarantees good results.
- if, on the other hand, the error at the new iteration is too large compared to the previous one, the bisection of the correction made will be apply, halving it: in this way, these equations of motion are integrated with the attempt values:

$$p^{r+1} = p^r + K_1 \Delta p / 2 \quad (33)$$

thus, repeating the comparison between the new maximum error obtained and that of the previous iteration and, if necessary, repeating the bisection. A maximum number of 5 bisections is set, after which the procedure stops, meaning that the chosen attempt solution is not able to lead to convergence.

2. Optimization of space trajectories with the indirect method

2.4 Optimization of space trajectories

The preliminary analysis of spacecraft trajectories is typically carried out assuming a point mass spacecraft under the influence of a single body, nevertheless, the two-body model can also be used to deal with interplanetary trajectories, as the patched-conic approximation that is usually employed in the initial analyses. An efficient approach only analyses the heliocentric legs; at the patch points with the planetocentric legs, suitable boundary conditions take the manoeuvres inside the planets' spheres of influence into account.

In the following pages, the formulation of the trajectory optimization in the two-body problem will give, making particular reference to the heliocentric legs of an interplanetary trajectory, due to the peculiarity of the relevant boundary conditions.

The state of the spacecraft is described by position r , velocity v , and mass m and the state equations are the following

$$\frac{dr}{dt} = v \quad (34)$$

$$\frac{dv}{dt} = g + \frac{T}{m} \quad (35)$$

$$\frac{dm}{dt} = -\frac{T}{c} \quad (36)$$

where T is the engine thrust and g is the gravitational acceleration, while the propellant mass-flow rate is expressed by the ratio of the thrust magnitude to the constant effective exhaust velocity c .

Furthermore, it is even possible to see the Hamiltonian, defined by equation (7)

$$H = \lambda_r^T v + \lambda_r^T \left(g + \frac{T}{m} \right) - \lambda_m \frac{T}{c} \quad (37)$$

and the Euler–Lagrange equations for the adjoint variables, equation (8), provide

$$\left[\frac{d\lambda_r}{dt} \right]^T = -\lambda_r^T \left[\frac{\partial g}{\partial r} \right] \quad (38)$$

$$\left[\frac{d\lambda_v}{dt} \right]^T = -\lambda_r^T \quad (39)$$

2. Optimization of space trajectories with the indirect method

$$\frac{d\lambda_m}{dt} = \frac{\lambda_v T}{m^2}$$

where the gravity-gradient matrix appears in equation (38).

Equations (34) – (36) and (38) – (39) constitute the system of differential equations, which is integrated numerically.

The thrust direction and its magnitude are typically the control variables, which must maximize H in agreement with PMP. The optimal thrust direction is therefore parallel to the velocity adjoint vector λ_v , which is named primer vector.

In addition, the switching function

$$S_F = \frac{\lambda_v}{m} - \frac{\lambda_m}{c} \quad (41)$$

has been introduced so to be possible to rewritten the equation (37) as

$$H = \lambda_r^T v + \lambda_r^T g + T S_F \quad (42)$$

The thrust magnitude assumes its maximum value when the switching function S_F is positive, whereas it is set to zero when S_F is negative, again to maximize the Hamiltonian.

Singular arcs occur when S_F remains zero during a finite time; the equation (42) is not sufficient to decide the optimal thrust magnitude (singular arcs are here excluded and, in addition, they may be required during atmospheric flight).

To improve the numerical accuracy, the trajectory is split into maximum-thrust arcs and coast arcs.

The number and order of the arcs, i.e., the trajectory switching structure, are assigned a priori, and the arc time-lengths are additional unknowns. The boundary conditions for optimality state that the switching function S_F must be null at the extremities of each thrust arc.

The numerical procedure provides the optimal solution that corresponds to the assigned switching structure.

This solution is then checked in the light of PMP, by means of an analysis of the switching function; if PMP is violated, coast or propelled arcs are inserted or removed, in accordance with the behaviour of S_F , to obtain an improved solution (e.g., a coast arc is introduced when S_F becomes negative during a propelled arc).

Suitable boundary conditions define the mission and here the reference is made to interplanetary trajectories: a similar (and usually simpler) analysis can be carried out for different cases (for example, orbital manoeuvres of an Earth satellite).

2. Optimization of space trajectories with the indirect method

At the exit from Earth's sphere of influence, spacecraft and Earth positions coincide (to notice that the influence sphere's dimension can be neglected) and the mass is typically a function of the hyperbolic excess velocity $v_{\infty 0} = v_0 - v_E(t_0)$, where subscript E refers to the Earth.

The boundary conditions at the initial point (subscript 0) are

$$r_0 = r_E(t_0) \quad (43)$$

$$m_0 = f(v_{\infty 0}) \quad (44)$$

The arrival at the target body with zero-hyperbolic excess velocity is here considered, as it appears to be the most general end condition, corresponding to the rendezvous with an asteroid or to the minimum-energy approach to a planet.

The relevant boundary conditions at the final point (subscript n) are therefore

$$r_n = r_T(t_n) \quad (45)$$

$$v_n = v_T(t_n) \quad (46)$$

where subscript T denotes the target body.

The final mass m_n is the performance index which is maximized.

In some cases, the spacecraft would fly too close to the planet surface, where a constraint on the periapsis height might be required. In this occurrence, an additional condition on the velocity turn arises

$$v_{\infty g+}^T v_{\infty g-} = -\cos 2\phi v_{\infty g-}^2 \quad (47)$$

where $\cos \phi = \frac{V_p^2}{v_{\infty g-}^2 + V_p^2}$, with $V_p = \sqrt{\mu_p/R_p}$ being the circular velocity at the minimum allowable distance from the planet surface.

To improve the convergence, the trajectories are first optimized by introducing additional degrees of freedom and letting the relevant bodies assume the best phasing with the Earth. The corresponding trajectories, which define the most favourable positions of the target planets at encounter, could be flown every year departing on the same day.

The positions of the planets on the encounter day of each year in the launch window are then compared to the optimal-phasing positions; favourable opportunities occur when differences are small. [10] [11] [12] [13] [14] [15]

2. Optimization of space trajectories with the indirect method

Wanting to sum up, it is possible to see as the indirect method's procedure is a powerful means to deal with the optimization of spacecraft trajectories. The necessary conditions for optimality are easily obtained even for complex problems. This has permitted the extension of the indirect approach to problems that were usually left to direct methods. When the problem is formulated in a convenient way, for instance by following the guidelines provided here, extremely accurate solutions can be obtained with very short computation times. Robustness is typically an issue when indirect methods are adopted; however, tentative solutions which allow for convergence can be built by properly splitting the trajectory in elementary legs (optimized separately), or by employing continuation techniques, or, finally, by exploiting periodicities in the motion of the relevant bodies and building on existing solutions.

2.5 Electric propulsion

In order to achieve the mission, a Hall effect thruster will be used, this because the electric propulsion (EP) can boost the performance of interplanetary missions due to the low propellant consumption in comparison to chemical propulsion.

It is important to notice how the missions could be performed using one or more thrusters, and so a problem of power partitioning among the thrusters exist and where the propellant gains can be obtained with an optimal power splitting. Nevertheless, in this thesis, the power partitioning will be not considered, but a little consideration is available in the programming code: in fact, the thrust magnitude and propellant mass flow rate of a thruster are related to its input power and, as a consequence, the effective exhaust velocity is also a function of the input power.

Then cubic relations have been assumed for T and q

$$T = a_0 + a_1P + a_2P^2 + a_3P^3 \quad (48)$$

$$q = b_0 + b_1P + b_2P^2 + b_3P^3 \quad (49)$$

In addition, many EP systems could present the capability of varying specific impulse and thrust magnitude at constant thrust power. High thrust and low specific impulse are used where the thrust can be favourably exploited to reduce the trip time. Where the thrust is less useful, a large specific impulse is adopted to reduce the propellant consumption.

Furthermore, the engine could operate using a fraction of the available power, and one has $T = 2P/c$ with $0 \leq P \leq P_a$. Then, the Hamiltonian could be rewritten as

$$H = \lambda_r^T v + \lambda_r^T g + \left(\frac{\lambda_v}{m} - \frac{\lambda_m}{c} \right) 2 \frac{P}{c} \quad (50)$$

2. Optimization of space trajectories with the indirect method

where the optimal specific impulse is first determined.

Now, by nullifying $\partial H / \partial c$

$$c_{opt} = 2 \frac{m \lambda_m}{\lambda_v} \quad (51)$$

Here, it is possible to see as the Hamiltonian linearly depends on P and a bang-bang control arises and if the specific impulse is unbounded, the engine can operate with $c = c_{opt}$. In addition, it is possible to find that the power coefficient in the Hamiltonian is always positive and the thruster is always on at maximum power ($P = P_a$). On the contrary, in the presence of bounds on the attainable values of c , variable between c_{min} and c_{max} , coast arcs may be required depending on the sign of the power switching function

$$S_P = \frac{\lambda_v}{m} - \frac{\lambda_m}{c_{max}} \quad (52)$$

It is even important to notice as these considerations hold even for solar electric power (SEP) systems, where the available power depends on the distance between Satellite (and even the solar arrays inclination) and Sun. [11]

Chapter 3

3. Fortran code to find and analyse the trajectories

3.1 Introduction

At this point of the discussion, after the description of the methodology underlying the problem (where even astrodynamics' equations have been implemented, not considering the atmosphere effects), it is possible to describe how the FORTRAN code works. [16]

The implemented FORTRAN code allows to analyse the various trajectories based on the received inputs, which are read by the program in order to give the trajectory for the required case from the input values. To note how the developed code allows to analyse any asteroid / case simply changed the input values.

Another important aspect to note is that, for the going and return trip, two different codes (ARM1 for the going trip and ARM2 for the return trip) has been compiled (but the methodology is the same), where the first considers a direct mission from Earth to asteroid, while the second one considers a trip from asteroid to Earth but with even a flyby (necessary to reach the final orbit around the Earth); by this, is clear to note as two different input values will be required.

3.2 ARM1v0

Just like previous said, the methodology described in the previous chapter has been used and implemented in the ARM1v0 code, where the initial velocity v_0 has been set as fixed (this is the reason because v_0 appeared in the code name after ARM1).

Then, one time that the code has been implemented, the input values has been used to found and analyse the different trajectories for this case.

In particular, the values that appeared in the input code are attempt values, which came from previous study and / or cases about the asteroid 2008 EV₅.

This has been done for two reasons:

1. the orbital parameters available in the input code are, both for the Earth and for the asteroid, always the same. All this is true in most cases, but some changes are necessary if you need to analyse the trajectories in different time intervals (this it will be explained shortly);

3. Fortran code to find and analyse the trajectories

2. these codes are used only as a starting point, this because the program is able to calculate the new correct values for the case in question.

Now, wanting to start from the beginning, it is possible to see how the (default) input code (for the direct mission case) assumes the following compilation

```

          1          4          4          4          4          4
          4          4          4          4          4          4
          4          4          4          4          4          4
141.136070562914      148.514529387352      -5.722968078190543E-002
  0.00
4.364658218747921E-002  1.01600517904995      10.9435867356728
4.852208294033913E-005  4.254573453187422E-004      1.00036337289207
-4.028952039142544E-002  0.441697045729119      0.134538513272825
-0.150716260529239      0.584179851769581      -1.44781573915660
  1.000000000000000
mf (kg)=  0.859942131374788
Dt =    7.37845882443787
Dt (days)=  428.927821301569
Vinf (km/s)=  1.30000699075990

```

Figure 5: Default input values for the ARMIv0 code

It is possible to see as the first three rows are made by 18 sequential numbers, that could go from 0 to 4, and which have the following meaning:

- if the number 0 appeared, this mean that the satellite is in a *coasting phase*, where the thruster is turn off ($T = 0$);
- if the number 1 appeared, this mean that the satellite is in a *propulsive g phase*; here, it is possible to see that if $S_F > 0$, the thruster is turn on ($T \neq 0$), while if $S_F < 0$, the thruster is turn off ($T = 0$);
- if the number 2 or 3 appeared, this mean that a flyby is required; in this case, the flyby is not required, but it is possible to note how the number 2 allows to have a flyby at free height, while the number 3 to have a flyby at constrained height;
- if the number 4 appeared, the code ignores this phase because there is a phase.

In this particular case, it is possible to see as only a number 1 appeared: this mean that the code must find the solution only for a direct trajectory from Earth to asteroid.

3. Fortran code to find and analyse the trajectories

Furthermore, it is possible to explain the remaining 17 numbers, which represent the unknown values of the problem (these values are the constant parameters and the initial unknown values provided by the previous studies). In order, these values are:

$$t_0 \quad t_1 \quad \lambda_{\vartheta_{01}} \quad t^* \quad v_{\infty 0} \quad r_0 \quad \vartheta_0 \quad \varphi_0 \quad u_0 \quad v_0 \quad w_0 \quad \lambda_{r_0} \quad \lambda_{\varphi_0} \quad \lambda_{u_0} \quad \lambda_{v_0} \quad \lambda_{w_0} \quad m_0$$

where t_0 and t_1 are the departure and arrival date, $\lambda_{\vartheta_{01}}$ takes into account the location of the Earth based on the day considered, t^* is the optimal time to perform the mission (in these cases has been set to be null because this value will be found during the analysis), while the others data are the initial values referred at the satellite position, as its velocity, acceleration and initial mass.

The final values that include mf, Dt, Dt (days) and vinf will be not explain because this are output values; in fact, the FORTRAN program reads the input values and then prints the results in the same input values code.

At this point, it is important to notice two aspects.

The first one is that the default t_0 and t_1 times will be used to analyse only the first case (and its “subcase” at different durations), while, for subsequent cases these values will be increased or decreased, in accord to find the trajectory solution for different years and months.

The second one is about the w_0 , λ_{w_0} , λ_{φ_0} and ϑ_0 values, which could be modified according to the node from which the satellite will start (this will be better explained in the "Results" chapter).

In this way, everything about the input values that will be used by the program has been said; then, it is possible to talk about how the code will work.

The FORTRAN program will read the input values and then, by user input, some additional values could be provided. In particular, the code will require the iteration interval values so to use them to reach the convergence, the duration (dimensionless) and the escape velocity.

The iteration interval values are required because, it is possible that, for the default interval values, the program could not be able to reach the convergence. In this case, in fact, these values could be reduced so to try to achieve the convergence (the convergence is reached when all 17 unknown values reached a value at least of 10^{-6}).

The duration user input is required in order to find the trajectory solution for different times. In fact, during the first run, a duration value of 0 will be imposed in order to find the optimal case for the trip

3. Fortran code to find and analyse the trajectories

time imposed in t_0 and t_1 . Subsequently, the runs will be evaluated starting by the nearest duration value that allows to have the convergence until a duration value around 20, in order to have different solutions for the same departure date (in fact, increasing the duration value, the departure date will be approximately the same (it could change a few days) while the arrival date will increase).

For the escape velocity user input, a value will be imposed and this same value will be used for all these analysis, in order to be able to analyse every trajectory so to find the best one.

In this way, for every time and for each duration, it will be possible to find the data about each trajectory from Earth to asteroid.

3.3 ARM2vf

For the return trip, the same method used for the going trip has been adopted, but with just a little consideration. In this case, in fact, the mission requires a flyby around the Earth, in order to allow, to the satellite, to reach a stable orbit around the Earth so to leave the boulder that will be taken by asteroid 2008ev5.

In addition, the FORTRAN code is a little different because, in this case, it has been imposed that the final velocity, that is the velocity which the satellite will arrive in the stable orbit around the Earth, is imposed (for this reason in the code name appeared vf after ARM2).

By these considerations, the (default) input values will include even the flyby, and it is possible to see how the input values appeared

```

          1          2          1          4          4          4
          4          4          4          4          4          4
          4          4          4          4          4          4
149.972170514062      156.942583208604      -6.840881939255349E-002
164.448167572196      1.416156053984300E-002
  0.00
  0.115369767303375      0.996594259371727      4.893758489903172E-006
-0.177819939156362      6.954117070617290E-008      -1.07374015032439
  0.180180110754843      8.847646298755199E-007      -6.492064524413279E-023
  0.937738284308750      13.4115322114909      -9.194177644693673E-002
  8.417254743371960E-002      1.03590826261240      9.530889117956413E-002
  1.01540240654099      0.733850399834630      -0.325159082146237
  0.895718405619162      -0.626839152053041      1.000000000000000
mf (kg)=  0.901071727065775
Dt =  14.4759970581340
Dt (days)=  841.525042973510
Vinff (km/s)=  0.700003760575483
```

Figure 6: Default input values for the ARM2vf code

3. Fortran code to find and analyse the trajectories

It is possible to see like the satellite will leave the asteroid, then will perform a flyby and then will follow a trajectory that will put it in the final orbit around the Earth (from the numerical sequence 1-2-1). Here, it is important to notice like the flyby value has been imposed to be 2, this because a flyby at free height is preferred. However, in the FORTRAN program there is a check that, in the case that the flyby will be too short, will recommend to change the value from 2 to 3 (however, this “problem” could be solved changing the iteration interval that will be imposed by the user, just like the `amr1v0` code).

So, from this new code, it is possible to see like the unknown values will be no more 17 but 27; in particular

$$t_0 \quad t_1 \quad \lambda_{\vartheta_{01}} \quad t_3 \quad \lambda_{\vartheta_{23}} \quad t^* \quad u_2 \quad v_2 \quad w_2 \quad \lambda_{r_2} \quad \lambda_{\varphi_2} \quad \lambda_{u_2} \quad \lambda_{v_2} \quad \lambda_{w_2} \quad v_{\infty 0}$$
$$r_0 \quad \vartheta_0 \quad \varphi_0 \quad u_0 \quad v_0 \quad w_0 \quad \lambda_{r_0} \quad \lambda_{\varphi_0} \quad \lambda_{u_0} \quad \lambda_{v_0} \quad \lambda_{w_0} \quad m_0$$

and, even for this case, the explanation is the same for the going trip, with the addition of the time, position and velocity values after the flyby.

To note as this code runs just like the previous one, even if there are small differences.

In fact, the code required, as user input, to insert the iteration values, the duration value, the initial mass and the final velocity. But in case, while for the iteration values the approach is the same to the `amr1v0` code, here it is possible that a problem about the initial mass value exists.

In fact, in this case, it is possible that a determined initial mass value could be reach the convergence for some duration but could not converge for the next one. In this case, if this problem appears, will be necessary to check the switching function value to understand if there is a problem about the thruster and, eventually, to solve it reducing the initial mass value for the considered case (further explanations will be provided in the following chapter) or if is only a convergence problem.

At the end, the last user input will be the final velocity v_{inf} , that is the value at which the satellite will arrive in the target orbit around Earth.

Another important aspect to notice is that, in this case and in general, the optimal duration is higher than the going trip case and the maximal duration for each case will arrive until 30 or almost and no more 20, in order to have more time to perform the mission and, in general, to allow to have a save of propellant consumption.

3. Fortran code to find and analyse the trajectories

Even in this case, different solutions for different time will be found but, in order to find them, only multiples of one year will be considered, because only a node of the asteroid's orbit is the best to perform the mission with the lowest Δv , and so the lowest propellant consumption (also here, further explanations will be provided in the following chapter).

Even in this case, just like the previous one, for every time and for each duration will be possible to find the data about each trajectory from asteroid to Earth, included the flyby around this last one.

3.4 Expected results

Using these FORTRAN code, it will be possible to evaluate how the performance change with duration and year for both cases, in order to find all the possible trajectories that will be able to perform the mission. In fact, the first results that will be obtained will be about the trend of the dimensionless mass compared with the different durations.

Done this, the best results will be found/analysed in order to have the highest final mass at the end of the mission and an appropriate coincidence time among the arrival date on the asteroid and the departure date from the latter.

In this way, the best results will be obtained for the going and return case and in this way will be possible to obtain the complete optimal trajectory. Then, from this, it will be possible to represent and report all mission characteristics, both in terms of trajectory travelled, both in terms of consumption and durations, as well as having other useful values.

Chapter 4

4. Results: from individual trips to the complete mission

4.1 Initial conditions

In this section, the previous FORTRAN codes will be used in order to study the different solutions for the going and return trip, and then to find the best solution able to perform the mission.

It is important to notice that the study will be interested only in the interplanetary trip and not the launch. However, the launcher with the satellite will be launched by Cape Canaveral (28° 27' 20'' N, 80° 31' 40'' W) and, after the separation, the satellite will perform a flyby around the moon in order to achieve the desired escape velocity, which will be used to find the trajectory to reach the asteroid 2008ev5.

In addition, in this thesis, no information about the satellite components is known, except for the propeller (which is Hall effect thruster).

4.2 Going trip

To allow to perform the mission, a Delta IV Heavy launcher will be used so to insert the satellite in a LEO orbit at 500 km from Earth's surface; furthermore, thanks to Moon flyby will be possible to provide an escape velocity of $v_{\infty} = 1.3 \text{ km/s}$ and an escape mass of 10000 kg (which includes a propellant mass of 5000 kg, value estimated for the ARM mission).

To notice that, for this going trip, further flyby will not be required to reach 2008 EV₅.

In order to start the analysis, a FORTRAN code has been developed in order to, using an iterative process, solve the optimal problem. In this way, the code has been used to evaluate the final mass trend compared to the trajectory duration, starting by 1 year (about value 6 referred to dimensionless time) until the case at 3-3.5 years (about value 19-20).

Then, following this procedure, a default case where the parameters have been taken by previous studies about this mission (just like said previously) has been analysed (to notice that, for the going trip, a high duration value (>20) is not required otherwise the mission will take too much time in order to be completed). So, by this first analysis, for the default case the following results have been founded

4. Results: from individual trips to the complete mission

	Duration	Days	m _f (dim. Less)	Departure date	Arrival date
Default	0 (optimal case for 7.378)	428.93	0.8599	18/06/2022	21/08/2023
	6.5	377.86	0.8453	18/06/2022	01/07/2023
	7	406.93	0.8573	22/06/2022	03/08/2023
	7.5	435.99	0.86	18/06/2022	28/08/2023
	8	465.06	0.86	16/06/2022	24/09/2023
	8.5	494.12	0.8601	18/06/2022	25/10/2023
	9	523.19	0.8634	04/07/2022	09/12/2023
	9.5	552.26	0.8708	07/07/2022	11/01/2024
	10	581.32	0.8764	02/07/2022	04/02/2024
	10.5	610.39	0.8793	24/06/2022	25/02/2024
	11	639.45	0.88	19/06/2022	20/03/2024
	11.5	668.52	0.88	19/06/2022	17/04/2024
	12	697.59	0.8801	20/06/2022	18/05/2024
	13	755.72	0.8803	20/06/2022	14/07/2024
	14	813.85	0.88	14/06/2022	05/09/2024
	15	871.98	0.8803	21/06/2022	09/11/2024
	16	930.12	0.883	20/06/2022	05/01/2025
	17	988.25	0.8833	15/06/2022	27/02/2025
	18	1046.38	0.8834	15/06/2022	27/04/2025
19	1104.51	0.8834	15/06/2022	23/06/2025	

Table 3: Default case results for the going trip

By this figure, it is possible to notice as some rows have been coloured with a different colour. This is because, in the general case, the converge has been obtained relatively quickly. But, in some cases, it was necessary to relax the procedure (ie, to multiply the theoretical corrections by a small coefficient) to overcome some convergence difficulties.

At this point, using the values available in the Table 3, the dimensionless final mass-duration graph has been plotted

4. Results: from individual trips to the complete mission

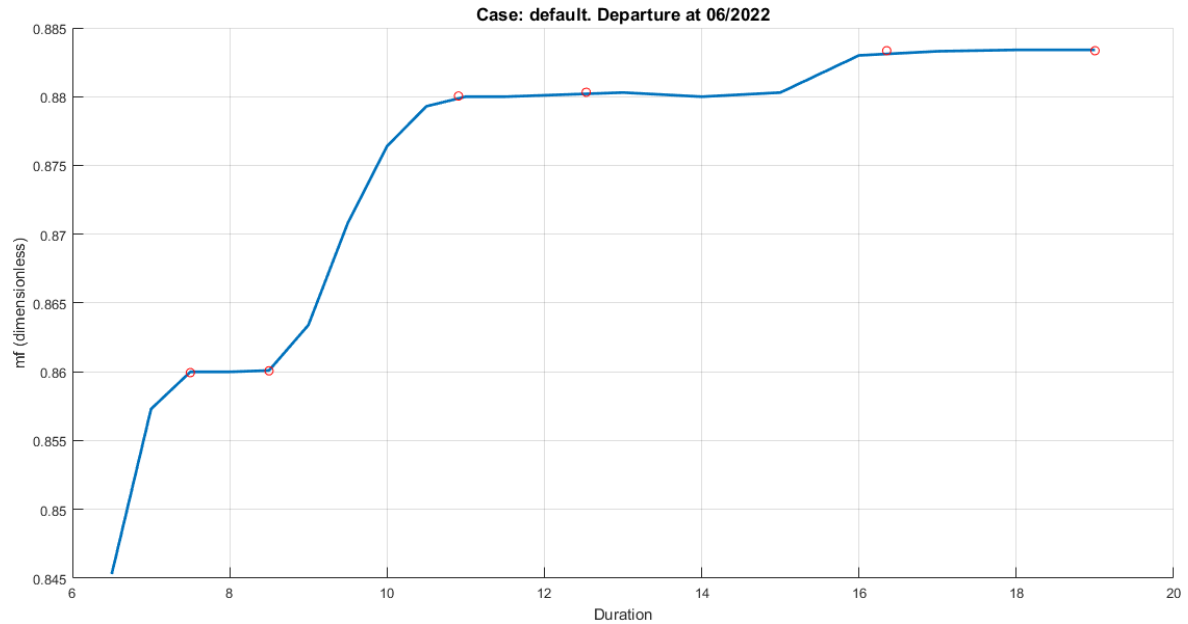


Figure 7: Graph for the default case, where the dimensionless mass is compared with the duration

By this figure it is possible to notice how the mass grows with increasing duration, as is obvious, because more time is available to perform the mission, so there is no hurry to reach the asteroid (in this way, it is possible to make lower ΔV manoeuvres and be able to save more propellant).

By the figure it is even possible to see like, for some sections, the final mass is constant and could be explain in the following way: in these sections the mission ends with a non-propelled arc, which is added to obtain the required duration but, in reality, the rendezvous is obtained at the duration corresponding to the left end of the “landing”: in these sections, the duration is optimal because is possible to perform the trip in different times and with the same mass amount. Then, in order to choose the optimal duration, the dimensionless final mass value and the duration must be carefully evaluated on the basis of the results to be obtained, i.e. high mass and acceptable duration.

After this first case, other solutions have been found changing the default case in order to achieve new trajectories at different times. In particular the solutions at ± 6 , ± 12 , $+18$ and -24 months have been found, but to find them, a significant correction on the tentative solution have been done: the v_{∞} velocity is exploited to change the plane and therefore the departure takes place near a node, because here is easier to change the inclination plane, however the attempt solution changes according to how much the mission is moved. In fact

4. Results: from individual trips to the complete mission

- If the mission is moved by a whole number of years, the node and the attempt solution do not change;
- If instead the mission is moved by an odd multiple of 6 months, the node changes and the attempt values of the quantities relative to the motion outside the plane ($w_0, \lambda_{w_0}, \lambda_{\varphi_0}$) are to be changed sign while ϑ_0 increases of π .

For example, for the +6 months case, the ϑ_0 value has been increased to +3 (because +6 is one year, correctly is 6.28, and +3 are +6 months) while to $w_0, \lambda_{w_0}, \lambda_{\varphi_0}$ the signs have been changed.

A detailed file with all results (tables and graphs for each case) is available in Appendix I.

At this point of the study, every value of the going trip for each case has been found, so to allow to obtain the following summary graph

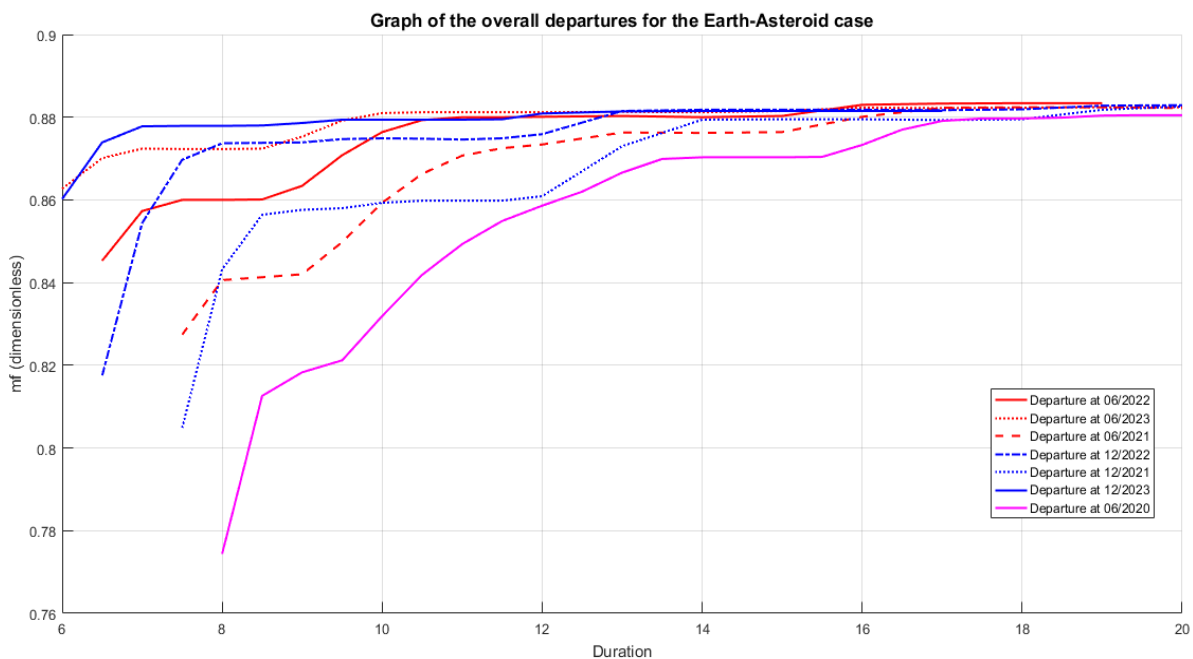


Figure 8: Graph for the overall departures

Analysing this graph has been possible to see that the interesting solutions are the one with a high dimensionless mass and a high optimal duration range (that is, where the mass is kept constant).

From this is possible to see that the best solutions, for different durations, are the following

4. Results: from individual trips to the complete mission

	Case	Duration	Departure date	Arrival date	m_f (dim. less)	
For short durations	+6 months	7	27/12/2022	07/02/2024	0.8544	
		9	13/12/2022	19/05/2024	0.8739	
		12	23/12/2022	20/11/2024	0.8759	
	+18 months	7	18/12/2023	28/01/2025	0.8778	
		9	22/12/2023	29/05/2025	0.8786	
12		27/12/2023	24/11/2025	0.8809		

	Case	Duration	Departure date	Arrival date	m_f (dim. less)
For long durations	Default	18	15/06/2022	27/04/2025	0.8834
	+6 months		21/12/2022	02/11/2025	0.8819
	-6 months		13/12/2021	25/10/2024	0.8795
	+12 months		12/06/2023	23/04/2026	0.8823
	-12 months		21/06/2021	02/05/2024	0.8824
	-24 months		24/06/2020	07/05/2023	0.8797

Table 4: Optimal results for the going trip

It is important to note that these solutions will be useful to find the best return trip solution, because have a good temporal coincidence and a high mf is essential.

4.3 Return trip

For the return trip solutions, the same approach used for the going trip has been used, but with some differences. The most important one is that, in this case, the flyby around Earth is necessary in order to be sure to be in the same plane of the Earth and to be able to reach the final velocity required in order to arrive in the final orbit where the boulder will stay.

The other difference is the reference mass, namely the mass of boulder taken from 2008 EV₅, because this value has a strong influence on the return trajectory and his convergence. But first to consider the “mass boulder convergence problem”, the default analysis will be analysed.

Just like done for the going trip, the analysis starts by the new default case, where the flyby had been considered and furthermore, a reference mass of 30000 kg is considered (to notice as this mass includes the dry mass, the residual propellant mass of the going journey and the mass boulder) and a final velocity $v_{fin} = 0.7 \text{ km/s}$ have been imposed.

In this first iteration of the optimal default case, the following results have been obtained

4. Results: from individual trips to the complete mission

```

149.9722156.9426 -0.0684164.4482 0.0142 0.1154 0.9966 0.0000 -0.1778 0.0000
-1.0737 0.1802 0.0000 0.0000
0.9377 13.4115 -0.0919 0.0842 1.0359 0.0953 1.0154 0.7339 -0.3252 0.8957 -0.6268 1.0000 1.0000
0.9836 20.4512 0.0000 0.0320 0.9983 0.1136 -0.2497 0.0229 -0.3190 0.1643 -1.0279 0.9532 1.0638
0.9836 20.4512 0.0000 0.1154 0.9966 0.0000 -0.1778 0.0000 -1.0737 0.1802 0.0000 0.9532 1.0638
0.9916 27.9923 0.0000 0.0145 0.9848 0.0000 0.4950 0.0000 0.0066 1.5735 0.0001 0.9011 1.1608
mf (kg)= 27032.1518119732
Dt = 14.4759970581340
Dt (days)= 841.525042973510
Vinf (km/s)= -1.933641412169573E-021
14/11/2023
23/12/2024
4/ 3/2026
1 -1.760049439921668E-006

```

Figure 9: Arm2vf results for the default case

In this figure, in addition to convergence of the code, it is possible to see the different dates for the various phases of the return trip and how the mass changes (the second last column from the right). In this way, the following mission steps have been founded:

- 1) the satellite leaves the asteroid on 14/11/2023 and the dimensionless mass goes from 1 (before to leaves) to 0.9532 (when the manoeuvres are required to get into the trajectory of the return);
- 2) after the previous step, the satellite reaches the node, on 23/12/24, where the flyby is required (in order to change the inclination plane) with a dimensionless mass of 0.9532 and, after the manoeuvres, the new value is 0.9011;
- 3) at this point, the Earth must be reach, because the satellite is already in the right plane compared to the Earth: so, to do this, a trip of more 2 years (the arrival date is on 04/03/2026) is necessary to re-intercept the Earth and reaches a stable orbit where the boulder will be released.

After this observation, as done in the previous paragraph, the complete duration values for this case have been found, with the only different that, in this case, the value of the duration reaches up to 30 or as far as convergence was possible.

4. Results: from individual trips to the complete mission

	Duration	Days	m f (dim. less)	Departure date	Flyby date	Arrival date
DEFAULT	0 (optimal case for 14.476)	841.52	0.901	14/11/2023	23/12/2024	04/03/2026
	14	813.85	0.899	12/12/2023	24/12/2024	05/03/2026
	14.5	842.92	0.901	12/11/2023	23/12/2024	04/03/2026
	15	871.98	0.901	14/10/2023	23/12/2024	04/03/2026
	15.5	901.05	0.901	15/09/2023	23/12/2024	04/03/2026
	16	930.12	0.901	17/08/2023	23/12/2024	04/03/2026
	16.5	959.18	0.901	19/07/2023	23/12/2024	04/03/2026
	17	988.25	0.902	20/06/2023	23/12/2024	04/03/2026
	18	1046.38	0.905	23/04/2023	23/12/2024	05/03/2026
	19	1104.52	0.91	22/02/2023	22/12/2024	02/03/2026
	20	1162.65	0.91	26/12/2022	22/12/2024	02/03/2026
	21	1220.78	0.91	29/10/2022	22/12/2024	02/03/2026
	22	1278.91	0.91	31/08/2022	22/12/2024	02/03/2026
	22.5	1307.98	0.91	02/08/2022	22/12/2024	02/03/2026
	23	1337.05	0.91	05/07/2022	22/12/2024	03/03/2026
	23.5	1366.11	0.91	06/06/2022	22/12/2024	03/03/2026
	24	1395.18	0.91	08/05/2022	22/12/2024	03/03/2026
	25	1453.31	0.91	10/03/2022	22/12/2024	02/03/2026
	26	1511.44	0.91	11/01/2022	22/12/2024	03/03/2026
	26.5	1540.51	0.91	13/12/2021	22/12/2024	03/03/2026
	27	1569.57	0.91	14/11/2021	22/12/2024	03/03/2026
	27.5	1598.64	0.91	16/10/2021	22/12/2024	03/03/2026
	28	1627.81	0.91	17/09/2021	22/12/2024	03/03/2026
	28.5	1656.77	0.91	19/08/2021	22/12/2024	03/03/2026
	29	1685.84	0.91	21/07/2021	22/12/2024	03/03/2026
	29.5	1714.91	0.91	22/06/2021	22/12/2024	03/03/2026
	30	1743.97	0.91	24/05/2021	22/12/2024	03/03/2026

Table 5: Default results for the return trip

and just like before the dimensionless final mass – duration graph has been plotted

4. Results: from individual trips to the complete mission

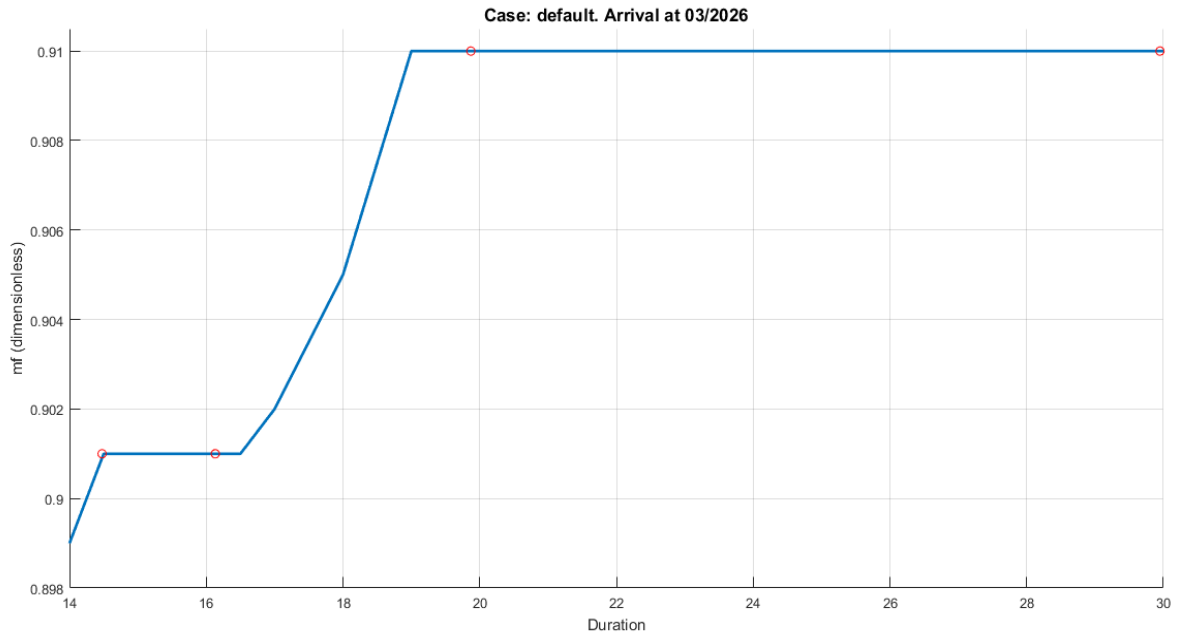


Figure 10: Graph for the return trip (default case)

At this point, it is easy to see how the same method used for the going trip has been used even for the return trip: in fact, even for this case, others different solutions have been evaluated. Nevertheless, in the following cases, a great constrain has been considered: in fact, while in the going cases the departure could be performed at the ascending or descending node, in the return case only one node could be used. In particular, only the descending node could be used in order to reach the Earth and the reason is very simple. Seeing the following figure

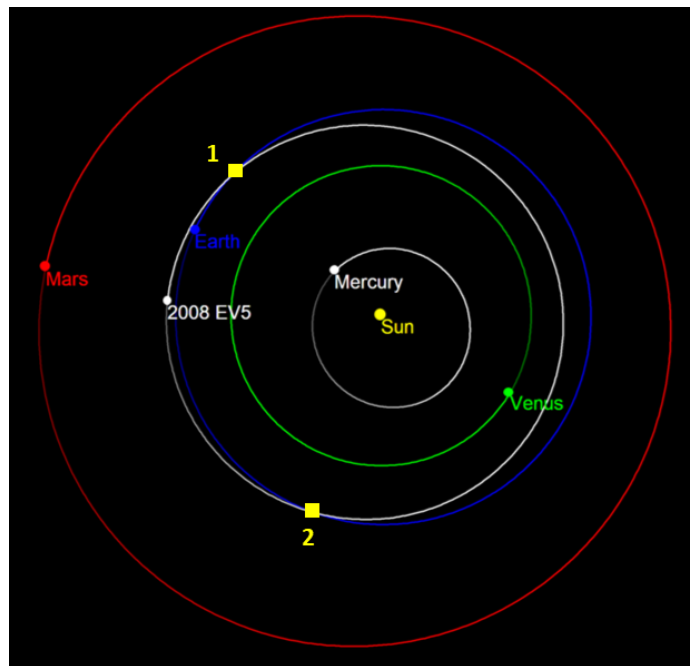


Figure 11: Nodes position for the asteroid's orbit

4. Results: from individual trips to the complete mission

It is possible to see how the two orbits (Earth and asteroid ones) intersect in two points (1 and 2), but only the higher point (number 1, which correspond to the descending node) will allow to achieve the manoeuvres with the less ΔV possible compared at the second one (which requires strong corrections, so a higher ΔV): this is the reason why it was chosen to operate only in the descending node, so to imply that only annual intervals can be used for the study of the different cases for the return.

Now, after this observation, even the cases with a dimensionless time of ± 6 and $+12$ have been analysed, but for the cases at $+6$ and $+12$ the “mass boulder convergence problem” appeared:

for these two cases, each optimal code was not able to reach the convergence for the reference mass of 30000 kg, while it was able only for 20000 kg (actually a little more, around 23500 kg, but for an easy comparison the 20000 kg has been set). The reason of this problem was in the switching function, which was always positive: this meant that the thruster was always on, suggesting that there is not enough acceleration to perform the transfer.

This explanation had been confirmed even by a preliminary analysis where, a comparison between the default mass at 20 ton ($m_{f_{default_{t_{20}}}}$) and the mass for the case at $+1$ year at 20 ton ($m_{f_{+1,20}}$) (even for the case at $+2$ year) was made; in fact, it was confirmed by the fact that the

$$m_{f_{default_{t_{20}}} \gg m_{f_{+1,20}} \quad (53)$$

proof that the fault is the lack of sufficient thrust (in fact the switching function signals it).

Having done this, only 4 cases were obtained.

However, wanting to have as many cases as possible so as to have even more chance of coinciding with the values of the going case, further analyses were carried out.

In fact, for each or almost of these cases, 3 sub-cases have been studied (this has been done in order to have a greater number of trajectories with different times distribution between the sections before and after the flyby): each single solution code has been modified so to obtain new solutions where:

- the flyby time (from the flyby position to final orbit around Earth) has been moved one year forward;
- the flyby time and the trip time (the time from asteroid to flyby position) have been moved one year forward;
- the flyby time has been moved two years forward (in this way the satellite have more time to reach the correct position, as well as allowing less consumption and more mass on board).

4. Results: from individual trips to the complete mission

Analysing these new values, some cases have been not able to reach the convergence for duration 30 but, in particular for some cases, the duration was much less (even around 20) and the reason was even the same: the switching function, which plays an important role because, when it is active, the engine pushes when it should not and in this way the trajectory is altered, so as to lose the convergence.

After all this, every value needed has been found (the results for the different cases for the return trip are in Appendix II) and the overall graph for the return trip could be plotted

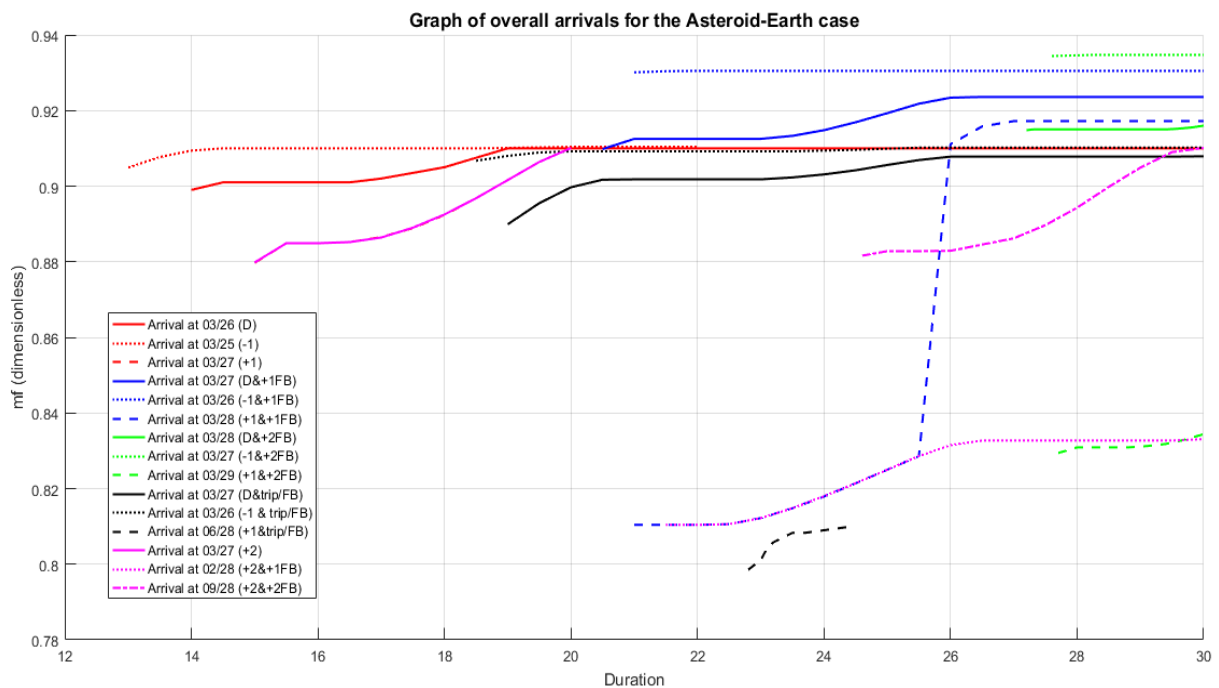


Figure 12: Graph of overall arrivals

Now, from this graph, just like for the going trip, the best values will be considered with the same method used before (the same for the going trip).

The best values, for different durations, are in Appendix 3.

4. Results: from individual trips to the complete mission

4.4 Complete trip

At this point, all the required information has been obtained and has been possible to find the best solution in order to achieve the mission in an acceptable time and, especially, to allow to have a high boulder mass and less propellant consumption as possible.

The first step was to find the best solution for the going trip. For do this has been important to compared the date of the going trip with the date of the return trip and, in order to have more coincidence and more final dimensionless mass as possible, the case at -24 months, at duration 18, has been chosen

	Case	Duration	Departure date	Arrival date	m_f (dim. less)
For long durations	Default	18	15/06/2022	27/04/2025	0.8834
	+6 months		21/12/2022	02/11/2025	0.8819
	-6 months		13/12/2021	25/10/2024	0.8795
	+12 months		12/06/2023	23/04/2026	0.8823
	-12 months		21/06/2021	02/05/2024	0.8824
	-24 months		24/06/2020	07/05/2023	0.8797

Table 6: Optimal result for the going trip

and the going trajectory has been possible to analyse.

In order to plot the following graphs, a MATLAB code has been implemented, using the output files of the chosen solution.

The first graph is useful to see the complete trajectory where Earth, asteroid and satellite appear together

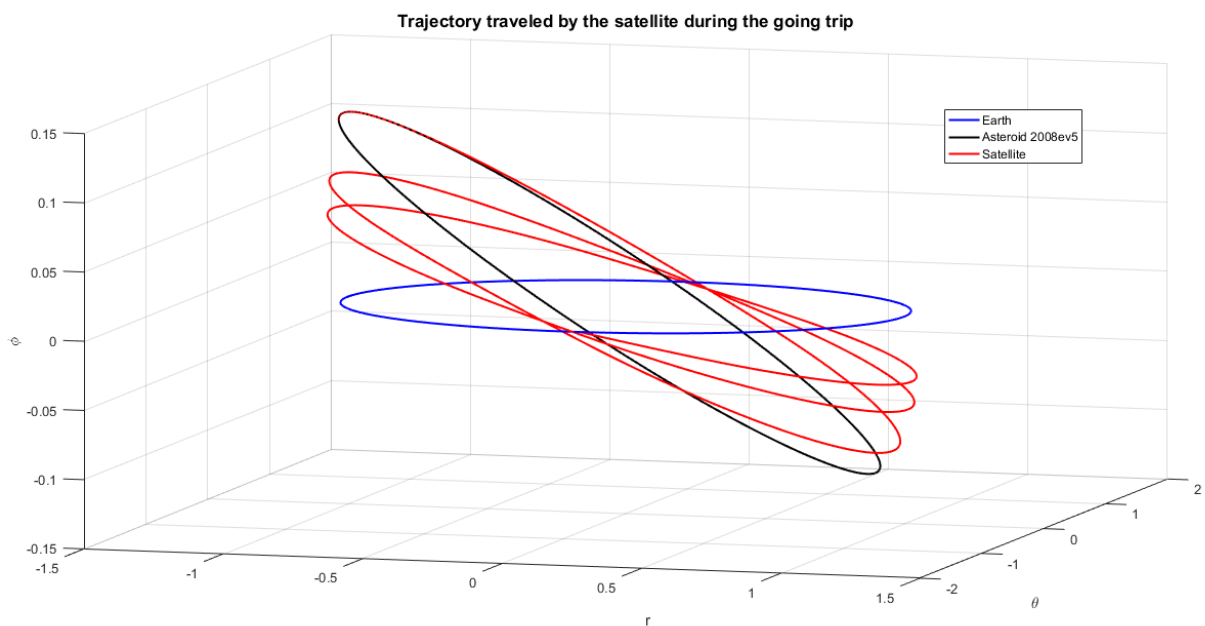


Figure 13: 3D Trajectory travelled by the satellite (referred to the best solution for the going trip)

4. Results: from individual trips to the complete mission

From this 3D graph, it is possible to notice how the satellite performs the inclination change in order to reach 2008 EV₅, and how the satellite starts its trip from the descending node. Now, for a better understanding of the satellite orbit, the 2D graph is showed

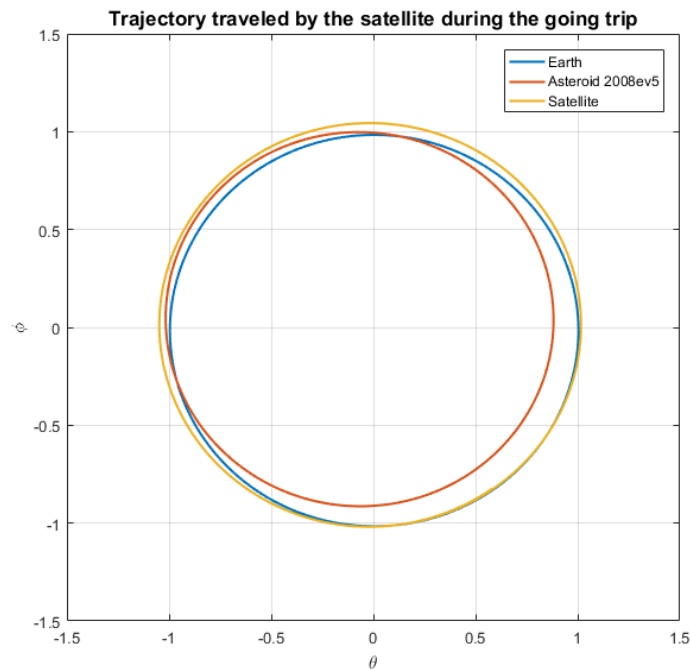


Figure 14: 2D Trajectory travelled by the satellite (referred to the best solution for the going trip)

In this 2D graph, even if only a stretch of orbit has been showed, it is easier to see the descending node (around coordinates (0 , -1)) and the elliptic orbit travelled by satellite.

To follow, another important graph shows the motion in the vertical plane

4. Results: from individual trips to the complete mission

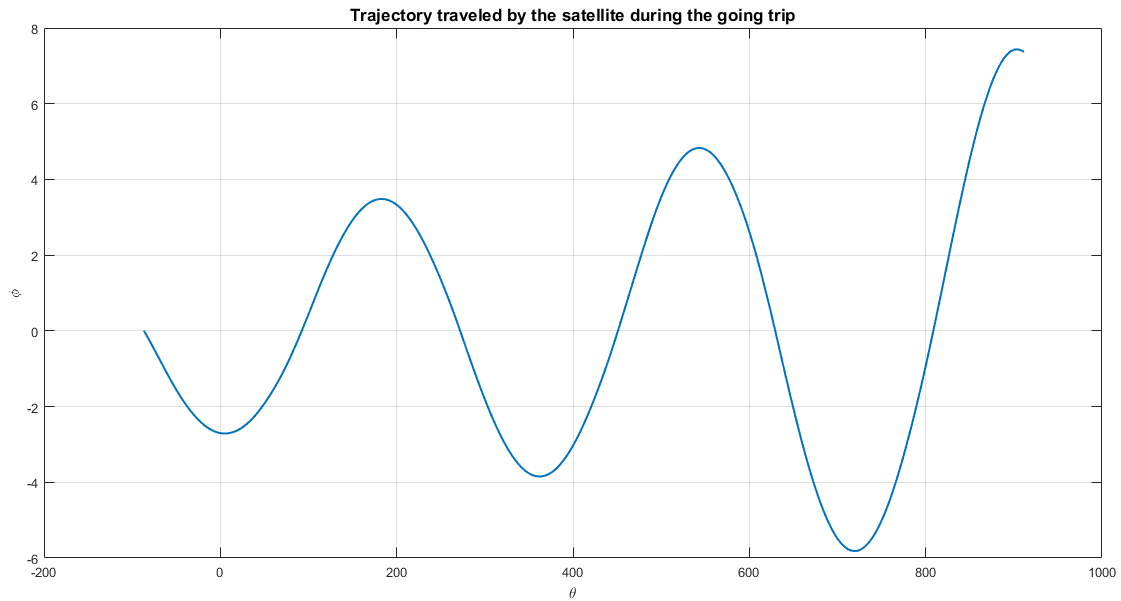


Figure 15: Satellite vertical motion for the optimal solution during the going trip

and it is possible to see how the satellite starts its travel from an inclination of 0° and then, after an inclination of 2.5° provided by the escape velocity, how the satellite is able to reach the asteroid at 7.4368° using the thruster.

Moreover, speaking about the thruster, it is possible to see how the latter works from the switching function graph

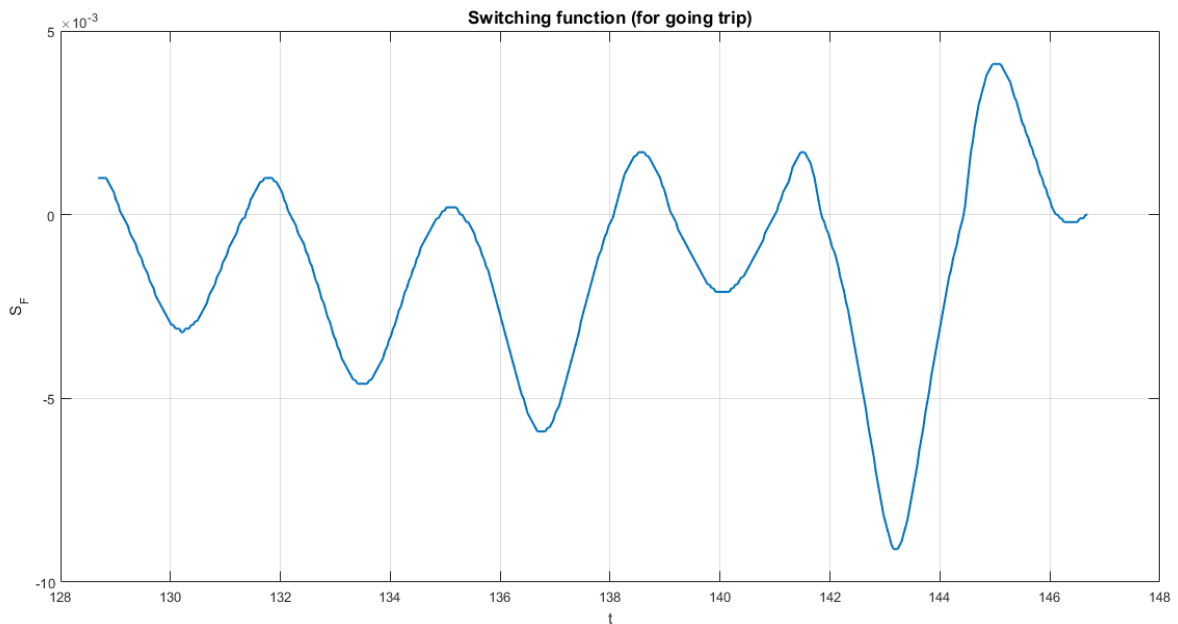


Figure 16: Switching function for the optimal solution during the going trip

4. Results: from individual trips to the complete mission

From this figure it is possible to see how the thruster is turned on when $S_F > 0$, while for $S_F < 0$ is turned off. To notice that the thruster is turned on for few time, and how the propellant consumption is of 1203 kg (obtained by the difference between the initial mass and the mass after landing on the asteroid)

$$m_{propellant\ return} = 10000(1 - 0.8797) = 1203\ kg \quad (54)$$

The final graph for the going trip that will be show allows to see the radius of perihelion and aphelion and how their change with the trip time. In order to find these values, the output file is required: in this file the energy and the eccentricity are provided for every time, but to find the radiuses a calculation is required. From the energy has been possible to calculate the semi-major axis as:

$$a = - \frac{\mu_{Earth}}{2E_g} \quad (55)$$

where $\mu_{Earth} = 398600\ km^3/s^2$ and represent the gravitational parameter of the Earth.

The next step was to found the radius of perihelion (r_p) and aphelion (r_a) as:

$$r_p = a(1 - e) \quad (56)$$

$$r_a = a(1 + e) \quad (57)$$

Done this, has been possible to obtain the following graph

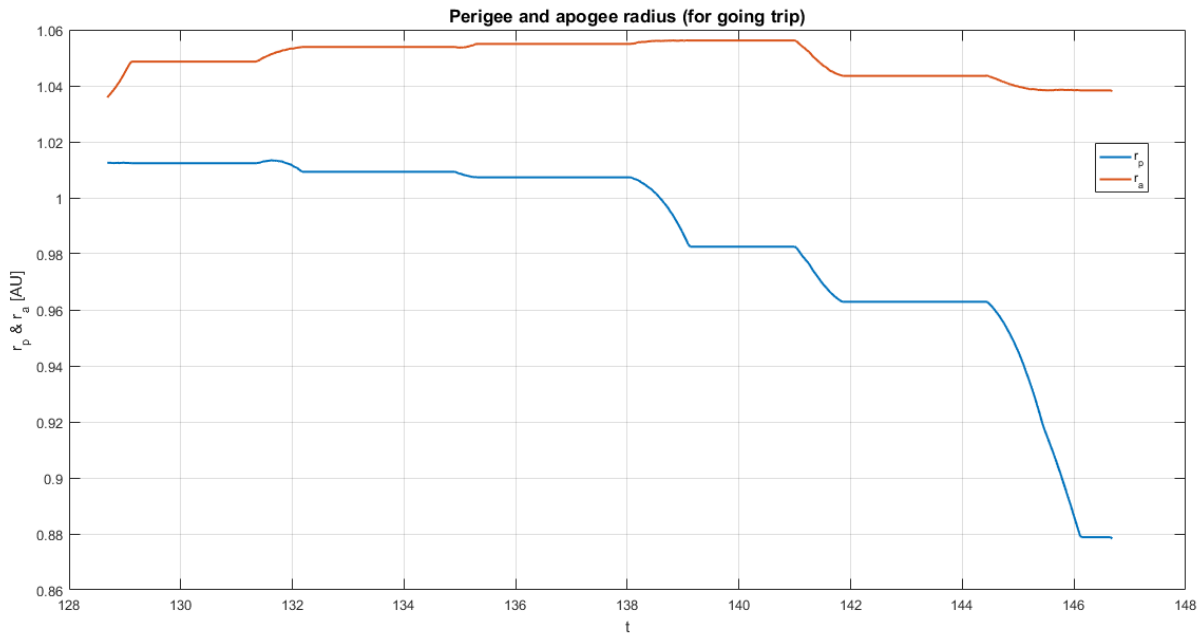


Figure 17: Apogee and perigee radius values for the optimal going trip

In conclusion, from the FORTRAN code used to find this solution, it was found that the required ΔV in order to perform this first trip is $\Delta V_{going} = 3.3472\ km/s$.

4. Results: from individual trips to the complete mission

At this point, the final step required to find the best return trip solution using the chosen going trip solution. In order to do this, the arrival date on the asteroid of the going trip have been considered in order to find the most possible solutions so to allow the coincidence among the arrival date of the going trip and the departure date of the return trip. Then, since the date of arrival on asteroid is fixed for 07/05/2023, the following return trip solutions have been founded

Case	Duration	Departure date	Flyby date	Arrival date	m_f (dim. less)
Default	15	14/10/2023	23/12/2024	04/03/2026	0.9010
Default (trip)	20	28/12/2023	22/12/2025	04/03/2027	0.8997
Default (trip)	22	02/09/2023	22/12/2025	04/03/2027	0.9018
+1 year (+1FB)	27	28/11/2023	23/12/2025	15/03/2028	0.9172
+1 year (+1FB)	28	30/09/2023	23/12/2025	15/03/2028	0.9172
Default (+2FB)		03/10/2023	23/12/2024	18/03/2028	0.9150
Default (+2FB)	30	09/06/2023	23/12/2024	18/03/2028	0.9160
+1 year (+1 FB)		06/06/2023	23/12/2025	15/03/2028	0.9172
+2 years (+2FB)		27/11/2023	23/12/2025	04/09/2028	0.9101

Table 7: Optimal results for the return trip

However, the solution chosen as optimal was the default one with duration 15 by the consideration of the following two reasons:

- 1) this solution allows to have the fastest return trip compared with the other ones, in addition to allowing to have almost 5 months in which it is possible to carry out studies of the asteroid;
- 2) this solution allows to have the highest dimensionless final mass (although slightly lower than the default case with duration 22, but the value is similar) because, just like said in the return trip paragraph, the default return trip allows to have a dimensionless final mass of 30 ton that is greater compared with the cases at 20 ton.

At this point, has been possible to make the same graphs likes the going trip. In fact, in the following graph is possible to see the 3D complete trajectories

4. Results: from individual trips to the complete mission

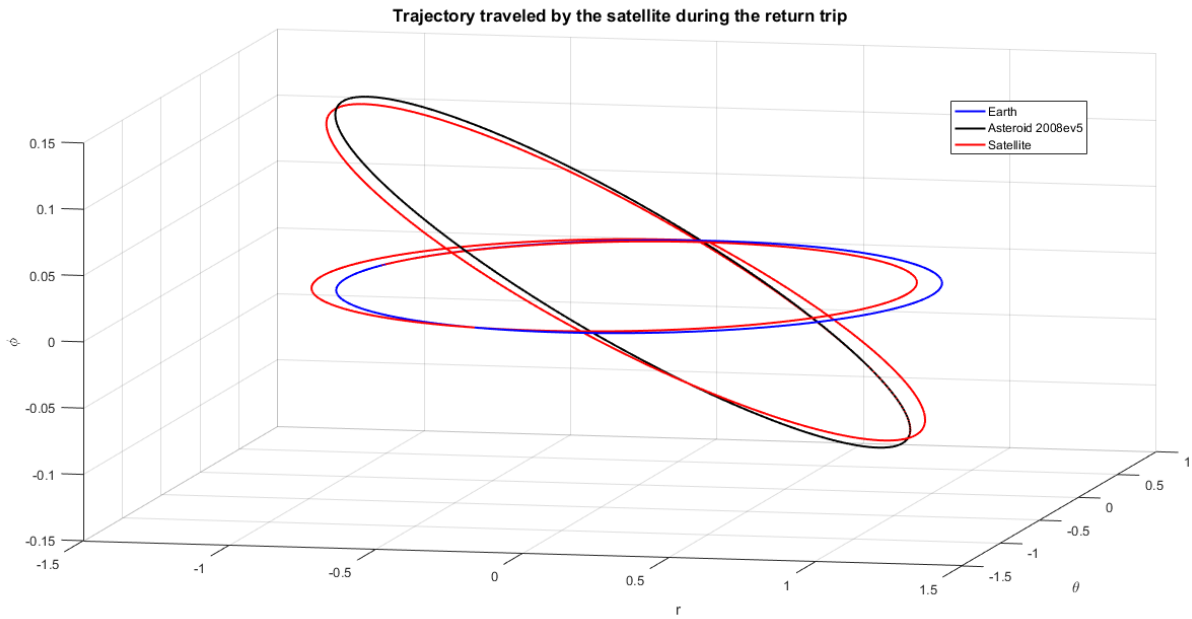


Figure 18: 3D Trajectory travelled by the satellite (referred to the best solution for the return trip)

where it is possible to see how the satellite, in order to reach the final orbit around the Earth, should start from the ascending node of the 2008 EV₅'s orbit and changes his inclination; then, after having travelled for an orbit, it is in a useful position to carry out the flyby of the Earth. In this way the satellite finds itself in an orbital coplanar with the terrestrial one and after a little more than a year, will meet the Earth and will achieve the desired final orbit.

The satellite orbit before the flyby is in the following 2D figure

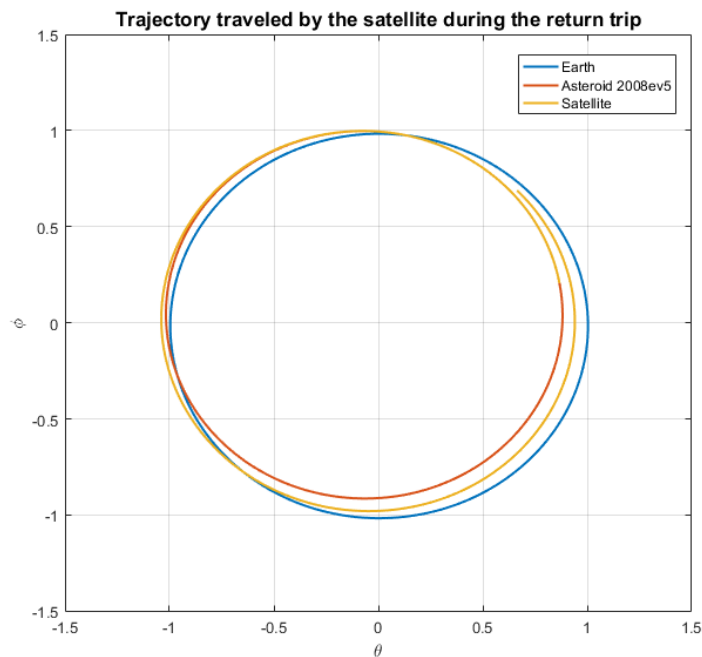


Figure 19: 2D Trajectory travelled by the satellite (referred to the best solution for the return trip)

4. Results: from individual trips to the complete mission

and it is possible even to see how the orbit trajectory changes during the trip

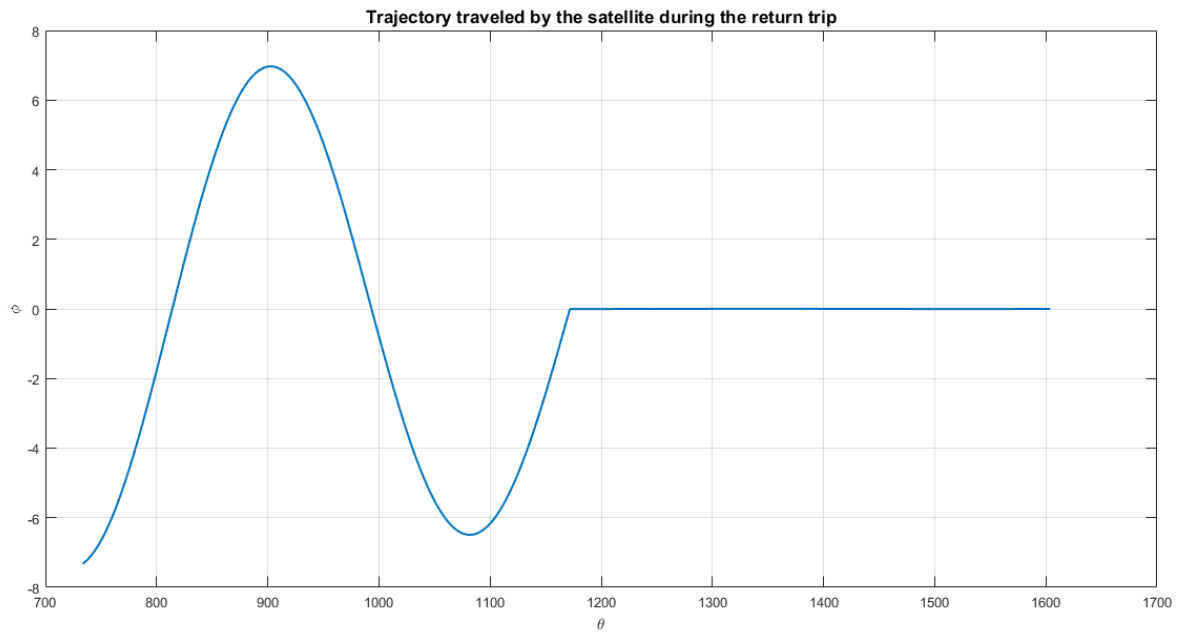


Figure 20: Satellite vertical motion for the optimal solution during the return trip

By this last figure, it is possible to notice how the satellite starts from the ascending node of 2008 EV₅ and as after having travelled the orbit, the flyby allows to zero the inclination of the satellite with respect to the terrestrial orbit, so to have the two orbits coplanar.

In conclusion, the last graphs useful to see are about the radius of perihelion and aphelion and the switching function. For the first one, it is possible to see like the radiuses, calculated in the same way like the previous case, change in the following mode

4. Results: from individual trips to the complete mission

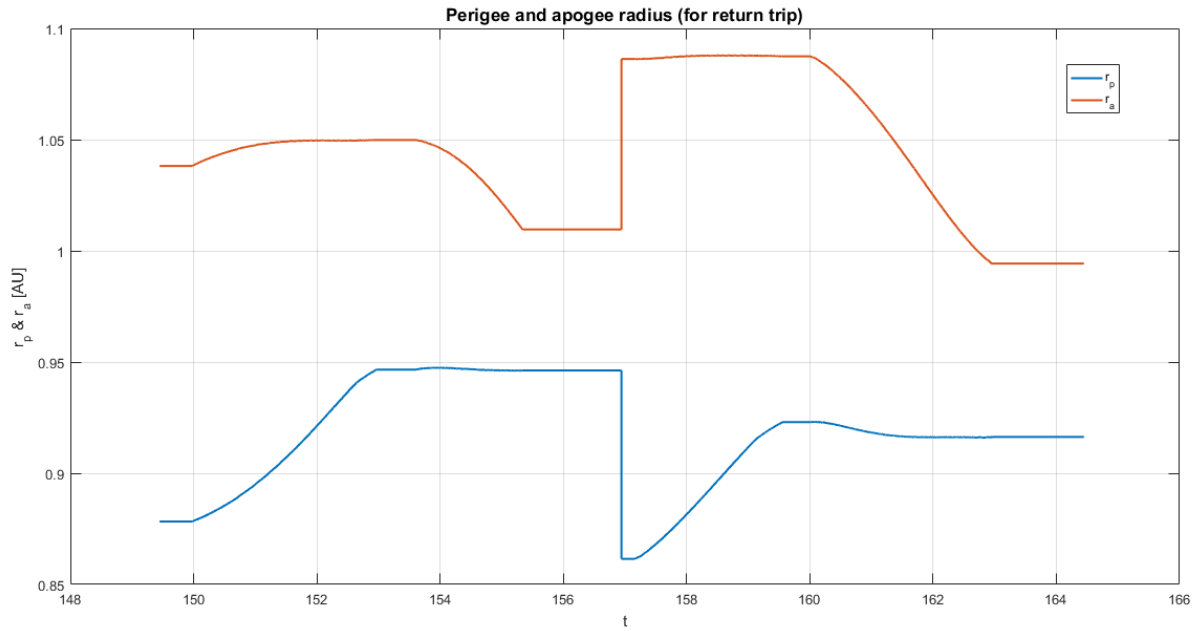


Figure 21: Apogee and perigee radius values for the optimal return trip

while the switching function graph shows like, in this case, the thruster works for more time (remembering that the thruster is switching on when $SF > 0$).

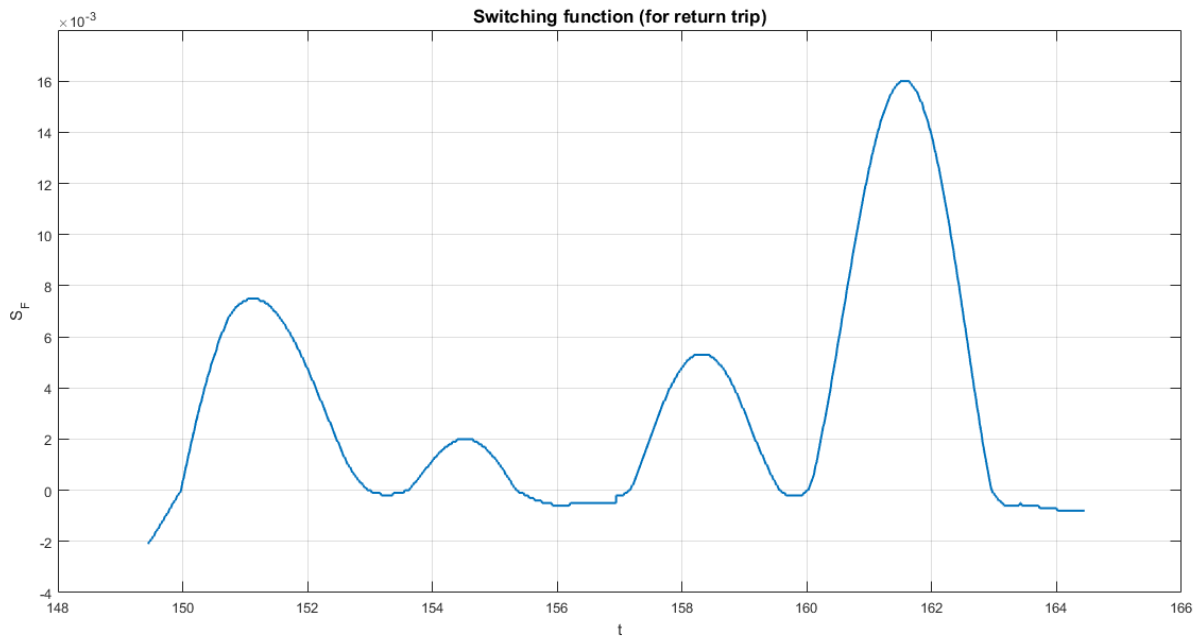


Figure 22: Switching function for the optimal solution during the going trip

4. Results: from individual trips to the complete mission

Finally, in order to calculate the propellant consumption, the solution code has been used and has been possible to calculate the propellant consumption before the flyby manoeuvre and the propellant consumption required to reach the destination.

$$m_{total\ propellant\ return} = m_{before\ FB} + m_{after\ FB} = 1404 + 1563 = 2967\ kg \quad (58)$$

Another important value to be considered is the radius which the flyby will be achieved and, in order to calculate it, the FORTRAN code is required again. Then, from the code, the required values are

```

rotazione, vp, vpmx
54.1494014600512      0.143034618253222      0.259525517570559
Vrel (km/s)
3.58325451166553
    
```

Figure 23: Flyby results for the optimal case

which they represent the rotation, the velocity at perihelion, the circular velocity at the minimum perihelion (velocities expressed in the heliocentric reference system) and the relative velocity (that is v_{∞}).

Now, in order to find the radius where the flyby will be achieved, the following expression has been used

$$\sin\left(\frac{\delta}{2}\right) = \frac{\frac{\mu}{R_p}}{\frac{\mu}{R_p} + v_{\infty}^2} \quad (59)$$

referred at the following figure

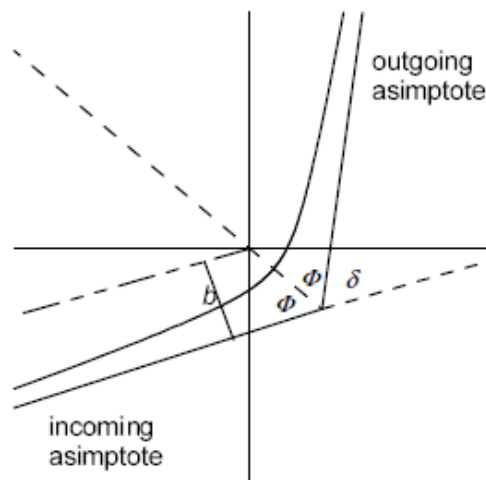


Figure 24: Flyby scheme

4. Results: from individual trips to the complete mission

Using this expression, the R_p has been calculated as

$$R_p = -\frac{\mu \left[\sin\left(\frac{\delta}{2}\right) - 1 \right]}{\sin\left(\frac{\delta}{2}\right) v_\infty^2} = -\frac{398600 \left[\sin\left(\frac{54.1494}{2}\right) - 1 \right]}{\sin\left(\frac{54.1494}{2}\right) 3.5832^2} = 37163 \text{ km} \quad (60)$$

Furthermore, the required ΔV s have been obtained considering a specific impulse of $I_{sp} = 2600 \text{ s}$ (remembering that a Hall effect thruster will be used). Then, by

$$I_{sp} = \frac{c}{g} \Rightarrow c = I_{sp} \cdot g = 2600 \text{ s} \cdot 9.81 \frac{\text{m}}{\text{s}^2} = 25506 \frac{\text{m}}{\text{s}} \quad (61)$$

and using the Tsiolkovsky's equation

$$\Delta V_{before \text{ FB}} = c \ln\left(\frac{m_{0 \text{ rif}}}{m_{0 \text{ rif}} - m_{before \text{ FB}}}\right) = 25506 \ln\left(\frac{30000}{30000 - 1404}\right) = 530.93 \text{ m/s} \quad (62)$$

$$\Delta V_{after \text{ FB}} = c \ln\left(\frac{m_{0 \text{ rif}}}{m_{0 \text{ rif}} - m_{after \text{ FB}}}\right) = 25506 \ln\left(\frac{28596}{28596 - 1563}\right) = 622.63 \text{ m/s} \quad (63)$$

So, the total ΔV value required for the return trip is

$$\Delta V_{return \text{ tot}} = \Delta V_{before \text{ FB}} + \Delta V_{after \text{ FB}} = 1.153 \text{ km/s} \quad (64)$$

4.4.1 Results summary

As previously said, for the ARM mission a mass of 5000 kg for the propellant and for the dry mass was hypothesized, for a total of 10000 kg.

Since the going trip will require a propellant mass of 1203 kg, it is possible to see how the mass still available (and therefore usable for the return) will be of 3797 kg and from this, bearing in mind that an initial mass of 30000 kg was imposed for the return, it is possible to see that it includes the dry mass (5000 kg), the residual propellant mass (3797 kg) and the boulder mass.

So, from all this, considering that the return trip will require a propellant consumption of 2967 kg, it is seen how the boulder mass that will be possible to withdraw from the asteroid 2008 EV₅ will be of 21203 kg and how the remaining propellant mass will be of 830 kg: this is an excellent result both because it

4. Results: from individual trips to the complete mission

is possible to carry out the mission with less propellant than the budgeted one, and because, in case of necessity of any kind, there will still be some propellant to be used to carry out any type of manoeuvre, always within the limits of the possible.

In the end, it is possible to see how the required ΔV for the return is lower than that the going, thanks to the flyby manoeuvre.

In conclusion, it is possible to see a summary table concerning the complete mission

	Departure date	Fly by date	Arrival date	ΔV [km/s]	m_0 [kg]	m_{fuel} [kg]
GOING TRIP	24/06/2020	x	07/05/2023	1.3	10000	1203
RETURN TRIP	14/10/2023	23/12/2024	04/03/2026	1.153	30000	2967
Total mission duration [days]					2080	
ΔV_{tot} [km/s]					2.453	
$m_{propellant\ tot}$ [kg]					4170	
$m_{boulder}$ [kg]					21203	

Table 8: Complete trip information

5. Conclusion

From this study, it has been possible to see, how a trajectory for whether space mission can be analysed in order to perform and achieve the mission with the best results. In fact, in this case, the target was to bring a boulder from asteroid 2008 EV₅ to a stable orbit around the Earth, having even the constrains to perform a mission that allows to have a save of propellant consumption (the total mission time was important but not very relevant). In order to achieve this, all the mission opportunities were found in a large launch window, from which the best in terms of fuel consumption convenience could be identified.

This was the strategy adopted in this study, but it is not said that it is the optimal one.

In fact, the same mission could be analysed imposing to execute it in the shortest time possible, therefore not considering the possible excessive propellant consumption; or could be possible to do even a longer mission or one that exploits more than one flyby or does it exploiting another celestial body (in all these cases, different FORTRAN codes should be implemented).

That said, it is possible to see how any mission (whether interplanetary or not) is influenced by many parameters and how, by modifying them (even small ones), the mission can be compromised.

All this make to think about the high difficulty that is present at the base of every space mission, be it past, present or future.

Bibliography

- [1] Nasa - Asteroid Redirect Mission (ARM), Formulation Assessment and Support Team (FAST) Final Report
- [2] Nasa - Asteroid Redirect Mission (ARM), Update to the NASA Advisory Council, Human Exploration and Operations Committee
- [3] Nasa - Overview of the Asteroid Redirect Mission (ARM)
- [4] Nasa JPL - Asteroid Retrieval Mission Feasibility Study
- [5] Asteroid 2008 ev5 – Wikipedia
- [6] <http://neo.ssa.esa.int/search-for-asteroids?sum=1&des=341843%202008EV5>
- [7] <https://ssd.jpl.nasa.gov/sbdb.cgi#top>
- [8] <https://nssdc.gsfc.nasa.gov/planetary/factsheet/earthfact.html>
- [9] ALMA, A Low-cost Mission to an Asteroid - Weiskircher, Busch, Shah
- [10] Indirect Methods for the Optimization of Spacecraft Trajectories - Guido Colasurdo and Lorenzo Casalino
- [11] Ottimizzazione Indiretta di Traiettorie Spaziali - Lorenzo Casalino
- [12] Indirect Methods for the Optimization of Spacecraft Trajectories (Slides) - Lorenzo Casalino
- [13] OPTIMAL POWER PARTITIONING FOR ELECTRIC THRUSTERS - Lorenzo Casalino and Matthew A. Vavrina
- [14] A Survey of Numerical Methods for Trajectory Optimization - John T. Betts
- [15] Optimization of Low-thrust Trajectories Using An Indirect Shooting Method without Guesses of Initial Costates - LIN Hou-yuan, ZHAO Chang-yin
- [16] Fundamentals of Astrodynamics - Bate, Mueller, and White
- [17] DIRECT AND INDIRECT METHODS FOR TRAJECTORY OPTIMIZATION - O. yon STRYK and R. BULIRSCH
- [18] DESIGN OF LUNAR-GRAVITY-ASSISTED ESCAPE MANEUVERS - Lorenzo Casalino and Gregory Lantoine
- [19] Space Engineering - Modeling and Optimization with Case Studies - Giorgio Fasano and János D. Pintér
- [20] Spacecraft Trajectory Optimization – Bruce A. Conway
- [21] Returning an Entire Near-Earth Asteroid in Support of Human Exploration Beyond Low-Earth Orbit - John R. Brophy and Louis Friedman

Appendixes

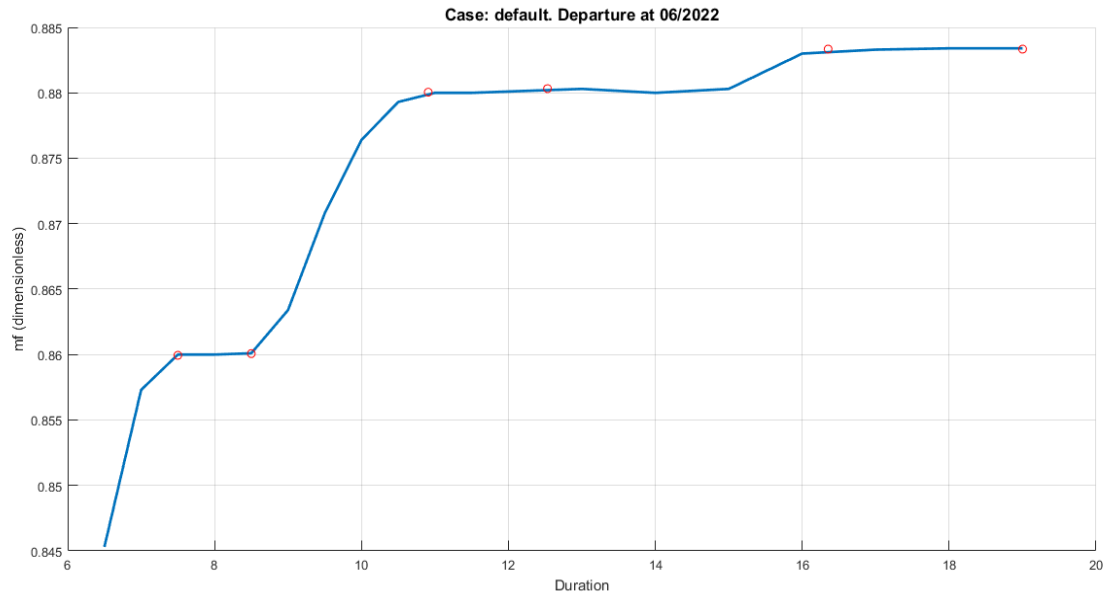
Appendix I: Results for the going trip

Interval iteration values		
1	2	500 (default)
0.1	2	500
0.01	2	2000

Case: Default

	Duration	Days	m_f (dim. less)	Departure date	Arrival date
Default	0 (optimal case for 7.378)	428.93	0.8599	18/06/2022	21/08/2023
	6.5	377.86	0.8453	18/06/2022	01/07/2023
	7	406.93	0.8573	22/06/2022	03/08/2023
	7.5	435.99	0.86	18/06/2022	28/08/2023
	8	465.06	0.86	16/06/2022	24/09/2023
	8.5	494.12	0.8601	18/06/2022	25/10/2023
	9	523.19	0.8634	04/07/2022	09/12/2023
	9.5	552.26	0.8708	07/07/2022	11/01/2024
	10	581.32	0.8764	02/07/2022	04/02/2024
	10.5	610.39	0.8793	24/06/2022	25/02/2024
	11	639.45	0.88	19/06/2022	20/03/2024
	11.5	668.52	0.88	19/06/2022	17/04/2024
	12	697.59	0.8801	20/06/2022	18/05/2024
	13	755.72	0.8803	20/06/2022	14/07/2024
	14	813.85	0.88	14/06/2022	05/09/2024
	15	871.98	0.8803	21/06/2022	09/11/2024
	16	930.12	0.883	20/06/2022	05/01/2025
	17	988.25	0.8833	15/06/2022	27/02/2025
	18	1046.38	0.8834	15/06/2022	27/04/2025
19	1104.51	0.8834	15/06/2022	23/06/2025	

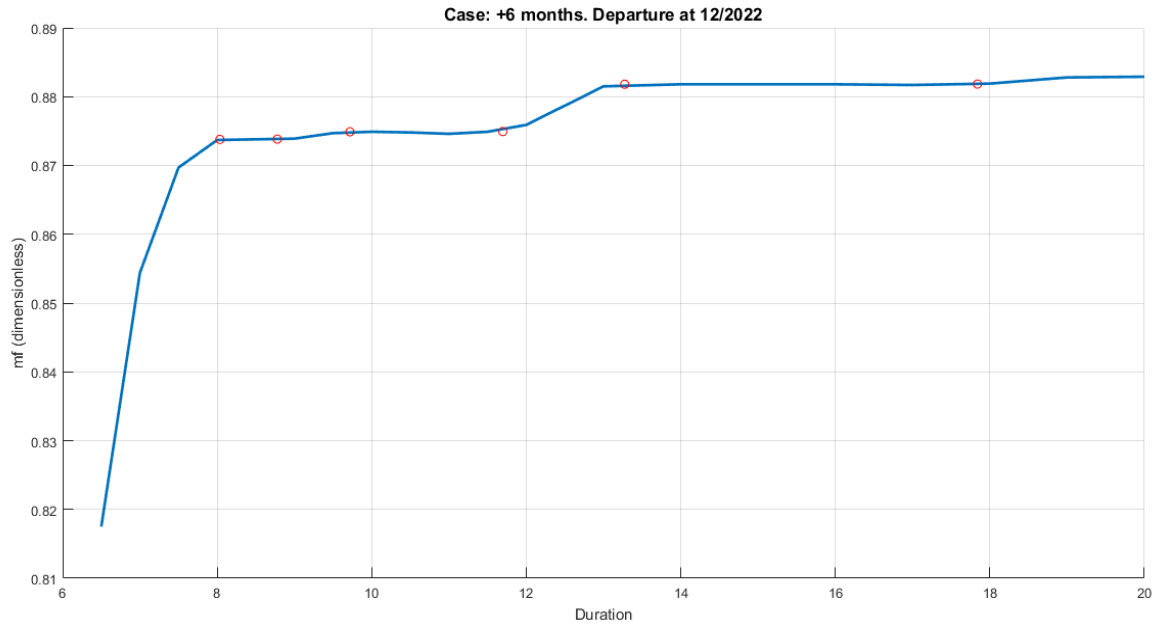
Appendixes



Case: +6 months

	Duration	Days	m_f (dim. less)	Departure date	Arrival date
	0 (optimal case for 8.034)	467.08	0.8737	11/12/2022	22/03/2024
+ 6 months	6	348.79	0.8627	15/06/2023	29/05/2024
	6.5	377.86	0.8175	25/12/2022	07/01/2024
	7	406.92	0.8544	27/12/2022	07/02/2024
	7.5	435.99	0.8697	19/12/2022	28/02/2024
	8	465.06	0.8737	11/12/2022	20/03/2024
	8.5	494.12	0.8738	11/12/2022	18/04/2024
	9	523.19	0.8739	13/12/2022	19/05/2024
	9.5	552.26	0.8747	16/12/2022	20/06/2024
	10	581.32	0.8749	14/12/2022	18/07/2024
	10.5	610.39	0.8748	12/12/2022	13/08/2024
	11	639.45	0.8746	09/12/2022	09/09/2024
	11.5	668.52	0.8749	13/12/2022	12/10/2024
	12	697.58	0.8759	23/12/2022	20/11/2024
	13	755.72	0.8815	21/12/2022	14/01/2025
	14	813.85	0.8818	18/12/2022	11/03/2025
	15	871.98	0.8818	19/12/2022	09/05/2025
	16	930.12	0.8818	17/12/2022	05/07/2025
	17	988.25	0.8817	16/12/2022	30/08/2025
	18	1046.38	0.8819	21/12/2022	02/11/2025
	19	1104.51	0.8828	21/12/2022	29/12/2025
20	1162.65	0.8829	20/12/2022	24/02/2026	

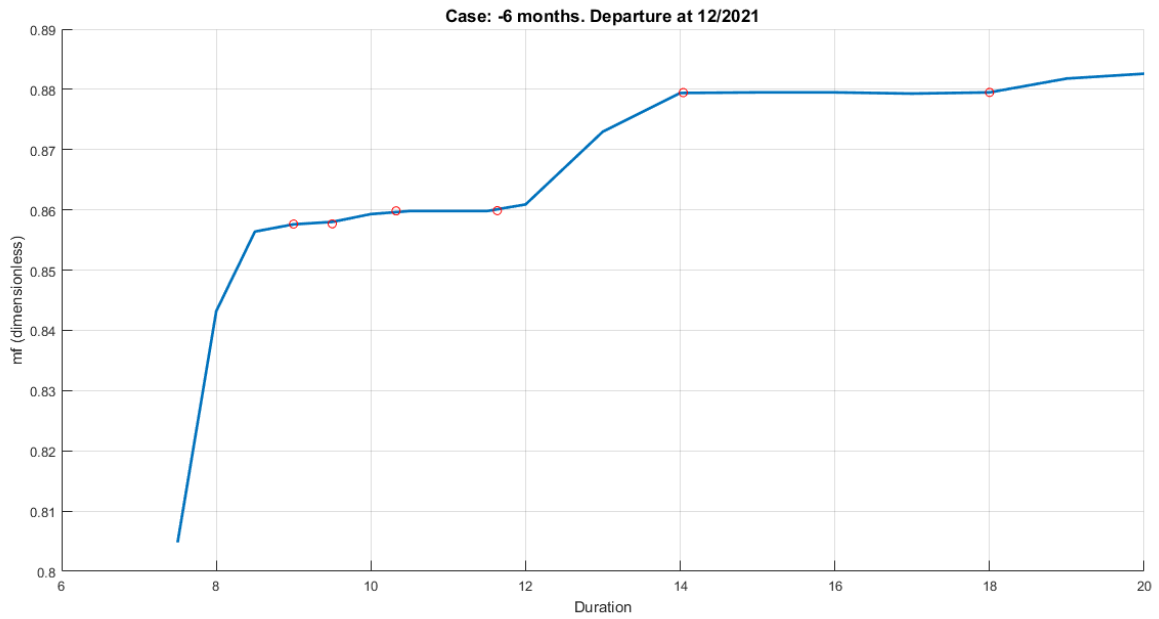
Appendixes



Case: -6 months

	Duration	Days	m f (dim. less)	Departure date	Arrival date
- 6 months	0 (optimal case for 8.778)	510.31	0.8576	08/12/2021	02/05/2023
	7.5	435.99	0.8048	12/12/2021	20/02/2023
	8	465.06	0.8432	18/12/2021	28/03/2023
	8.5	494.12	0.8564	11/12/2021	19/04/2023
	9	523.19	0.8576	08/12/2021	15/05/2023
	9.5	552.26	0.858	12/12/2021	17/06/2023
	10	581.32	0.8593	14/12/2021	19/07/2023
	10.5	610.39	0.8598	11/12/2021	14/08/2023
	11	639.45	0.8598	10/12/2021	10/09/2023
	11.5	668.52	0.8598	11/12/2021	10/10/2023
	12	697.59	0.8609	18/12/2021	16/11/2023
	13	755.72	0.873	24/12/2021	19/01/2024
	14	813.85	0.8794	15/12/2021	08/03/2024
	15	871.98	0.8795	14/12/2021	04/05/2024
	16	930.12	0.8795	14/12/2021	01/07/2024
	17	988.25	0.8793	10/12/2021	24/08/2024
	18	1046.38	0.8795	13/12/2021	25/10/2024
	19	1104.52	0.8818	20/12/2021	29/12/2024
	20	1162.65	0.8826	17/12/2021	22/02/2025

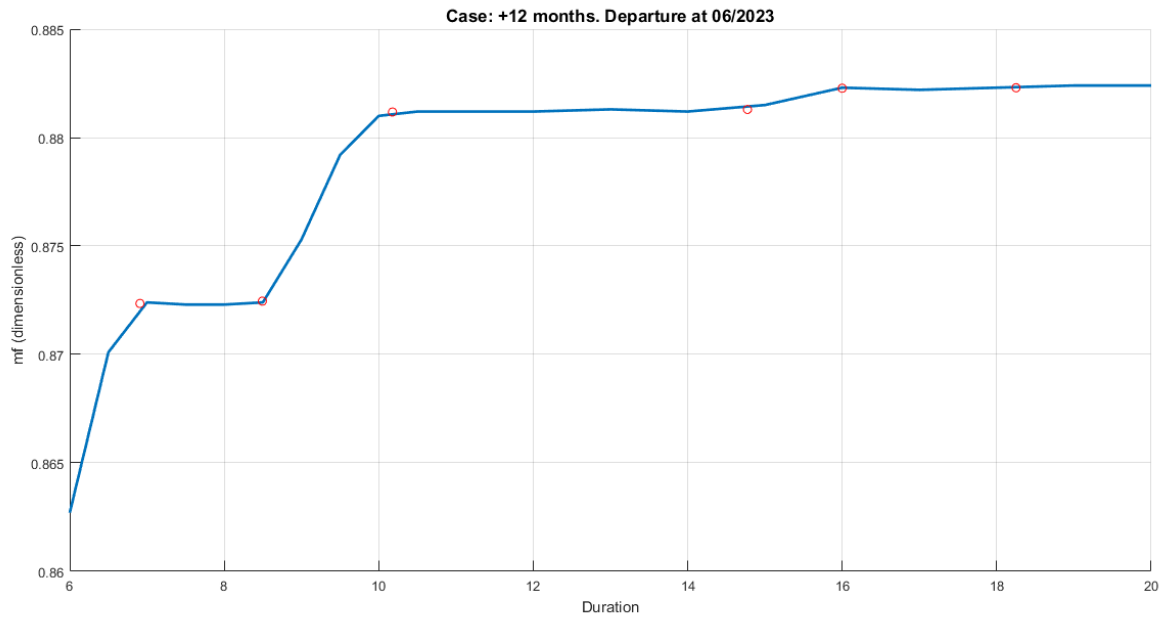
Appendixes



Case: +12 months

	Duration	Days	m_f (dim. less)	Departure date	Arrival date
+ 12 months	0 (optimal case for 6.908)	401.608	0.8723	17/06/2023	22/07/2024
	6	348.79	0.8627	15/06/2023	29/05/2024
	6.5	377.86	0.8701	20/06/2023	02/07/2024
	7	406.92	0.8724	16/06/2023	27/07/2024
	7.5	435.99	0.8723	14/06/2023	23/08/2024
	8	465.06	0.8723	13/06/2023	20/09/2024
	8.5	494.12	0.8724	17/06/2023	23/10/2024
	9	523.19	0.8753	26/06/2023	30/11/2024
	9.5	552.26	0.8792	23/06/2023	26/12/2024
	10	581.34	0.881	15/06/2023	16/01/2025
	10.5	610.39	0.8812	12/06/2023	11/02/2025
	11	639.45	0.8812	10/06/2023	11/03/2025
	11.5	668.52	0.8812	11/06/2023	09/04/2025
	12	697.59	0.8812	12/06/2023	10/05/2025
	13	755.72	0.8813	13/06/2023	07/07/2025
	14	813.85	0.8812	11/06/2023	01/09/2025
	15	871.99	0.8815	16/06/2023	04/11/2025
	16	930.12	0.8823	12/06/2023	28/12/2025
	17	988.25	0.8822	09/06/2023	22/02/2026
	18	1046.38	0.8823	12/06/2023	23/04/2026
19	1104.52	0.8824	12/06/2023	21/06/2026	
20	1162.65	0.8824	11/06/2026	17/08/2026	

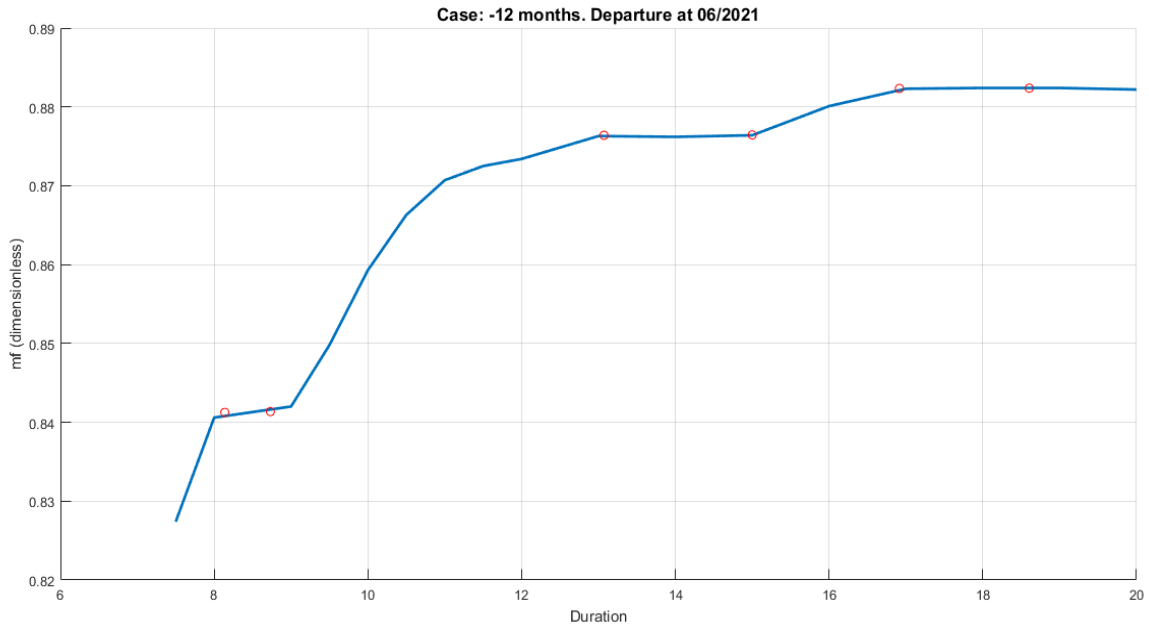
Appendixes



Case: -12 months

	Duration	Days	m_f (dim. less)	Departure date	Arrival date
- 12 months	0 (optimal case for 8.137)	473.06	0.8412	13/06/2021	29/09/2022
	7.5	435.99	0.8274	16/06/2021	26/08/2022
	8	465.06	0.8406	15/06/2021	23/09/2022
	8.5	494.12	0.8413	13/06/2021	20/10/2022
	9	523.19	0.842	21/06/2021	26/11/2022
	9.5	552.25	0.8498	09/07/2021	13/01/2023
	10	581.32	0.8593	12/07/2021	14/02/2023
	10.5	610.39	0.8663	08/07/2021	30/09/1901
	11	639.45	0.8707	30/06/2021	31/03/2023
	11.5	668.52	0.8725	23/06/2021	23/04/2023
	12	697.59	0.8734	24/06/2021	22/05/2023
	13	755.72	0.8763	25/06/2021	21/07/2023
	14	813.85	0.8762	19/06/2021	11/09/2023
	15	871.99	0.8764	23/06/2021	12/11/2023
	16	930.12	0.8801	02/07/2021	18/01/2024
	17	988.25	0.8823	21/06/2021	05/03/2024
	18	1046.38	0.8824	21/06/2021	02/05/2024
	19	1104.52	0.8824	21/06/2021	29/06/2024
	20	1162.65	0.8822	15/06/2021	21/08/2024

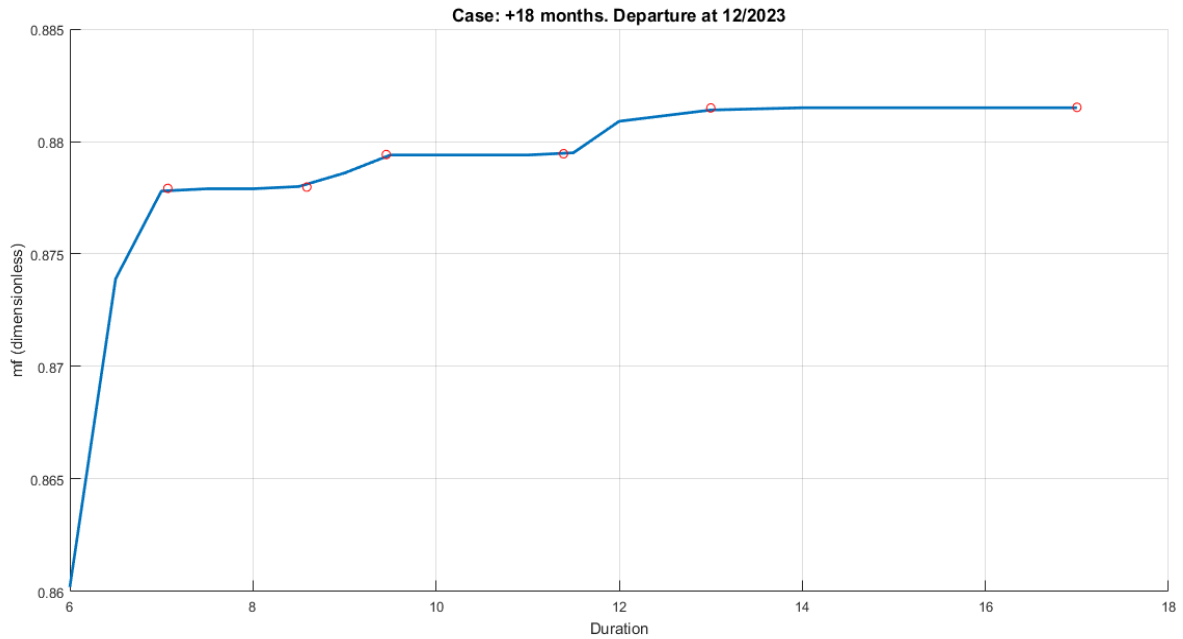
Appendixes



Case: +18 months

	Duration	Days	m_f (dim. less)	Departure date	Arrival date
+ 18 months	0 (optimal case for 7.069)	410.99	0.8779	17/12/2023	31/01/2025
	6	348.79	0.8602	29/12/2023	12/12/2024
	6.5	377.86	0.8739	25/12/2023	06/01/2025
	7	406.92	0.8778	18/12/2023	28/01/2025
	7.5	435.99	0.8779	16/12/2023	24/02/2025
	8	465.06	0.8779	16/12/2023	25/03/2025
	8.5	494.12	0.878	17/12/2023	24/04/2025
	9	523.19	0.8786	22/12/2023	29/05/2025
	9.5	552.26	0.8794	21/12/2023	25/06/2025
	10	581.34	0.8794	19/12/2023	22/07/2025
	10.5	610.39	0.8794	18/12/2023	19/08/2025
	11	639.45	0.8794	19/12/2023	18/09/2025
	11.5	668.52	0.8795	23/12/2023	22/10/2025
	12	697.59	0.8809	27/12/2023	24/11/2025
	13	755.72	0.8814	23/12/2023	16/01/2026
	14	813.85	0.8815	22/12/2023	15/03/2026
	15	871.99	0.8815	24/12/2023	14/05/2026
16	930.12	0.8815	23/12/2023	10/07/2026	
17	988.25	0.8815	24/12/2023	07/09/2026	

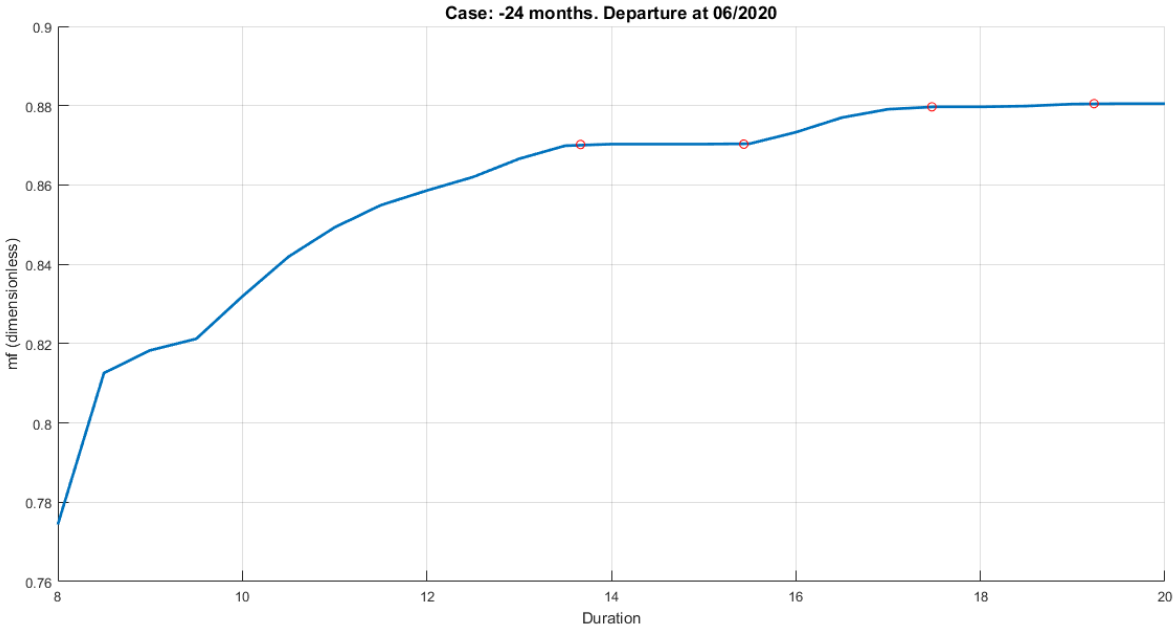
Appendixes



Case: -24 months

	Duration	Days	m_f (dim. less)	Departure date	Arrival date
-24 months	0 (optimal case for 13.6658)	794.43	0.8702	24/06/2020	28/08/2022
	8	465.06	0.7744	14/06/2020	22/09/2021
	8.5	494.12	0.8126	10/06/2020	17/10/2021
	9	523.19	0.8183	09/06/2020	14/11/2021
	9.5	552.26	0.8212	27/06/2020	31/12/2021
	10	581.32	0.8319	15/07/2020	17/02/2022
	10.5	610.39	0.8419	16/07/2020	18/03/2022
	11	639.45	0.8493	10/07/2020	10/04/2022
	11.5	668.52	0.8549	01/07/2020	01/05/2022
	12	697.59	0.8586	22/06/2020	21/05/2022
	12.5	726.65	0.862	24/06/2020	21/06/2022
	13	755.72	0.8666	29/06/2020	25/07/2022
	13.5	784.79	0.8699	26/06/2020	20/08/2022
	14	813.85	0.8703	23/06/2020	14/09/2022
	15	871.98	0.8703	20/06/2020	09/11/2022
	15.5	901.05	0.8704	27/06/2020	15/12/2022
	16	930.12	0.8733	07/07/2020	24/01/2023
	16.5	959.18	0.877	05/07/2020	19/02/2023
	17	988.25	0.8791	29/06/2020	14/03/2023
	17.5	1017.32	0.8797	24/06/2020	08/04/2023
	18	1046.38	0.8797	24/06/2020	07/05/2023
18.5	1075.45	0.8799	26/06/2020	06/06/2023	
19	1104.52	0.8804	26/06/2020	05/07/2023	
19.5	1133.58	0.8805	23/06/2020	01/08/2023	
20	1162.65	0.8805	20/06/2020	27/08/2023	

Appendixes

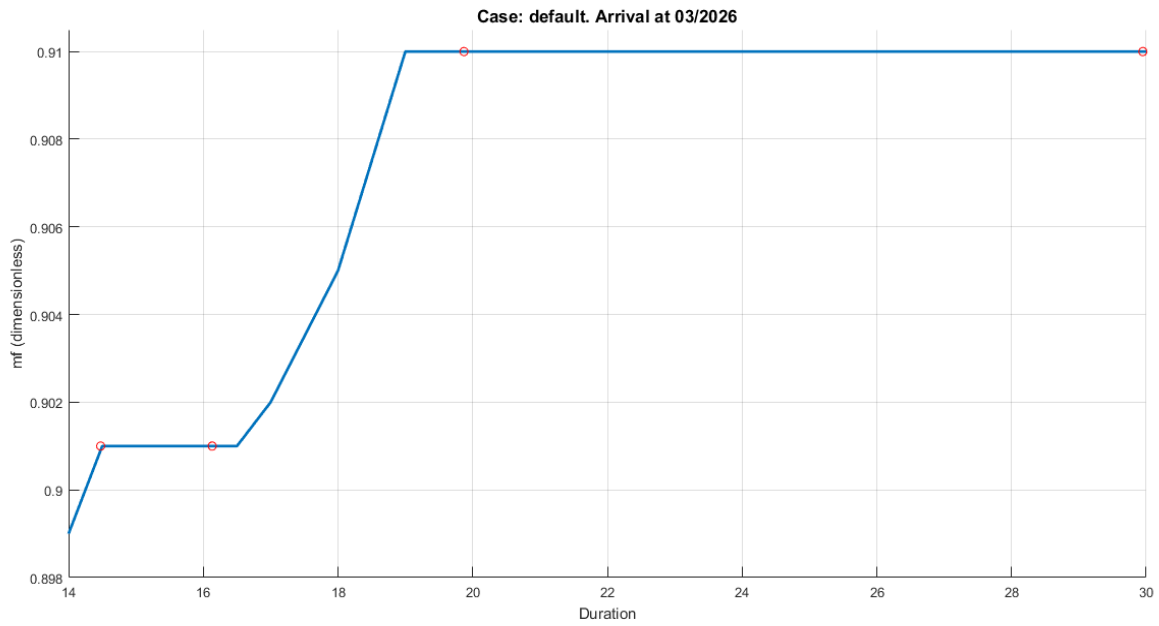


Appendix II: Results for the return trip

Case: Default

	Duration	Days	m f (dim. less)	Departure date	Flyby date	Arrival date
DEFAULT	0 (optimal case for 14.476)	841.52	0.901	14/11/2023	23/12/2024	04/03/2026
	14	813.85	0.899	12/12/2023	24/12/2024	05/03/2026
	14.5	842.92	0.901	12/11/2023	23/12/2024	04/03/2026
	15	871.98	0.901	14/10/2023	23/12/2024	04/03/2026
	15.5	901.05	0.901	15/09/2023	23/12/2024	04/03/2026
	16	930.12	0.901	17/08/2023	23/12/2024	04/03/2026
	16.5	959.18	0.901	19/07/2023	23/12/2024	04/03/2026
	17	988.25	0.902	20/06/2023	23/12/2024	04/03/2026
	18	1046.38	0.905	23/04/2023	23/12/2024	05/03/2026
	19	1104.52	0.91	22/02/2023	22/12/2024	02/03/2026
	20	1162.65	0.91	26/12/2022	22/12/2024	02/03/2026
	21	1220.78	0.91	29/10/2022	22/12/2024	02/03/2026
	22	1278.91	0.91	31/08/2022	22/12/2024	02/03/2026
	22.5	1307.98	0.91	02/08/2022	22/12/2024	02/03/2026
	23	1337.05	0.91	05/07/2022	22/12/2024	03/03/2026
	23.5	1366.11	0.91	06/06/2022	22/12/2024	03/03/2026
	24	1395.18	0.91	08/05/2022	22/12/2024	03/03/2026
	25	1453.31	0.91	10/03/2022	22/12/2024	02/03/2026
	26	1511.44	0.91	11/01/2022	22/12/2024	03/03/2026
	26.5	1540.51	0.91	13/12/2021	22/12/2024	03/03/2026
	27	1569.57	0.91	14/11/2021	22/12/2024	03/03/2026
	27.5	1598.64	0.91	16/10/2021	22/12/2024	03/03/2026
	28	1627.81	0.91	17/09/2021	22/12/2024	03/03/2026
	28.5	1656.77	0.91	19/08/2021	22/12/2024	03/03/2026
	29	1685.84	0.91	21/07/2021	22/12/2024	03/03/2026
	29.5	1714.91	0.91	22/06/2021	22/12/2024	03/03/2026
	30	1743.97	0.91	24/05/2021	22/12/2024	03/03/2026

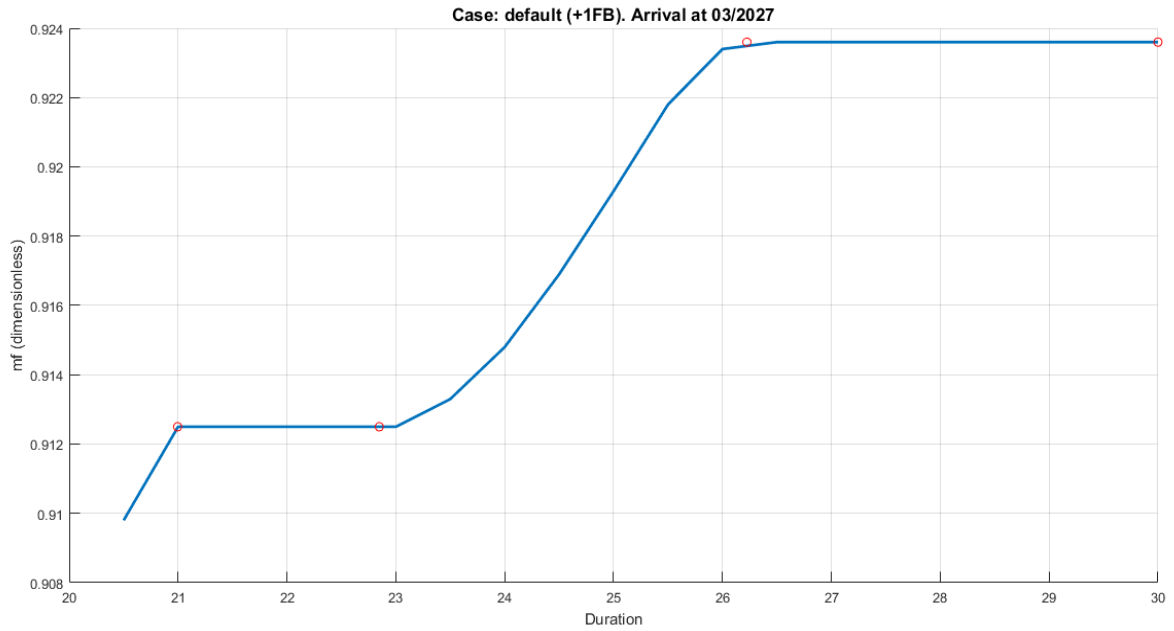
Appendixes



Case: Default (+1FB)

	Duration	Days	m f (dim. less)	Departure date	Flyby date	Arrival date
DEFAULT (+1FB)	0 (optimal case for 20.99)	1220.52	0.9125	11/11/2023	23/12/2024	15/03/2027
	20.5	1191.71	0.9098	10/12/2023	23/12/2024	16/03/2027
	21	1220.78	0.9125	11/11/2023	23/12/2024	15/03/2027
	21.5	1249.85	0.9125	13/10/2023	23/12/2024	15/03/2027
	22	1278.91	0.9125	13/09/2023	23/12/2024	15/03/2027
	22.5	1307.98	0.9125	15/08/2023	23/12/2024	15/03/2027
	23	1337.05	0.9125	17/07/2023	23/12/2024	15/03/2027
	23.5	1366.11	0.9133	19/06/2023	23/12/2024	16/03/2027
	24	1395.18	0.9148	21/05/2023	23/12/2024	16/03/2027
	24.5	1424.24	0.9169	22/04/2023	23/12/2024	16/03/2027
	25	1453.25	0.9193	23/03/2023	23/12/2024	15/03/2027
	25.5	1482.37	0.9218	21/02/2023	23/12/2024	15/03/2027
	26	1511.44	0.9234	23/01/2023	23/12/2024	14/03/2027
	26.5	1540.51	0.9236	25/12/2022	23/12/2024	14/03/2027
	27	1569.57	0.9236	26/11/2022	23/12/2024	14/03/2027
	27.5	1598.64	0.9236	28/10/2022	23/12/2024	14/03/2027
	28	1627.71	0.9236	29/09/2022	23/12/2024	14/03/2027
	28.5	1656.77	0.9236	31/08/2022	23/12/2024	14/03/2027
	29	1685.84	0.9236	02/08/2022	23/12/2024	14/03/2027
	29.5	1714.91	0.9236	04/07/2022	23/12/2024	14/03/2027
30	1743.97	0.9236	05/06/2022	23/12/2024	15/03/2027	

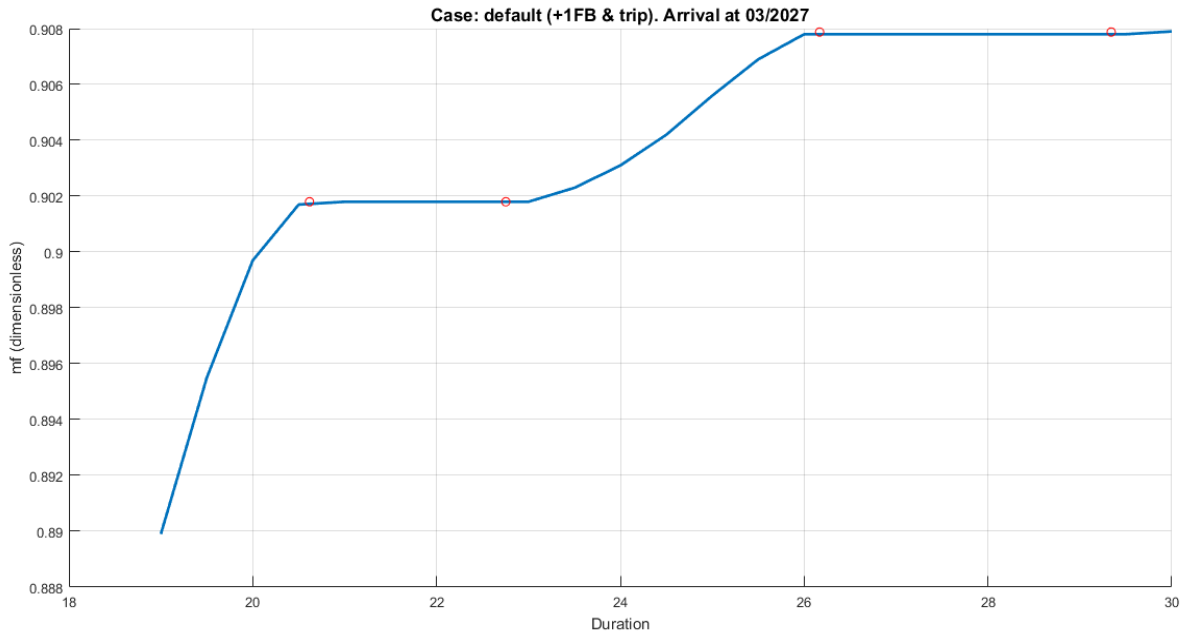
Appendixes



Case: Default (+1FB & trip)

	Duration	Days	m f (dim. less)	Departure date	Flyby date	Arrival date
DEFAULT (+1 FB & trip)	0 (optimal case for 20.6177)	1198.56	0.9018	21/11/2023	22/12/2025	04/03/2027
	19	1104.52	0.8899	26/02/2024	24/12/2023	07/03/2027
	19.5	1133.58	0.8955	27/01/2024	23/12/2025	06/03/2027
	20	1162.65	0.8997	28/12/2023	22/12/2025	04/03/2027
	20.5	1191.71	0.9017	28/11/2023	22/12/2025	04/03/2027
	21	1220.78	0.9018	30/10/2023	22/12/2025	04/03/2027
	21.5	1249.85	0.9018	01/10/2023	22/12/2025	04/03/2027
	22	1278.91	0.9018	02/09/2023	22/12/2025	04/03/2027
	22.5	1307.98	0.9018	04/08/2023	22/12/2025	04/03/2027
	23	1337.05	0.9018	06/07/2023	22/12/2025	04/03/2027
	23.5	1366.11	0.9023	08/06/2023	22/12/2025	05/03/2027
	24	1395.18	0.9031	10/05/2023	23/12/2025	05/03/2027
	24.5	1424.24	0.9042	10/04/2023	22/12/2025	04/03/2027
	25	1453.31	0.9056	11/03/2023	22/12/2025	03/03/2027
	25.5	1482.37	0.9069	09/02/2023	21/12/2025	02/03/2027
	26	1511.44	0.9078	11/01/2023	21/12/2025	02/03/2027
	26.5	1540.51	0.9078	13/12/2022	21/12/2025	03/03/2027
	27	1569.57	0.9078	14/11/2022	21/12/2025	03/03/2027
	27.5	1598.64	0.9078	16/10/2022	21/12/2025	03/03/2027
	28	1627.71	0.9078	17/09/2022	21/12/2025	03/03/2027
	28.5	1656.77	0.9078	19/08/2022	21/12/2025	03/03/2027
	29	1685.84	0.9078	21/07/2022	21/12/2025	03/03/2027
	29.5	1714.91	0.9078	22/06/2022	21/12/2025	03/03/2027
	30	1746.97	0.9079	24/05/2022	22/12/2025	03/03/2027

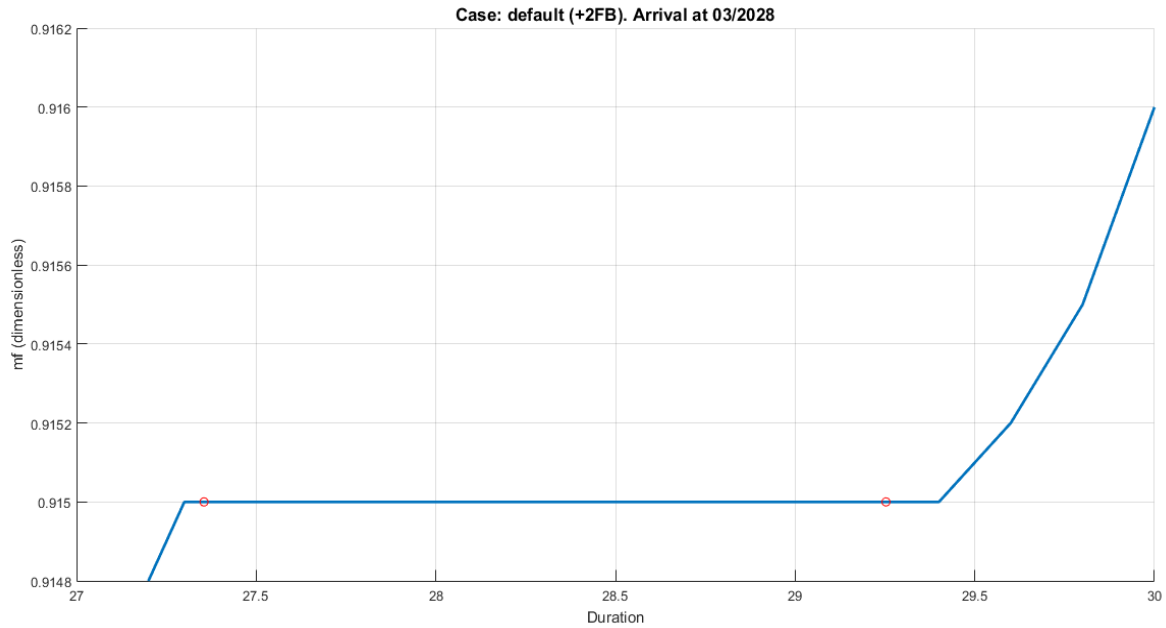
Appendixes



Case: Default (+2FB)

	Duration	Days	m_f (dim. less)	Departure date	Flyby date	Arrival date
DEFAULT (+2 FB)	0 (optimal case for 27.3548)	1590.20	0.915	10/11/2023	23/12/2024	18/03/2028
	27.2	1581.20	0.9148	19/11/2023	23/12/2024	18/03/2028
	27.3	1587.01	0.915	13/11/2023	23/12/2024	18/03/2028
	27.4	1592.83	0.915	07/11/2023	23/12/2024	18/03/2028
	27.6	1604.45	0.915	26/10/2023	23/12/2024	18/03/2028
	27.8	1616.08	0.915	15/10/2023	23/12/2024	18/03/2028
	28	1627.71	0.915	03/10/2023	23/12/2024	18/03/2028
	28.2	1639.33	0.915	22/09/2023	23/12/2024	18/03/2028
	28.4	1650.96	0.915	10/09/2023	23/12/2024	18/03/2028
	28.6	1662.59	0.915	29/08/2023	23/12/2024	18/03/2028
	28.8	1674.21	0.915	18/08/2023	23/12/2024	18/03/2028
	29	1685.84	0.915	06/08/2023	23/12/2024	18/03/2028
	29.2	1697.47	0.915	25/07/2023	23/12/2024	18/03/2028
	29.4	1709.09	0.915	14/07/2023	23/12/2024	18/03/2028
	29.6	1720.72	0.9152	02/07/2023	23/12/2024	18/03/2028
	29.8	1732.35	0.9155	21/06/2023	23/12/2024	18/03/2028
	30	1743.97	0.916	09/06/2023	23/12/2024	18/03/2028

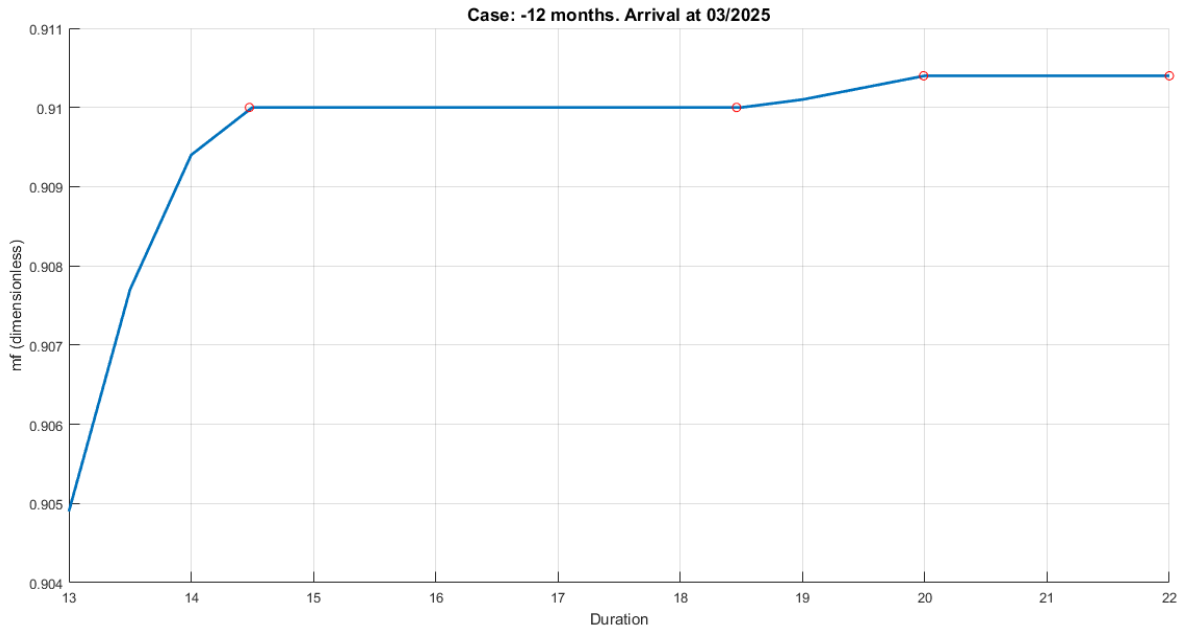
Appendixes



Case: -12 months

	Duration	Days	m_f (dim. less)	Departure date	Flyby date	Arrival date
-1 year	0 (optimal case for 14.445)	839.75	0.9098	17/11/2022	26/12/2023	06/03/2025
	13	755.72	0.9049	09/02/2023	27/12/2023	06/03/2025
	13.5	784.78	0.9077	11/01/2023	27/12/2023	05/03/2025
	14	813.85	0.9094	13/12/2022	26/12/2023	06/03/2025
	14.5	842.92	0.91	14/11/2022	26/12/2023	06/03/2025
	15	871.98	0.9100	16/10/2022	26/12/2023	06/03/2025
	15.5	901.05	0.91	16/09/2022	26/12/2023	05/03/2025
	16	930.12	0.91	18/08/2022	26/12/2023	05/03/2025
	16.5	959.18	0.91	20/07/2022	26/12/2023	05/03/2025
	17	988.25	0.91	21/06/2022	26/12/2023	05/03/2025
	17.5	1017.31	0.91	23/05/2022	26/12/2023	05/03/2025
	18	1046.38	0.91	24/04/2022	26/12/2023	05/03/2025
	18.5	1075.45	0.91	26/03/2022	26/12/2023	05/03/2025
	19	1104.51	0.9101	24/02/2022	25/12/2023	05/03/2025
	20	1162.65	0.9104	28/12/2021	25/12/2023	05/03/2025
	20.2	1174.27	0.9104	16/12/2021	25/12/2023	05/03/2025
	20.4	1185.90	0.9104	05/12/2021	25/12/2023	05/03/2025
	20.6	1197.53	0.9104	23/11/2021	25/12/2023	05/03/2025
	20.8	1209.15	0.9104	12/11/2021	25/12/2023	05/03/2025
	21	1220.78	0.9104	31/10/2021	25/12/2023	05/03/2025
	21.2	1232.41	0.9104	19/10/2021	25/12/2025	05/03/2025
	21.4	1244.03	0.9104	08/10/2021	25/12/2023	05/03/2025
21.6	1255.66	0.9104	26/09/2021	25/12/2023	05/03/2025	
21.7	1261.47	0.9104	20/09/2021	25/12/2023	05/03/2025	
21.8	1267.29	0.9104	14/09/2021	25/12/2023	05/03/2025	
22	1278.91	0.9104	03/09/2021	25/12/2023	05/03/2025	

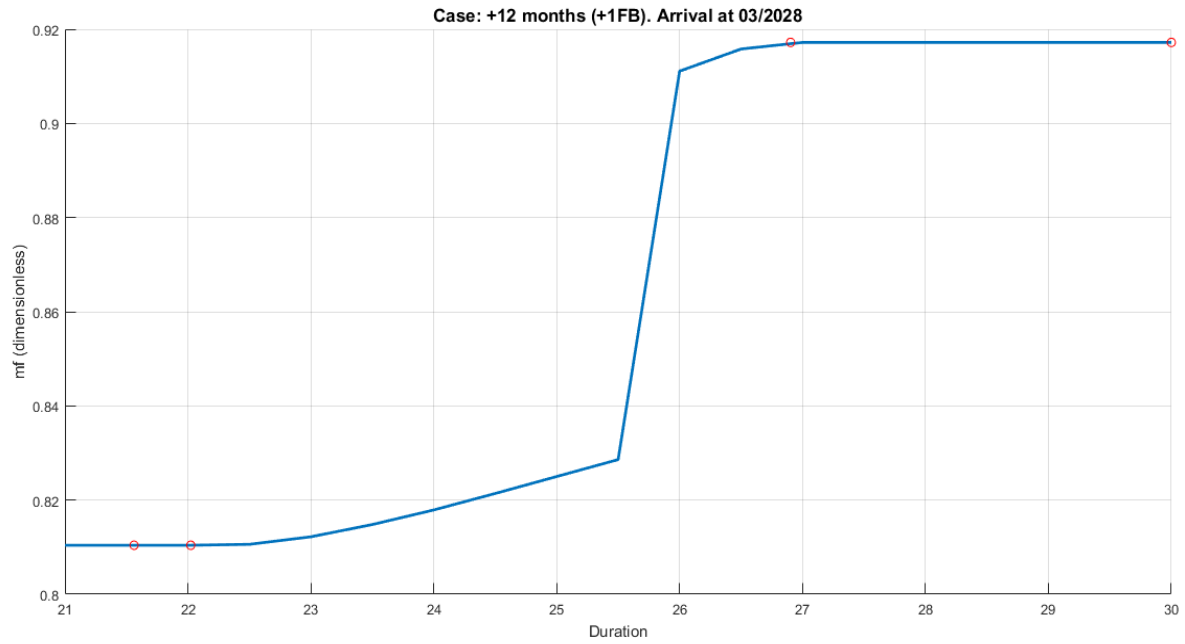
Appendixes



Case: -12 months (+1FB)

	Duration	Days	m f (dim. less)	Departure date	Flyby date	Arrival date
-1 year (+1 FB)	0 (optimal case for 21.97)	1277.36	0.9305	13/09/2022	25/12/2023	14/03/2026
	21	1220.78	0.9301	09/11/2022	25/12/2023	14/03/2026
	21.5	1249.85	0.9304	11/10/2022	25/12/2023	14/03/2026
	22	1278.91	0.9305	12/09/2022	25/12/2023	14/03/2026
	22.5	1307.98	0.9305	14/08/2022	25/12/2023	14/03/2026
	23	1337.05	0.9305	16/07/2022	25/12/2023	14/03/2026
	23.5	1366.11	0.9305	17/06/2022	25/12/2023	14/03/2026
	24	1395.18	0.9305	19/05/2022	25/12/2023	14/03/2026
	24.5	1424.24	0.9305	19/04/2022	25/12/2023	14/03/2026
	25	1453.31	0.9305	21/03/2022	25/12/2023	14/03/2026
	25.5	1482.38	0.9305	20/02/2022	25/12/2023	14/03/2026
	26	1511.44	0.9305	22/01/2022	25/12/2023	14/03/2026
	26.5	1540.51	0.9305	24/12/2021	25/12/2023	14/03/2026
	27	1569.57	0.9305	25/11/2021	25/12/2023	14/03/2026
	27.5	1598.64	0.9305	27/10/2021	25/12/2023	14/03/2026
	28	1627.71	0.9305	28/09/2021	25/12/2023	14/03/2026
	28.5	1656.77	0.9305	30/08/2021	25/12/2023	14/03/2026
	29	1685.84	0.9305	01/08/2021	25/12/2023	14/03/2026
	29.5	1714.91	0.9305	03/07/2021	25/12/2023	14/03/2026
	30	1743.97	0.9305	04/06/2021	25/12/2023	14/03/2026

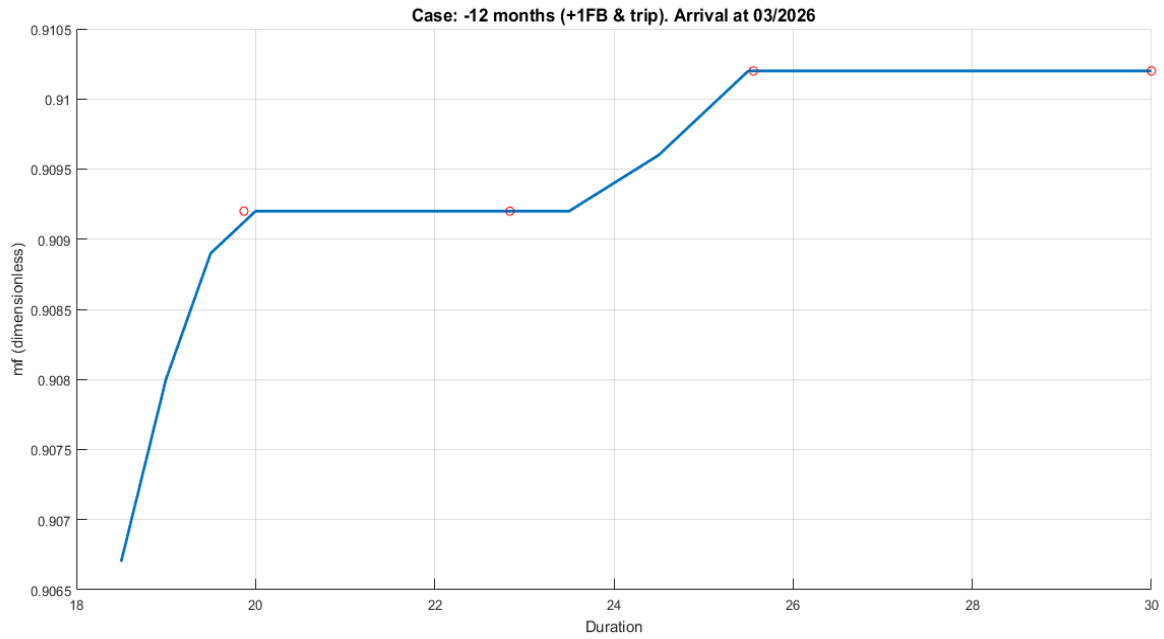
Appendixes



Case: -12 months (+1FB & trip)

	Duration	Days	m f (dim. less)	Departure date	Flyby date	Arrival date
-1 year (+1 FB & trip)	0 (optimal case for 19.87)	1155.09	0.9092	02/01/2023	22/12/2024	02/03/2026
	18.5	1075.45	0.9067	24/03/2023	22/12/2024	03/03/2026
	19	1104.52	0.908	22/02/2023	21/12/2024	02/03/2026
	19.5	1133.58	0.9089	23/01/2023	21/12/2024	02/03/2026
	20	1162.65	0.9092	26/12/2022	22/12/2024	02/03/2026
	20.5	1191.71	0.9092	27/11/2022	22/12/2024	02/03/2026
	21	1220.78	0.9092	29/10/2022	22/12/2024	02/03/2026
	21.5	1249.85	0.9092	30/09/2022	22/12/2024	02/03/2026
	22	1278.91	0.9092	31/08/2022	22/12/2024	02/03/2026
	22.5	1307.98	0.9092	02/08/2022	22/12/2024	02/03/2026
	23	1337.05	0.9092	05/07/2022	22/12/2024	03/03/2026
	23.5	1366.11	0.9092	06/06/2022	22/12/2024	03/03/2026
	24	1395.18	0.9094	08/05/2022	22/12/2024	03/03/2026
	24.5	1424.24	0.9096	08/04/2022	22/12/2024	03/03/2026
	25	1453.31	0.9099	10/03/2022	22/12/2024	02/03/2026
	25.5	1482.37	0.9102	09/02/2022	22/12/2024	02/03/2026
	26	1511.44	0.9102	11/01/2022	22/12/2024	03/03/2026
	26.5	1540.51	0.9102	13/12/2021	22/12/2024	03/03/2026
	27	1569.57	0.9102	14/11/2021	22/12/2024	03/03/2026
	27.5	1598.64	0.9102	16/10/2021	22/12/2024	03/03/2026
	28	1627.71	0.9102	17/09/2021	22/12/2024	03/03/2026
	28.5	1656.77	0.9102	19/08/2021	22/12/2024	03/03/2026
	29	1685.84	0.9102	21/07/2021	22/12/2024	03/03/2026
	29.5	1714.91	0.9102	22/06/2021	22/12/2024	03/03/2026
	30	1743.97	0.9102	24/05/2021	22/12/2024	03/03/2026

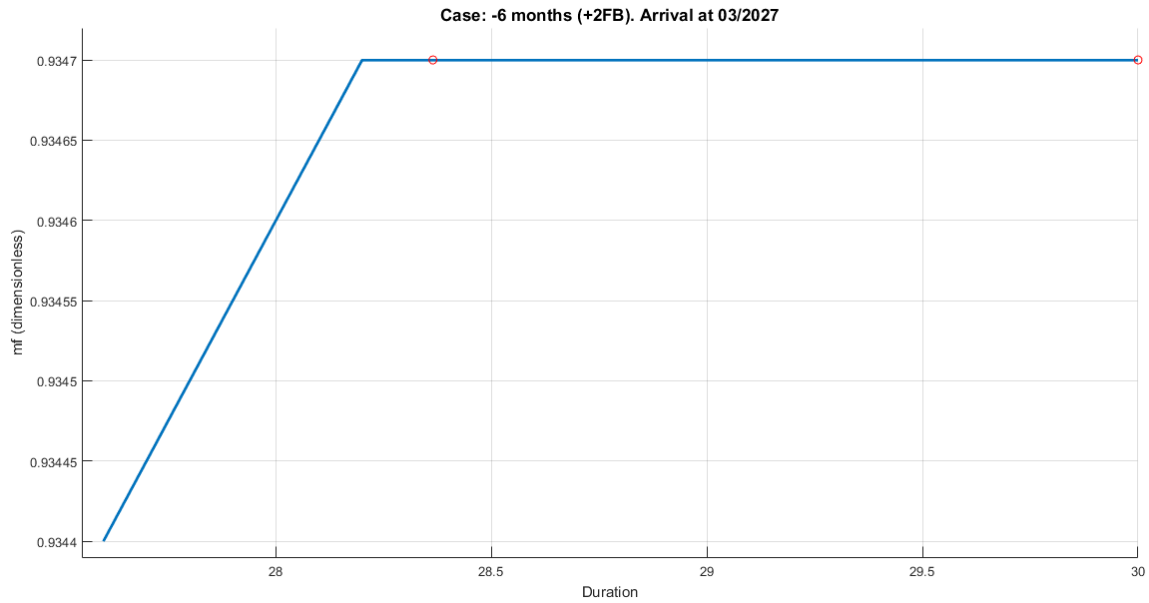
Appendixes



Case: -12 months (+2FB)

	Duration	Days	m_f (dim. less)	Departure date	Flyby date	Arrival date
-1 year (+2 FB)	0 (optimal case for 28.3644)	1648.89	0.9347	11/09/2022	25/12/2023	18/03/2027
	27.6	1604.45	0.9344	26/10/2022	25/12/2023	18/03/2027
	27.8	1616.08	0.9345	14/10/2022	25/12/2023	18/03/2027
	28	1627.71	0.9346	02/10/2022	25/12/2023	18/03/2027
	28.2	1639.33	0.9347	21/09/2022	25/12/2023	18/03/2027
	28.4	1650.96	0.9347	09/09/2022	25/12/2023	18/03/2027
	28.6	1662.59	0.9347	28/08/2022	25/12/2023	18/03/2027
	28.8	1674.21	0.9347	17/08/2022	25/12/2023	18/03/2027
	28.9	1680.03	0.9347	11/08/2022	25/12/2023	18/03/2027
	29	1685.84	0.9347	05/08/2022	25/12/2023	18/03/2027
	29.2	1697.47	0.9347	24/07/2022	25/12/2023	18/03/2027
	29.4	1709.09	0.9347	13/07/2022	25/12/2023	18/03/2027
	29.6	1720.72	0.9347	01/07/2022	25/12/2023	18/03/2027
	29.8	1732.35	0.9347	20/06/2022	25/12/2023	18/03/2027
30	1743.97	0.9347	08/06/2022	25/12/2023	18/03/2027	

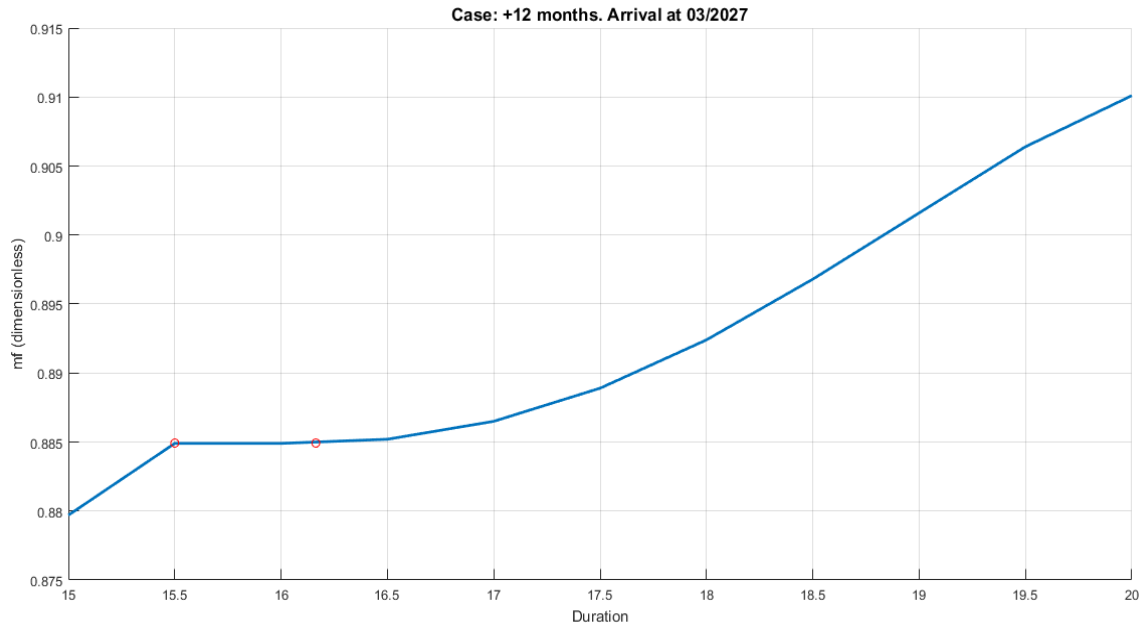
Appendixes



Case: +12 months

	Duration	Days	m_f (dim. less)	Departure date	Flyby date	Arrival date
+1 year (20 ton)	0 (optimal case for 15.4454)	897.87	0.8849	19/09/2024	22/12/2025	06/03/2027
	15	871.98	0.8797	17/10/2024	24/12/2025	08/03/2027
	15.5	897.88	0.8849	19/09/2024	22/12/2025	06/03/2027
	16	930.12	0.8849	18/08/2024	22/12/2025	06/03/2027
	16.5	959.18	0.8852	20/07/2024	22/12/2025	06/03/2027
	17	988.25	0.8865	22/06/2024	22/12/2025	07/03/2027
	17.5	1017.32	0.8889	25/05/2024	22/12/2025	08/03/2027
	18	1046.38	0.8924	26/04/2024	23/12/2025	09/03/2027
	18.5	1075.45	0.8968	28/03/2024	23/12/2025	09/03/2027
	19	1104.52	0.9016	27/02/2024	22/12/2025	07/03/2027
	19.5	1133.58	0.9064	27/01/2024	21/12/2025	06/03/2027
	20	1162.65	0.9101	28/12/2023	21/12/2025	05/03/2027

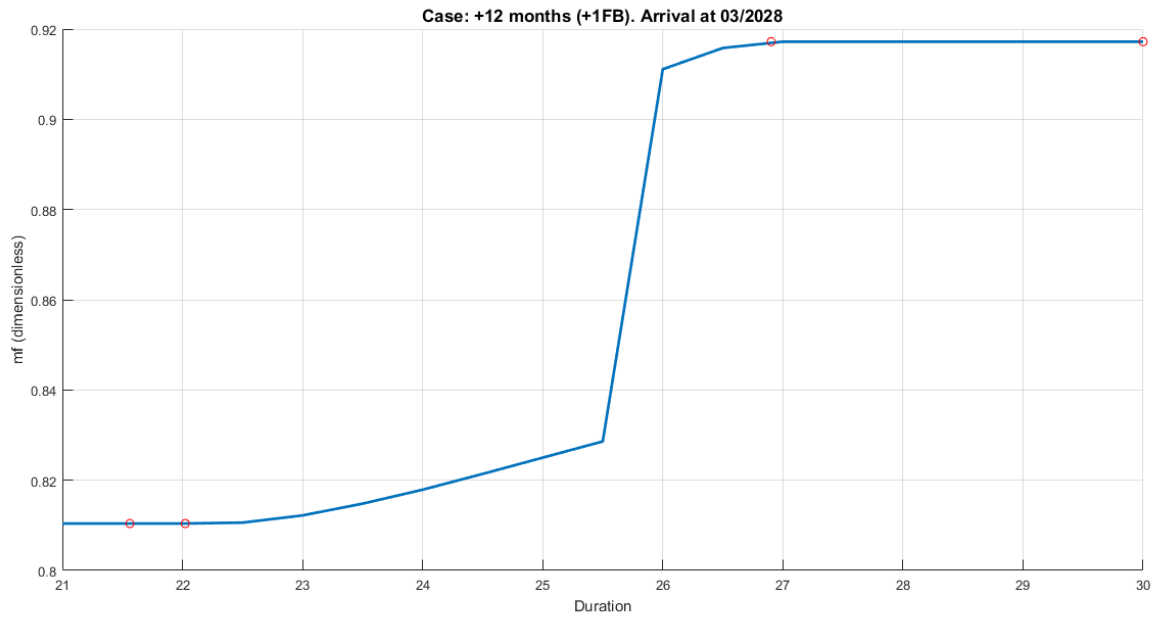
Appendixes



Case: +12 months (+1FB)

	Duration	Days	m_f (dim. less)	Departure date	Flyby date	Arrival date
	0 (optimal case for 21.5619)	1253.45	0.8104	20/09/2024	20/12/2025	26/02/2028
+1 year (+1 FB)	21	1220.78	0.8104	28/10/2024	23/12/2025	02/03/2028
	21.5	1249.85	0.8104	24/09/2024	20/12/2025	26/02/2028
	22	1278.91	0.8104	26/08/2024	20/12/2025	26/02/2028
	22.5	1307.98	0.8106	27/07/2024	19/12/2025	25/02/2028
	23	1337.05	0.8122	28/06/2024	19/12/2025	25/02/2028
	23.5	1366.11	0.8148	31/05/2024	20/12/2025	26/02/2028
	24	1395.18	0.8179	03/05/2024	21/12/2025	27/02/2028
	24.5	1424.24	0.8214	04/04/2024	21/12/2025	27/02/2028
	25	1453.31	0.825	05/03/2024	20/12/2025	26/02/2028
	25.5	1482.38	0.8286	03/02/2024	18/12/2025	24/02/2028
	26	1511.44	0.9111	25/01/2024	22/12/2025	15/03/2028
	26.5	1540.51	0.9158	26/12/2023	22/12/2025	15/03/2028
	27	1569.57	0.9172	28/11/2023	23/12/2025	15/03/2028
	27.5	1598.64	0.9172	29/10/2023	23/12/2025	15/03/2028
	28	1627.71	0.9172	30/09/2023	23/12/2025	15/03/2028
	28.5	1656.77	0.9172	01/09/2023	23/12/2025	15/03/2028
29	1685.84	0.9172	03/08/2023	23/12/2025	15/03/2028	
29.5	1714.91	0.9172	05/07/2023	23/12/2025	15/03/2028	
30	1743.97	0.9172	06/06/2023	23/12/2025	15/03/2028	

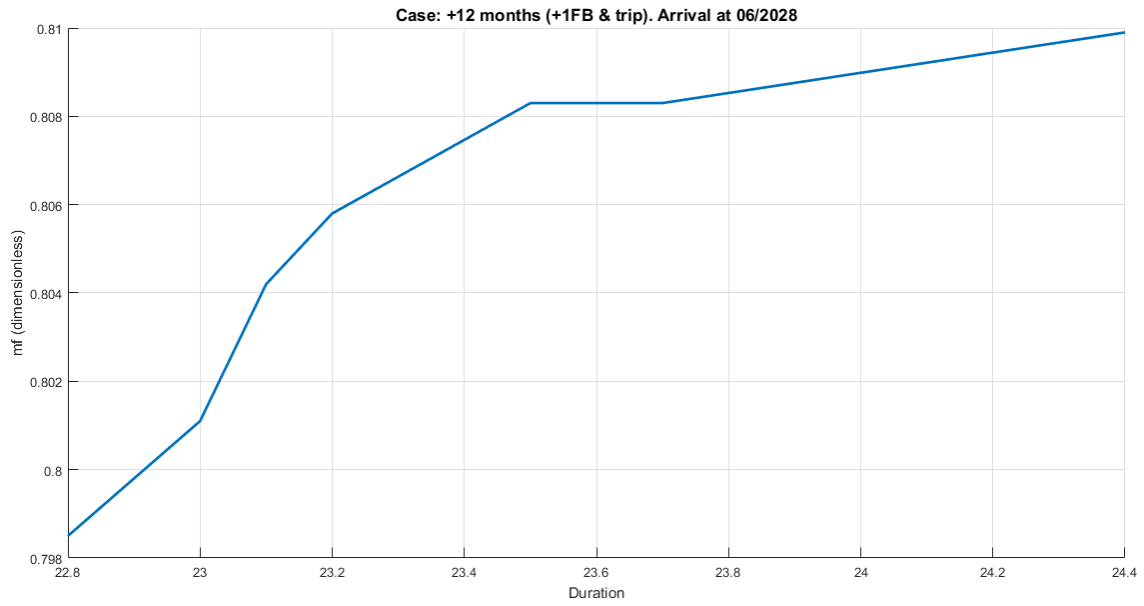
Appendixes



Case: +12 months (+1FB & trip)

	Duration	Days	m_f (dim. less)	Departure date	Flyby date	Arrival date
+1 year (+1 FB & trip)	0 (optimal case for 22.8495)	1328.297	0.7957	23/10/2024	08/11/2026	12/06/2028
	22.8	1325.42	0.7985	27/10/2024	09/11/2026	13/06/2028
	23	1337.05	0.8011	27/10/2024	06/11/2026	25/06/2028
	23.1	1342.86	0.8042	22/10/2024	07/11/2026	26/06/2028
	23.2	1348.67	0.8058	17/10/2024	07/11/2026	27/06/2028
	23.5	1366.11	0.8083	08/10/2024	08/11/2026	05/07/2028
	23.7	1377.74	0.8083	29/09/2024	08/11/2026	07/07/2028
	24.4	1418.43	0.8099	06/10/2024	03/12/2026	25/08/2028

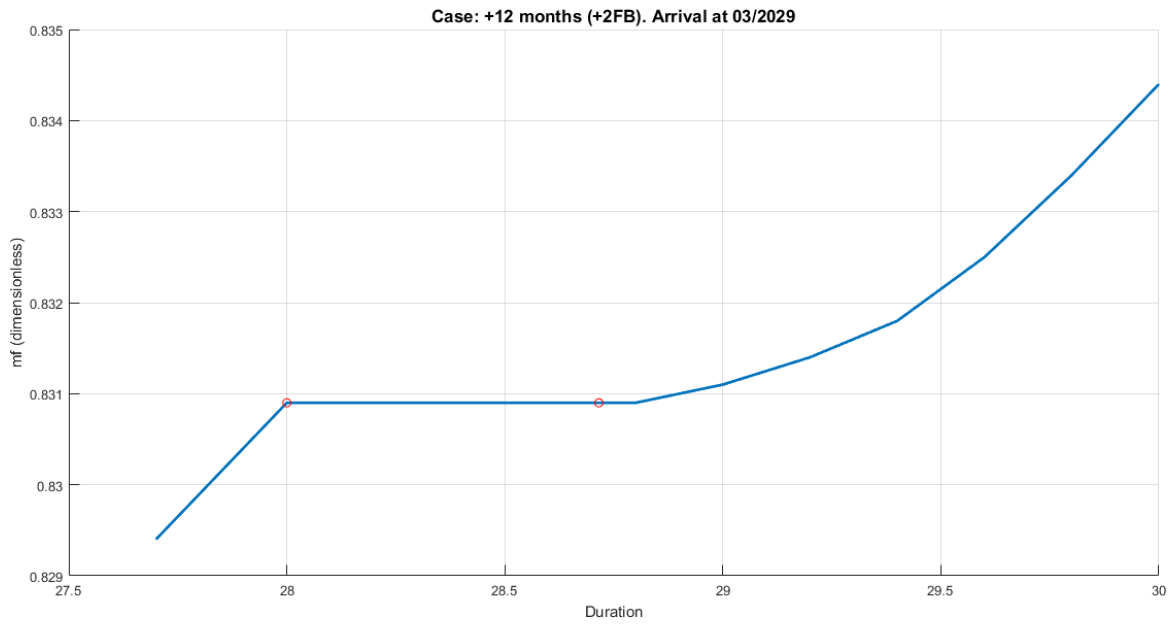
Appendixes



Case: +12 months (+2FB)

	Durata	Giorni	m_f (dim. less)	Data partenza	Data flyby	Data arrivo
+1 year (+2 FB)	0 (optimal case for 27.9677)	1625.83	0.8309	18/09/2024	22/12/2025	02/03/2029
	27.7	1610.27	0.8294	05/10/2024	22/12/2025	03/03/2029
	28	1627.71	0.8309	17/09/2024	22/12/2025	02/03/2029
	28.2	1639.33	0.8309	05/09/2024	22/12/2025	02/03/2029
	28.4	1650.96	0.8309	24/08/2024	22/12/2025	02/03/2029
	28.6	1662.59	0.8309	12/08/2024	22/12/2025	02/03/2029
	28.8	1674.21	0.8309	01/08/2024	21/12/2025	02/03/2029
	29	1685.84	0.8311	20/07/2024	21/12/2025	02/03/2029
	29.2	1697.47	0.8314	08/07/2024	21/12/2025	02/03/2029
	29.4	1709.09	0.8318	27/06/2024	21/12/2025	02/03/2029
	29.6	1720.72	0.8325	16/06/2024	21/12/2025	02/03/2029
	29.8	1732.35	0.8334	04/06/2024	22/12/2025	03/03/2029
	30	1743.97	0.8344	24/05/2024	22/12/2025	03/03/2029

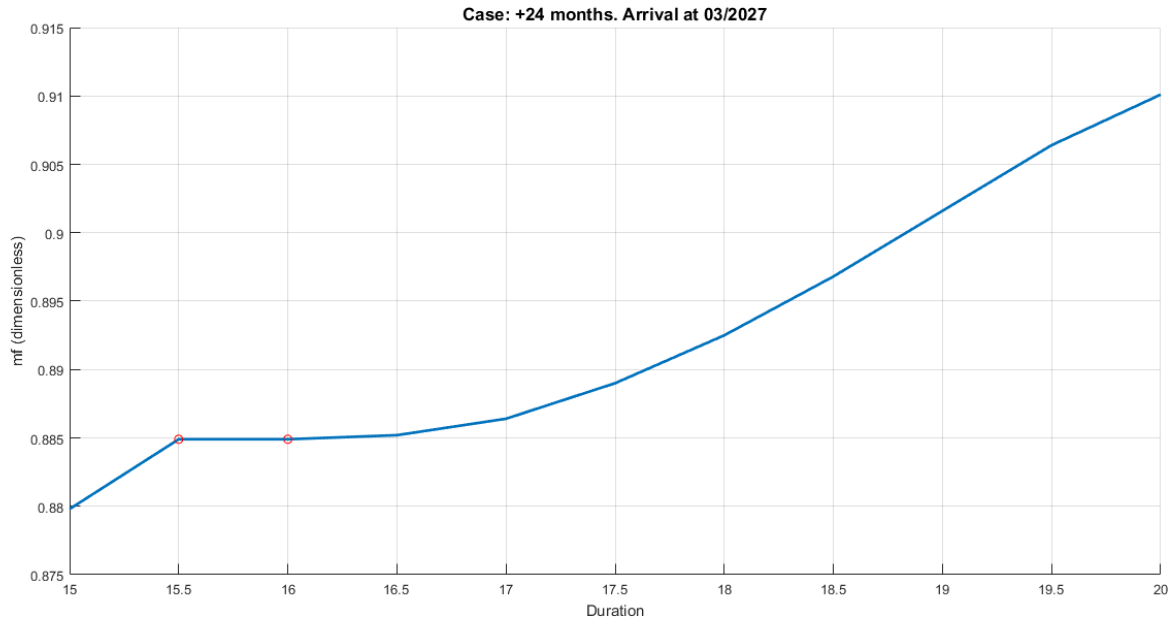
Appendixes



Case: +24 months

	Duration	Days	m f (dim. less)	Departure date	Flyby date	Arrival date
+2 years	0 (optimal case for 15.4454)	897.88	0.8849	19/09/2024	22/12/2025	06/03/2027
	15	871.99	0.8798	17/10/2024	24/12/2025	08/03/2027
	15.5	901.05	0.8849	16/09/2024	22/12/2025	06/03/2027
	16	930.12	0.8849	18/08/2024	22/12/2025	06/03/2027
	16.5	959.18	0.8852	20/07/2024	22/12/2025	06/03/2027
	17	988.25	0.8864	22/06/2024	22/12/2025	07/03/2027
	17.5	1017.32	0.889	25/05/2024	22/12/2025	08/03/2027
	18	1046.38	0.8925	26/04/2024	23/12/2025	09/03/2027
	18.5	1075.45	0.8968	28/03/2024	23/12/2025	09/03/2027
	19	1104.52	0.9016	27/02/2024	22/12/2025	07/03/2027
	19.5	1133.58	0.9064	27/01/2024	21/12/2025	06/03/2027
	20	1162.65	0.9101	28/12/2023	21/12/2025	05/03/2027

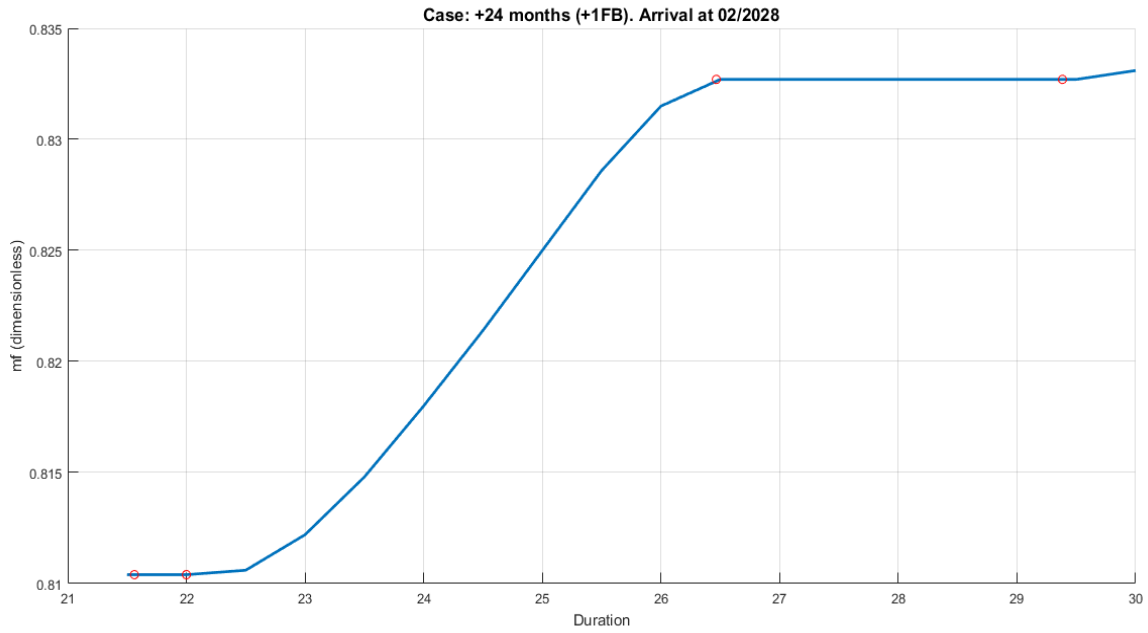
Appendixes



Case: +24 months (+1FB)

	Duration	Days	m f (dim. less)	Departure date	Flyby date	Arrival date
+2 years (+1 FB)	0 (optimal case for 21.5619)	1253.45	0.8104	20/09/2024	20/12/2025	26/02/2028
	21.5	1249.85	0.8104	24/06/2024	20/12/2025	26/02/2028
	22	1278.91	0.8104	26/08/2024	20/12/2025	26/02/2028
	22.5	1307.98	0.8106	27/07/2024	19/12/2025	25/02/2028
	23	1337.05	0.8122	28/06/2024	19/12/2025	25/02/2028
	23.5	1366.11	0.8148	31/05/2024	20/12/2025	26/02/2028
	24	1395.18	0.818	03/05/2024	21/12/2025	27/02/2028
	24.5	1424.24	0.8214	04/04/2024	21/12/2025	27/02/2028
	25	1453.31	0.825	05/03/2024	20/12/2025	26/02/2028
	25.5	1482.38	0.8286	03/02/2024	18/12/2025	24/02/2028
	26	1511.44	0.8315	04/01/2024	17/12/2025	23/02/2028
	26.5	1540.51	0.8327	06/12/2023	18/12/2025	24/02/2028
	27	1569.57	0.8327	07/11/2023	18/12/2025	24/02/2028
	27.5	1598.64	0.8327	09/10/2023	18/12/2025	24/02/2028
	28	1627.71	0.8327	10/09/2023	18/12/2025	24/02/2028
	28.5	1656.77	0.8327	12/08/2023	18/12/2025	24/02/2028
	29	1685.84	0.8327	14/07/2023	18/12/2025	24/02/2028
	29.5	1714.97	0.8327	15/06/2023	18/12/2025	24/02/2028
	30	1743.97	0.8331	17/05/2023	18/12/2025	24/02/2028

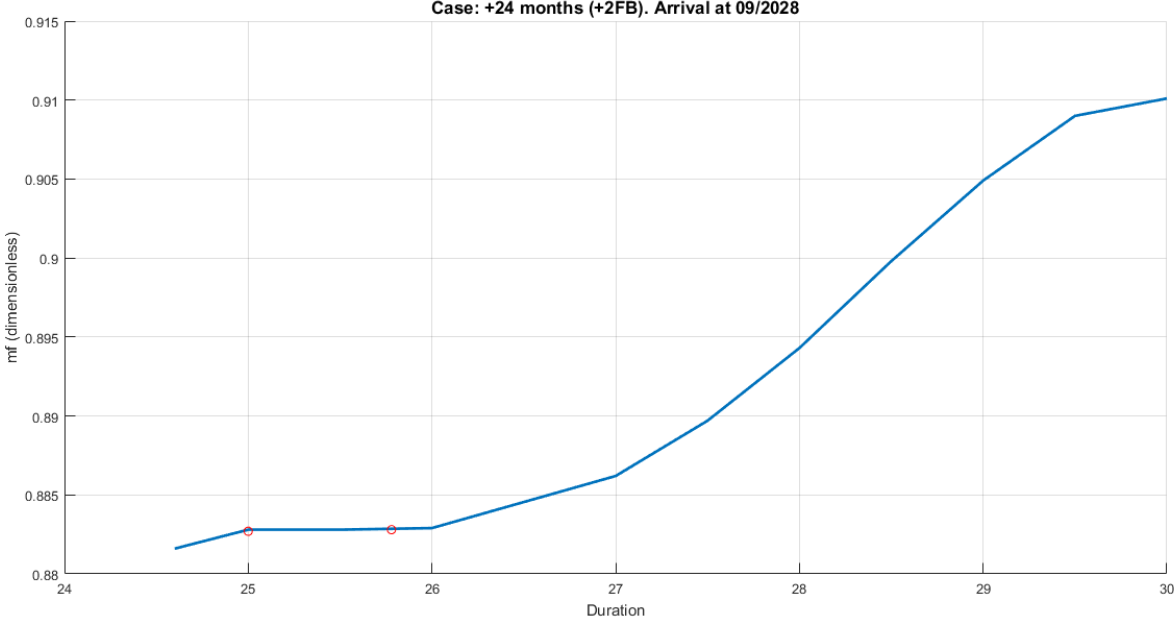
Appendixes



Case: +24 months (+2FB)

	Durata	Giorni	m_f (dim. less)	Data partenza	Data flyby	Data arrivo
	0 (optimal case for 24.8891)	1446.86	0.8828	16/09/2024	22/12/2025	02/09/2028
+2 years (+2 FB)	24.6	1430.06	0.8816	01/10/2024	23/12/2025	31/08/2028
	25	1453.31	0.8828	10/09/2024	22/12/2025	02/09/2028
	25.5	1482.38	0.8828	12/08/2024	22/12/2025	02/09/2028
	26	1511.44	0.8829	13/07/2024	22/12/2025	02/09/2028
	27	1569.57	0.8862	18/05/2024	23/12/2025	04/09/2028
	27.5	1598.64	0.8897	21/04/2024	23/12/2025	05/09/2028
	28	1627.71	0.8943	22/03/2024	23/12/2025	05/09/2028
	28.5	1656.77	0.8998	19/02/2024	23/12/2025	02/09/2028
	29	1685.84	0.9049	21/01/2024	22/12/2025	01/09/2028
	29.5	1714.91	0.909	24/12/2023	22/12/2025	03/09/2028
	30	1743.97	0.9101	27/11/2023	23/12/2025	04/09/2028

Appendix



Appendix III: Optimal results for the return trip

Case	Duration	Departure date	Flyby date	Arrival date	m_f (dim. less)
Default	15	14/10/2023	23/12/2024	04/03/2026	0.9010
-1 year		16/10/2022	26/12/2023	06/03/2025	0.9100
Default	20	26/12/2022	22/12/2024	02/03/2026	0.9100
-1 year		28/12/2021	25/12/2023	05/03/2025	0.9104
-1 year (trip)		26/12/2022	22/12/2024	02/03/2026	0.9092
Default (trip)		28/12/2023	22/12/2025	04/03/2027	0.8997
Default	22	31/08/2022	22/12/2024	02/03/2026	0.9100
-1 year (+1FB)		12/09/2022	25/12/2023	14/03/2026	0.9305
-1 year (trip)		31/08/2022	22/12/2024	02/03/2026	0.9092
Default (trip)		02/09/2023	22/12/2025	04/03/2027	0.9018
Default	25	10/03/2022	22/12/2024	02/03/2026	0.9100
-1 year (+1FB)		21/03/2022	25/12/2023	14/03/2026	0.9305
-1 year (trip)		10/03/2022	22/12/2024	02/03/2026	0.9099
Default	27	14/11/2021	22/12/2024	03/03/2026	0.9100
-1 year (+1FB)		25/11/2021	25/12/2023	14/03/2026	0.9305
-1 year (trip)		14/11/2021	22/12/2024	03/03/2026	0.9102
Default (+1FB)		26/11/2022	23/12/2024	14/03/2027	0.9236
Default (trip)		14/11/2022	21/12/2025	03/03/2027	0.9078
+1 year (+1FB)		28/11/2023	23/12/2025	15/03/2028	0.9172
Default	28	17/09/2021	22/12/2024	03/03/2026	0.9100
-1 year (+1FB)		28/09/2021	25/12/2023	14/03/2026	0.9305
-1 year (trip)		17/09/2021	22/12/2024	03/03/2026	0.9102
Default (+1FB)		29/09/2022	23/12/2024	14/03/2027	0.9236
Default (trip)		17/09/2022	21/12/2025	03/03/2027	0.9078
+1 year (+1FB)		30/09/2023	23/12/2025	15/03/2028	0.9172
Default (+2FB)		03/10/2023	23/12/2024	18/03/2028	0.9150
-1 year (+2FB)		02/10/2022	25/12/2023	18/03/2027	0.9346
Default	30	24/05/2021	22/12/2024	03/03/2026	0.9100
Default (+1FB)		05/06/2022	23/12/2024	15/03/2027	0.9236
Default (trip)		24/05/2022	22/12/2025	03/03/2027	0.9079
Default (+2FB)		09/06/2023	23/12/2024	18/03/2028	0.9160
-1 year (+1FB)		04/06/2021	25/12/2023	14/03/2026	0.9305
-1 year (+2FB)		08/06/2022	25/12/2023	18/03/2027	0.9347
-1 year (trip)		24/05/2021	22/12/2024	03/03/2026	0.9105
+1 year (+1 FB)		06/06/2023	23/12/2025	15/03/2028	0.9172
+2 years (+2FB)		27/11/2023	23/12/2025	04/09/2028	0.9101